

APPLICATION OF DISTANCE PROTECTION FOR TRANSFORMERS IN ESKOM TRANSMISSION

Kubendran Naicker

In partial fulfilment of the requirements for the degree
Master of Science in Power and Energy Systems
School of Engineering
Discipline of Electrical, Electronic & Computer Engineering
University of KwaZulu-Natal

November 2014

Supervisor: Professor I.E Davidson

Co-supervisor: A. Perera

“As the candidate’s Supervisor I agree/do not agree to the submission of this dissertation.”

Signed: _____
Professor I.E. Davidson

I, Kubendran Naicker, declare that:

- i. The research reported in this dissertation, except where otherwise indicated, is my original work.
- ii. The dissertation has not been submitted for any degree or examination at any other university.
- iii. This dissertation does not contain other persons’ data, pictures, graphs or other information, unless specifically acknowledged as being sourced from other persons.
- iv. This dissertation does not contain other persons’ writing, unless specifically acknowledged as being sourced from other researchers. Where other written sources have been quoted, then:
 - a) their words have been re-written but the general information attributed to them has been referenced;
 - b) where their exact words have been used, their writing has been placed inside quotation marks, and referenced.
- v. Where I have reproduced a publication of which I am an author, co-author or editor, I have indicated in detail which part of the publication was actually written by myself alone and have fully referenced such publications.
- vi. This dissertation does not contain text, graphics or tables copied and pasted from the Internet, unless specifically acknowledged, and the source being detailed in the dissertation and in the References sections.

Signed: 
Kubendran Naicker

ACKNOWLEDGEMENTS

The author would like to extend his appreciation and gratitude to the following persons:

- My supervisor, Professor I.E. Davidson for his guidance and support.
- My co-supervisor, Mr Anura Perera for his wisdom, guidance and support.
- My wife, Lolita and daughters Latika and Kriya for supporting me.
- My parents, family and friends for motivating me.
- Sri Sri Nitai & Gauranga for giving me this opportunity

ABSTRACT

Eskom is South Africa's state owned utility who is responsible for the generation, transmission and distribution of electricity. The transmission network in Eskom consists of thousands of kilometres of lines operating at voltages from 220kV to 765kV. Three winding transformers, two winding transformers and autotransformers are employed in Eskom's transmission network.

High Voltage (HV) Inverse Definite Minimum Time (IDMT) overcurrent protection and Medium Voltage (MV) IDMT overcurrent protection are employed to provide backup for these transformer's differential protection and for uncleared through faults. Eskom's Transmission setting philosophy states "that the HV and MV IDMT overcurrent elements must be stable at 2 x full load current of the transformer". This has resulted in MV and HV over-current protection not detecting MV multiphase busbar faults in substations with low MV fault levels which are located far away from generating stations.

In such cases a possible solution is to use distance protection for transformers. This research study investigates how the different vector groups of the power transformer affect the impedance measured by the protection relay, and how standard distance algorithms in protection relays respond to faults located on the MV side of the power transformer. The study consists of a literature review of current practices of transformer distance protection. Autotransformers and distance relays are discussed with manual fault calculation examples. The effects of tap-changers and transformer inrush current on transformer distance protection are also discussed. DigSilent Power Factory software version 15.0.2 was used in the modelling and simulation of faults. The response of distance elements for various faults located on the MV side of transformers are analysed and summarised in two tables which indicate which loops will measure the precise distance to fault through the various transformers and which loops will measure the distance to fault with a slight error.

Multifunction Intelligent Electronic Devices (IEDs) with both distance and differential functions are now being commissioned in the Eskom transmission network for the protection of transformers. The distance elements employed in transformer IEDs are similar to distance elements found in a line distance relay. These distance functions can be set to provide local backup protection for uncleared HV and MV busbar faults in the Eskom Transmission network.

LIST OF ABBREVIATIONS

B/B	Busbar
CbVV	Combined voltage variation
CFVV	Constant flux voltage variation
CT	Current Transformer
Dr	Doctor
Dy	Delta/star
EHV	Extra High Voltage
ESKOM	Electricity Supply Commission
HV	High Voltage
I_1	positive sequence component of current
I_2	negative sequence component of current
I_0	zero sequence component of current
I_b	blue phase current
IDMT	Inverse Definite Minimum Time
IED	Intelligent Electronic Device
I_r	red phase current or residual current
I_{sc}	short circuit current
I_w	white phase current
k_0	residual compensation factor
kV	kilovolt
LV	Low Voltage
MV	Medium Voltage
ms	milliseconds
MVA	Megavolt Ampere
NEC	Neutral Earthing Compensator
pu	per unit
RCA	Relay Characteristic Angle
s	seconds
S/S	Substation
TX	Transformer
VFVV	Variable flux voltage variation
V_p	Transformer primary voltage (line-to-line)
V_s	Transformer secondary voltage (line-to-line)

VT	Voltage Transformer
Yd	Star/delta
YNa0d1	Star connection auto transformer with a tertiary delta winding
Yy	Star/Star
Z1	Zone 1
Z2	Zone 2
Z3	Zone 3
Z_L	Positive sequence impedance of line
Z_s	Source Impedance
Z_T	Positive sequence impedance of transformer
Z_L	Positive sequence impedance of line

TABLE OF CONTENTS

ACKNOWLEDGEMENTS	iii
ABSTRACT	iv
LIST OF ABBREVIATIONS	v
TABLE OF CONTENTS	vii
LIST OF FIGURES	x
LIST OF TABLES	xii
1 INTRODUCTION	1
1.1 Background to the Research Problem	1
1.2 The Research Problem	2
1.3 Research Questions	2
1.4 The Hypothesis	2
1.5 The Importance of this Study	3
1.6 Outline of Dissertation	3
2 LITERATURE REVIEW	4
2.1 Instrument Transformer Connections.....	4
2.2 Zones of Transformer Distance Protection	9
2.3 Fault Current Distribution through Delta/Star Transformers	9
2.4 Distance Measurement through Transformers	10
2.5 Zero Sequence Impedance of Transformers.....	13
2.6 Tap-Changer and Transformer Inrush Currents	14
2.6.1 Transformer Magnetising Inrush Currents	14
2.6.2 Distance Relay Response and Solutions to Inrush Currents	16
2.6.3 On-Load Tap-Changers.....	17
2.7 Conclusion	18
3 METHODOLOGY AND APPLICATION	19
3.1 Autotransformer basics and fault calculations	19
3.1.1 Autotransformers.....	19
3.1.2 Review of zero sequence currents.....	24
3.1.3 Fault Calculation - Autotransformer (Line to Ground - MV side).....	25
3.1.4 Fault Calculation - Autotransformer (Line to Ground - HV side).....	25
3.1.5 Z Bus Method - Autotransformer (Line to Line Fault - MV side)	26
3.1.6 Z Bus Method - Autotransformer (Line to Ground Fault - MV side)	26
3.2 Distance Relays.....	26

3.2.1	Mho Characteristic	26
3.2.2	Quadrilateral Characteristic	32
3.2.3	Impedance Measurement – Phase to Phase Fault.....	32
3.2.4	Impedance Measurement – Single-Line-to-Ground Fault.....	34
3.2.5	Impedance Measurement – Line-to-Ground Fault through Autotransformer	37
3.2.6	Distance Relay Settings.....	39
3.3	Effects of Tap-Changer on Settings for Transformer Distance Protection	40
3.4	Conclusion	43
4	FAULT SIMULATIONS.....	45
4.1	Star/Star Transformer Fault Simulation and Analysis	47
4.1.1	Star/Star Transformer - 3-Phase Fault.....	48
4.1.2	Star/Star Transformer – Single-Line-to-Ground Fault.....	49
4.1.3	Star/Star Transformer – Phase-to-Phase Fault	49
4.1.4	Star/Star Transformer – Phase-to-Phase-to-Ground Fault	49
4.2	Star/Delta (YNd1) Transformer Fault Simulation and Analysis.....	50
4.2.1	Star/Delta Transformer – 3-Phase Fault.....	52
4.2.2	Star/Delta Transformer – Single Line-to-Ground Fault.....	52
4.2.3	Star/Delta Transformer – Phase-to-Phase Fault	53
4.2.4	Star/Delta Transformer – Phase-to-Phase-to-Ground Fault	54
4.3	Delta/Star (Dyn1) Transformer Fault Simulation and Analysis.....	54
4.3.1	Delta/Star Transformer – 3-Phase Fault.....	55
4.3.2	Delta/Star Transformer – Single-Line-to-Ground Fault.....	56
4.3.3	Delta/Star Transformer – Phase-to-Phase Fault	56
4.3.4	Delta\Star Transformer – Phase-to-Phase-to-Ground Fault	57
4.4	Star/Star/Delta (YNynd1) Transformer Fault Simulation and Analysis	58
4.4.1	Star/Star/Delta Transformer – 3-Phase Fault	61
4.4.2	Star/Star/Delta Transformer – Single-Line-to-Ground Fault	61
4.4.3	Star/Star/Delta Transformer – Phase-to-Phase Fault.....	62
4.4.4	Star/Star/Delta Transformer – Phase-to-Phase-to-Ground Fault.....	62
4.5	Autotransformer (YNa0d1) Fault Simulation and Analysis	62
4.6	Conclusion	63
5	CASE STUDIES AND SIMULATIONS	66
5.1	Case-Study-Example 1	66
5.2	Case-Study-Example 2.....	68
5.3	Case-Study-Example 3.....	71

5.4	Case-Study-Example 4.....	73
5.5	Case-Study-Example 5.....	79
5.6	Case-Study-Example 6.....	84
5.7	Case-Study-Example 7.....	92
5.8	Simulation-Example 1.....	101
5.9	Simulation-Example 2.....	102
5.10	Simulation-Example 3.....	103
5.11	Simulation-Example 4.....	104
5.12	Simulation-Example 5.....	105
5.13	Simulation-Example 6.....	107
5.14	Simulation-Example 7.....	108
5.15	Simulation-Example 8.....	109
5.16	Simulation-Example 9.....	111
5.17	Simulation-Example 10.....	112
5.18	Simulation-Example 11.....	113
5.19	Simulation-Example 12.....	115
5.20	Simulation-Example 13.....	115
6	CONCLUSIONS AND RECOMMENDATIONS.....	118
6.1	Conclusions.....	118
6.2	Recommendations.....	119
	REFERENCES.....	120
	APPENDIX 1.....	125
	APPENDIX 2.....	126
	APPENDIX 3.....	127
	APPENDIX 4.....	128

LIST OF FIGURES

<i>Figure 2-1: CT and VT located on the transformer primary side (Ziegler 2008).....</i>	<i>5</i>
<i>Figure 2-2: CT and VT located on the transformer secondary side (Ziegler 2008).....</i>	<i>6</i>
<i>Figure 2-3: CT on the secondary side and VT located on the primary side</i>	<i>6</i>
<i>Figure 2-4: CT on the primary side and VT located on the secondary side</i>	<i>7</i>
<i>Figure 2-5: Distance protection zones when applied through transformers</i>	<i>9</i>
<i>Figure 2-6: Fault current distribution in Delta/Star transformer (Ederhoff 2010).....</i>	<i>10</i>
<i>Figure 3-1: Schematic drawing of autotransformer (EPRI 2009).....</i>	<i>20</i>
<i>Figure 3-2: Equivalent positive sequence impedance diagram.....</i>	<i>22</i>
<i>Figure 3-3: Zero sequence equivalent circuit of an autotransformer (GEC Alsthom Measurements Limited 1987).....</i>	<i>23</i>
<i>Figure 3-4: Zero sequence model of a 3 winding transformer (GEC Alsthom Measurements Limited 1987)</i>	<i>24</i>
<i>Figure 3-5: Self-polarised mho-impedance diagram (Ziegler 2008).....</i>	<i>27</i>
<i>Figure 3-6: Self-polarised mho-voltage diagram (Ziegler 2008).....</i>	<i>29</i>
<i>Figure 3-7: Circular phase comparator (Perez 2006).....</i>	<i>30</i>
<i>Figure 3-8: Quadrilateral characteristic (Andrichak & Alexander n.d.).....</i>	<i>32</i>
<i>Figure 3-9: Impedance measurement – 3-phase fault (Alworthy 1999).....</i>	<i>33</i>
<i>Figure 3-10: Impedance measurement – single-line-to-ground fault (Alworthy 1999).....</i>	<i>35</i>
<i>Figure 3-11: Impedance measurement – single-line-to-ground fault sequence diagram (Alworthy 1999).....</i>	<i>35</i>
<i>Figure 3-12: Residual connection of CTs (Eaton 2014).....</i>	<i>37</i>
<i>Figure 3-13: Zone 3 for local HV feeder</i>	<i>39</i>
<i>Figure 4-1: Network diagram for fault simulations.....</i>	<i>45</i>
<i>Figure 4-2: Network diagram for fault simulations - YNd1.....</i>	<i>51</i>
<i>Figure 4-3: Network diagram for fault simulations - YNynd1</i>	<i>59</i>
<i>Figure 5-1: Network for Case-Study-Example 2</i>	<i>68</i>
<i>Figure 5-2: Network with an autotransformer – Case-Study-Example 4</i>	<i>73</i>
<i>Figure 5-3: Positive sequence reactance diagram for Case-Study-Example 4</i>	<i>74</i>
<i>Figure 5-4: Zero sequence reactance diagram for Case-Study-Example 4.....</i>	<i>75</i>
<i>Figure 5-5: Distribution of fault current for zero sequence reactance diagram - Case-Study- Example 4.....</i>	<i>76</i>

<i>Figure 5-6: Distribution of fault current for the positive/negative sequence reactance diagram - Case-Study-Example 4.....</i>	<i>77</i>
<i>Figure 5-7: Network diagram for Case-Study-Example 4 showing fault current distribution</i>	<i>79</i>
<i>Figure 5-8: Positive sequence reactance diagram for Case-Study-Example 5</i>	<i>79</i>
<i>Figure 5-9: Zero sequence reactance diagram for Case-Study-Example 5.....</i>	<i>80</i>
<i>Figure 5-10: Network diagram for Case-Study-Example 5.....</i>	<i>81</i>
<i>Figure 5-11: Distribution of fault current for zero sequence reactance diagram - Case-Study-Example 5.....</i>	<i>81</i>
<i>Figure 5-12: Distribution of fault current for the positive/negative sequence reactance diagram – Case-Study-Example 5.....</i>	<i>82</i>
<i>Figure 5-13: Network diagram for Case-Study-Example 5 showing fault current distribution</i>	<i>84</i>
<i>Figure 5-14: Network diagram for Case-Study-Example 6.....</i>	<i>85</i>
<i>Figure 5-15: Positive and negative sequence reactance diagram for Case-Study-Example 6</i>	<i>85</i>
<i>Figure 5-16: Distribution of fault current for the positive/negative sequence reactance diagram – Case-Study-Example 6 and 7.....</i>	<i>90</i>
<i>Figure 5-17: Network diagram for Case-Study-Example 7.....</i>	<i>92</i>
<i>Figure 5-18: Zero sequence reactance diagram for Case-Study-Example 7.....</i>	<i>93</i>
<i>Figure 5-19: Distribution of fault current for zero sequence reactance diagram - Case-Study-Example 7.....</i>	<i>99</i>

LIST OF TABLES

<i>Table 2-1: Formulae for Yyd and Yd11 transformers (Cigré 2008)</i>	11
<i>Table 2-2: Formulae for Dy1 Transformer (Cigré 2008)</i>	11
<i>Table 2-3: Phase distance element input for Yd1 and Dy1 transformer (GE Multilin 2011)</i> 12	
<i>Table 2-4: Harmonics of the magnetising inrush current (Horowitz, Phadke & Niemira 2008)</i>	15
<i>Table 3-1: Apparent impedance seen by self-polarised distance relays</i>	28
<i>Table 3-2: ΔU and V_{pol} for a self-polarised mho characteristic</i>	30
<i>Table 3-3: Inputs for cross-polarised distance relay</i>	31
<i>Table 3-4: HV/MV transformer impedance ranges (Goosen, (2004)</i>	40
<i>Table 3-5: Eros S/S - Transformer 1</i>	41
<i>Table 4-1: AC Voltage Source 1 & 2 data</i>	46
<i>Table 4-2: 420/22kV Generator Transformers T1 and T2 data</i>	46
<i>Table 4-3: 400kV Line 1 data</i>	46
<i>Table 4-4: 400kV Line 2 data</i>	46
<i>Table 4-5: General Load data</i>	47
<i>Table 4-6: 400/88 TX3 and TX4 data</i>	47
<i>Table 4-7: Fault currents - Star/Star Transformer</i>	48
<i>Table 4-8: Fault Voltages - Star/Star Transformer</i>	48
<i>Table 4-9: 88/6.6 TX5 data</i>	50
<i>Table 4-10: Fault currents - star/delta transformer</i>	51
<i>Table 4-11: Fault voltages - star/delta transformer</i>	52
<i>Table 4-12: Fault currents - delta/star transformer</i>	55
<i>Table 4-13: Fault voltages – delta/star transformer</i>	55
<i>Table 4-14: 400/88/22 TX3 and TX4 data</i>	59
<i>Table 4-15: Fault currents - star/star/delta transformer</i>	60
<i>Table 4-16: Fault voltages - star/star/delta transformer</i>	60
<i>Table 4-17: Formulae for distance measurement through YNyn and YNd1 transformer</i>	64
<i>Table 4-18: Formulae for distance measurement through Dyn1 and 3 winding transformers</i>	65

1 INTRODUCTION

Eskom which is a state owned utility in South Africa is also the largest producer of electricity in Africa. The generation, transmission and distribution of power in South Africa are performed by Eskom. In the Eskom Transmission Network HV IDMT overcurrent protection and MV IDMT overcurrent protection are employed to provide backup for the transformer's differential protection and for uncleared external faults. MV IDMT is also employed to backup the MV busbar protection scheme in the case of failure of the busbar protection scheme.

Tenaga Nasional Berhad (Malaysian Utility) has started using distance functions in place of IDMT overcurrent functions for transformer protection (Shukri, Hairi & Mohd Zin 2005). A joint venture study between Tenaga Nasional Berhad and Tokyo Electric Power Company concluded that the fault clearance requirements for Extra High Voltage (EHV) and HV networks are not met by the transformers' overcurrent backup protection. In Germany 75% of electric utilities employ distance function as backup in transformers rather than overcurrent (Herrmann 2005).

Multifunction IEDs with both distance and differential functions are now being commissioned in the Eskom Network for the protection of transformers. The distance elements employed in the transformer IEDs are similar to distance elements found in a line distance IED (Han, et al (2009)). For transformer protection the distance function is traditionally not used because overcurrent is used as backup protection. In this research investigation Transformer Distance Protection will not be used to replace conventional overcurrent protection, but rather to provide local backup for uncleared MV and HV busbar faults and backup the transformers' differential protection.

1.1 Background to the Research Problem

Eskom's Transmission setting philosophy states that the HV and MV IDMT overcurrent elements must be stable at 2 x full load current of the transformer (Eskom 2006). This has resulted in MV and HV overcurrent protection not detecting uncleared MV multiphase busbar faults in substations with low MV fault levels which are located far away from

generating stations. In these situations a reverse reaching zone of the local HV feeders are used to backup the MV busbar protection. If this is not possible then a forward reaching zone of all remote HV feeders is used to respond to uncleared MV busbar faults. This results in a total shutdown of a substation for a MV busbar protection failure. Zone 3 of the HV feeders (forward or reverse) have a standard delay of 1s in Eskom. This delay can be up to 5s due to co-ordination according to Eskom's Transmission setting philosophy (Eskom 2006).

1.2 The Research Problem

Two winding transformers with star/delta configuration, three winding transformers and autotransformers are employed in the Eskom Transmission Network. How would the traditional phase and ground distance elements in transformer IEDs respond to varying faults when reaching through different types of transformers?

1.3 Research Questions

- Can the impedance function in transformer IEDs be set to reach through transformers?
- Will the relay correctly measure the distance to fault through a transformer?
- How will the vector group of a transformer affect distance measurement for various fault types?
- What percentage error will the tap-changer introduce?
- Is vector group compensation required for instrument transformers when used for transformer distance protection?
- How to prevent the impedance function in the relay from operating during transformer inrush conditions.

1.4 The Hypothesis

Distance protection applied through transformers can provide local backup for uncleared MV and HV busbar faults and backup the transformer's differential protection.

1.5 The Importance of this Study

This study will assist setting engineers when applying distance protection functions in transformer IEDs and assist engineers and students to perform manual fault calculations in networks employing autotransformers.

1.6 Outline of Dissertation

Chapter 1 introduces the subject of applying distance protection function in transformer IEDs.

Chapter 2 presents a literature review of current practices of transformer distance protection. Factors that will effect distance measurement through power transformers such as zero sequence impedances of transformers, tap-changers and transformer inrush currents are discussed.

Chapter 3 reviews the sequence network diagrams for autotransformers. Fault calculations are performed that show the reversal of the current direction in the neutral of an autotransformer. Fault calculation case studies are also performed to determine the currents and voltages at the relaying point for a phase-to-phase and a single-line-to-ground fault. These values will be used to calculate distance to fault, through the autotransformer.

Chapter 3 also describes the Mho and Quadrilateral characteristics of distance relays and how impedance measurement is performed using traditional algorithms. The effects of a tap-changer on settings for transformer distance protection is also explained,

Chapter 4 deals with fault simulations. Digsilent Power Factory Simulation software is used to throw faults on one side of power transformers having varying vector groups. Voltages and currents are recorded at the other side of the transformer. These values are then used in traditional distance measurement algorithms to measure distance to fault through transformers.

Chapter 5 consists of all the Case-Study-Examples and Simulation Examples.

Chapter 6 summarises the findings of this research and presents the conclusion reached.

2 LITERATURE REVIEW

This chapter discusses how the positioning of the instrument transformers (Current Transformers (CTs) and Voltage Transformers (VTs)) affects the settings of distance relays when applied through power transformers. The CT and VT can be positioned on either side of power transformers. However, in these cases compensation is required. Compensation caters for the phase shift of the transformer. If both instrument transformers (connected to the distance relay) are located on the same side of the power transformer then vector group compensation is not required. Furthermore a review of current applications of transformer distance protection, impedance of transformers, tap-changers and transformer inrush currents is discussed.

2.1 Instrument Transformer Connections

Four possible options are used for the connection of current transformers and voltage transformers when distance protection is applied through transformers (Ziegler 2008). However, in practice, the instrument transformers for distance protection are typically positioned on the primary side or secondary side of the transformer. Figures 2-1 to 2-4 show the four possible positions of the instrument transformers. These figures show the application of distance protection with the intention of providing backup protection for the transformer unit protection and for providing backup protection for HV and MV busbar protection and the lines located on both sides of the transformer. In these figures Zone 1 is the forward zone and Zone 3 is the reverse zone. The zones are determined by the VT location. In other words, the protective zone starts at the location of the VT and then the intended direction (forward or reverse) must be considered. In Figure 2-1 the positive sequence impedance of the transformer is included in the Zone 1 setting. For the Zone 3 setting the positive sequence of the transformer is not included, because the transformer is not located between the VT and the intended reach point.

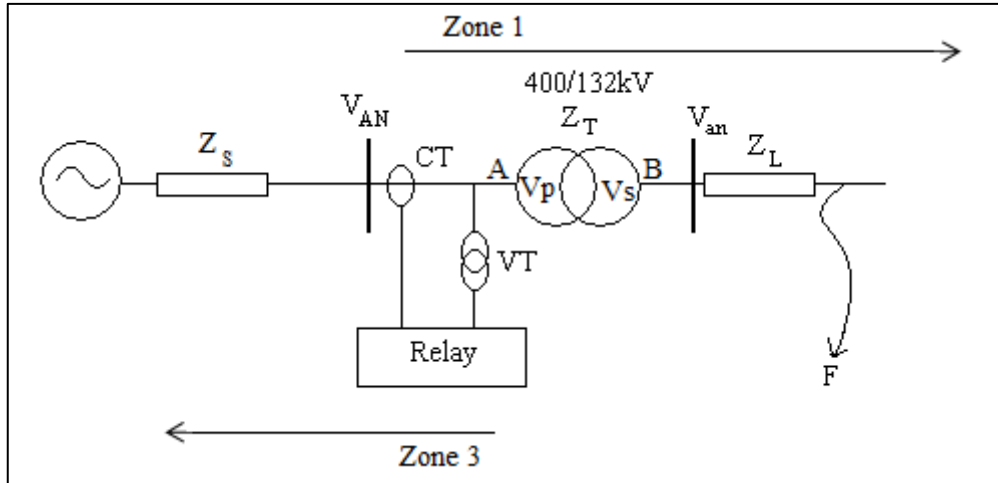


Figure 2-1: CT and VT located on the transformer primary side (Ziegler 2008)

The Zone 1 setting in primary ohms in Figure 2-1 is:-

$$Z1 = Z_T \text{ (at A) } + Z_L (V_p/V_s)^2 \text{ or } \quad (2.1)$$

$$Z1 = (Z_T \text{ (at B) } + Z_L) (V_p/V_s)^2 \quad (2.2)$$

The Zone 3 setting is:-

$$Z3 = Z_s \quad (2.3)$$

Where:

Z_s = Source impedance

Z_T = Positive sequence impedance of transformer

Z_L = Positive sequence impedance of line

V_p = Primary voltage of transformer (line-to-line)

V_s = Secondary voltage of transformer (line-to-line)

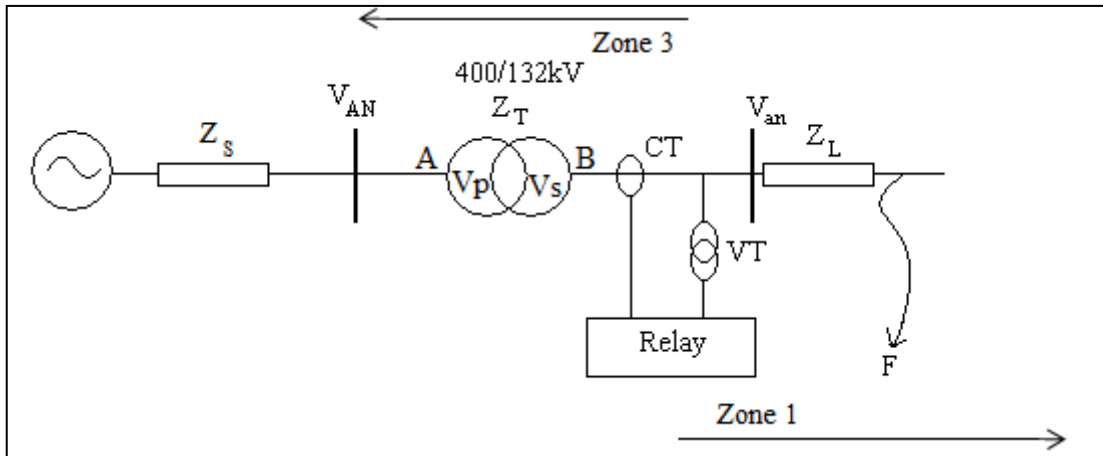


Figure 2-2: CT and VT located on the transformer secondary side (Ziegler 2008)

The Zone 3 setting in primary ohms in Figure 2-2 is:-

$$Z3 = Z_T \text{ (at B)} + Z_s \left(\frac{V_s}{V_p}\right)^2 \text{ or} \quad (2.4)$$

$$Z3 = (Z_T \text{ (at A)} + Z_s) \left(\frac{V_s}{V_p}\right)^2 \quad (2.5)$$

The Zone 1 setting is:-

$$Z1 = Z_L \quad (2.6)$$

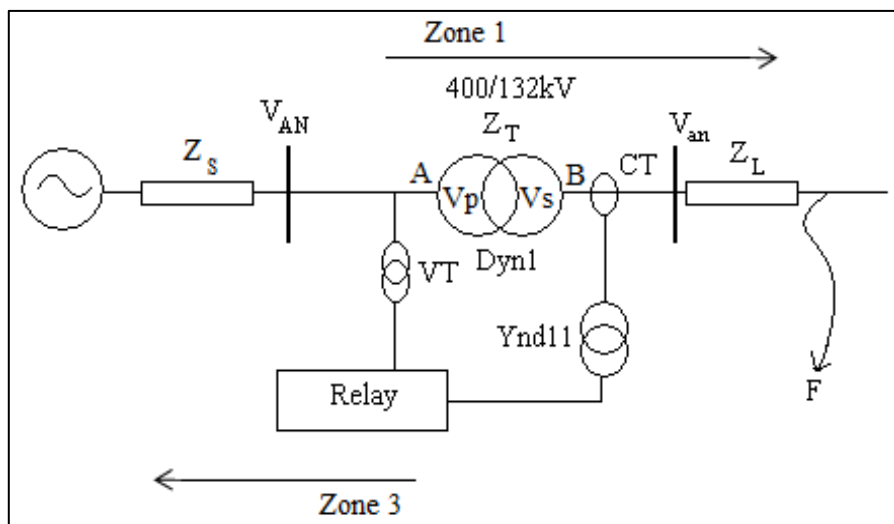
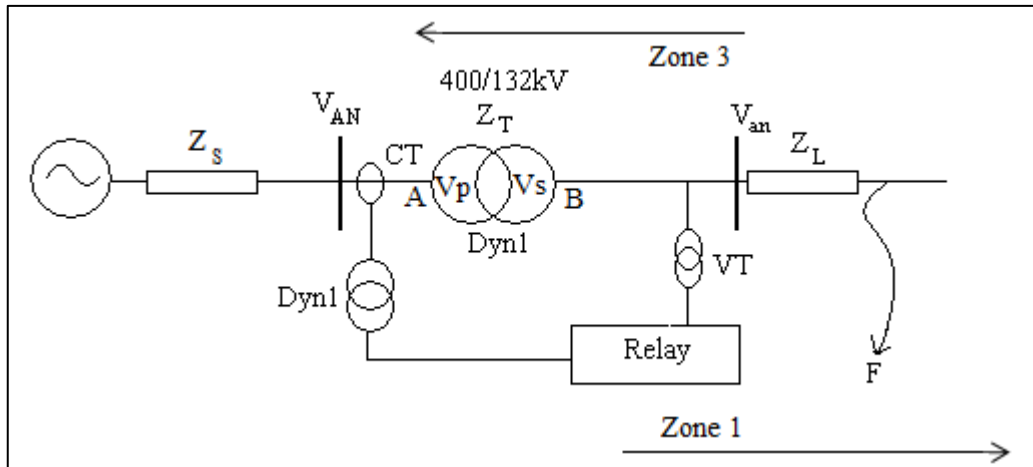


Figure 2-3: CT on the secondary side and VT located on the primary side (Ziegler 2008)



**Figure 2-4: CT on the primary side and VT located on the secondary side
(Ziegler 2008)**

In Figure 2-3 Zone 3 requires CT compensation (Yd11) and Zone 1 requires CT compensation (Yd11). In Figure 2-4 Zone 3 requires CT compensation (Dy1) and Zone 1 requires CT compensation (Dy1). Compensation can be achieved via an interposing transformer or within the software of the relay. The compensation accounts only for the phase shift of the power transformer. The setting in secondary ohms must take into account the position and ratios of the instrument transformers as well as the transformation ratio of the power transformer (GE Multilin 2011). In Figures 2-3 and 2-4 compensation is applied to the current transformer that is located on the other side of the transformer compared to the location of the voltage transformer. To convert primary ohms to secondary ohms one must multiply the primary ohms by the CT ratio/VT ratio.

The settings in secondary ohms in Figure 2-3 are:-

$$Z1 = (Z_T \text{ (at B)} + Z_L) (V_p/V_s)^2 (V_s/V_p) (\text{CT ratio}/\text{VT ratio}) \quad (2.7)$$

$$Z3 = Z_s (V_s/V_p) (\text{CT ratio}/\text{VT ratio}) \quad (2.8)$$

For the Zone 1 setting in Figure 2-3 shown above, the term $(V_p/V_s)^2$ is used to refer to the impedance on the secondary side of the transformer to the primary side. This is necessary since the VT is located on the primary side of the transformer, and the intended zone of protection is through the transformer. The term (V_s/V_p) caters for the change in the CT currents caused by the power transformer's ratio. This term corrects the value of the CT current relative to the position of the VT.

The settings in secondary ohms in Figure 2-4 are:-

$$Z3 = (Z_T \text{ (at A)} + Z_S) (V_s/V_p)^2 (V_p/V_s) (\text{CT ratio/VT ratio}) \quad (2.9)$$

$$Z1 = Z_L (V_p/V_s) (\text{CT ratio/VT ratio}) \quad (2.10)$$

Impedances from the secondary side of transformers are referred to the primary side by multiplying the secondary impedance by the square of the transformation ratio (Shepherd, Morton & Spence 1994). This is shown in Case-Study-Example 1, Chapter 5. Case-Study-Example 2, Chapter 5 shows a setting calculation where the CT and VT are located on either side of the power transformer and proves that the apparent distance measured by the relay is correct, with respect to the settings. In Case-Study-Example 1 the effect of the tap-changer has been neglected, but will be considered in Section 3.3.

Transformers used in the Eskom Transmission Grid are equipped with tap-changers. The typical tap-changer used consists of 17 taps. Tap number 5 is the nominal tap. The tapping range is usually -5% to +15%. Therefore maximum buck will be at tap number 1 and consequently the HV voltage will be at 1.05pu. Tap number 17 will be maximum boost and consequently the HV voltage will be at 0.85pu. The tap-changer causes the transformer ratio of the transformer to change by adding or subtracting turns in the HV winding. This action causes the impedance of the transformer to change. Some transformers operating at 400kV are equipped with a tap-changer having 13 taps. Here the tapping range is from +0% to +15%. Therefore this tap-changer only provides a boosting function.

2.2 Zones of Transformer Distance Protection

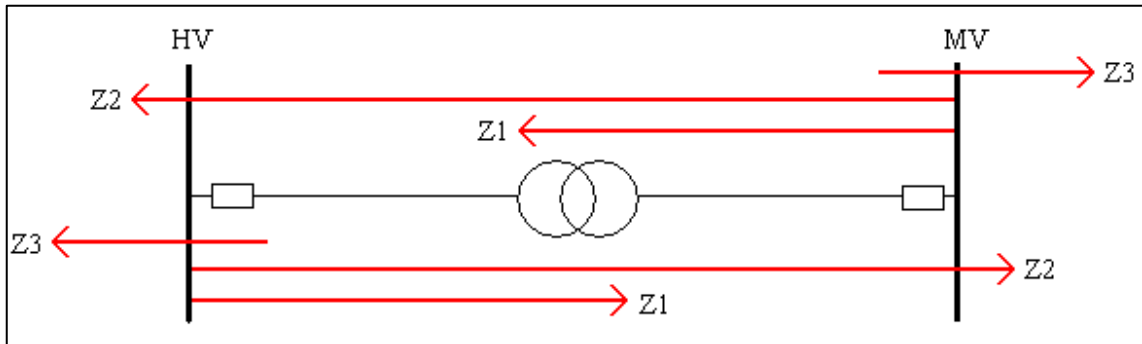


Figure 2-5: Distance protection zones when applied through transformers
(Cigré 2008)

Distance relays for transformer protection can be applied according to Figure 2-5 (Cigré 2008). The distance relays can be located on HV bus or MV bus. Zone 1 and Zone 2 are forward reaching zones and Zone 3 is a reversing reaching zone. The intention of Zone 1 is to provide backup to the transformers differential protection. Zone 1 can be set up to 70% of the transformers positive sequence impedance to operate instantaneously (Cigré 2008). As shown in Figure 2-5 Zone 1's instantaneous protection covering 70% of the transformer's impedance can be applied from both sides of the transformer in order to provide 100% instantaneous coverage (Herrmann 2005). Zone 2 and Zone 3 can be applied with time delay to provide backup protection for the HV and MV buses.

2.3 Fault Current Distribution through Delta/Star Transformers

Figure 2-6 shows the current distribution in a delta/star transformer during faults on the star side. For a 3-phase fault the current distribution is the same on both sides of the transformer. For a phase-to-phase fault there is a 2-1-1 current distribution on the delta side. During a single line to ground fault on the star side, currents flow on the delta side in two phases only, mimicking a phase-to-phase fault. Since the fault current distribution changes from the star side to the delta side or vice versa for asymmetrical faults it is essential that the protection IED simultaneously computes all fault loops (A-B, B-C, C-A, A-E, B-E and C-E) to determine if a fault exists within its zone of protection.

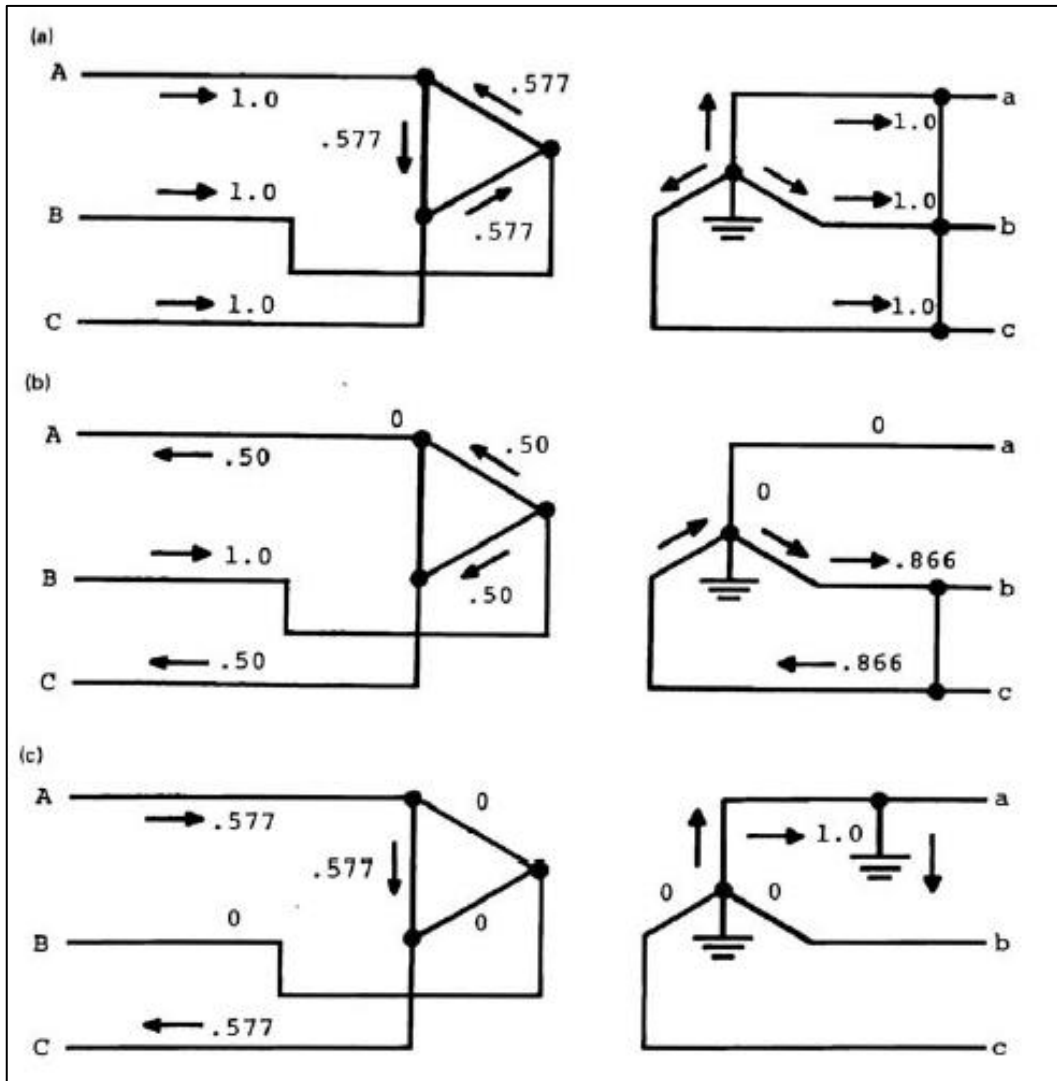


Figure 2-6: Fault current distribution in Delta/Star transformer (Ederhoff 2010)

2.4 Distance Measurement through Transformers

Table 2-1 and Table 2-2 show the formulae and the distance measured by the relay for various faults and transformer types (Cigré 2008). The distance relay is located on the LV side and the fault is on the HV side. In Tables 2-1 and 2-2 X_{1d} is the primary winding's (winding 1) positive sequence impedance and X_{2d} is the secondary winding's (winding 2) positive sequence impedance. Consequently $X_{1d} + X_{2d} = X_T$

X_T is the positive sequence impedance of the two winding transformer

X_{30} is the zero sequence impedance of the tertiary (third) winding

X_{10} is the zero sequence impedance of the primary (first) winding

X_n is the value of reactance inserted in the neutral of the system

Table 2-1: Formulae for Yyd and Yd11 transformers (Cigré 2008)

	Yyd Transformer Assuming $I_{0TR} = 0$ on LV Side	Yd11 Transformer
Phase-to-ground fault (A)	$\frac{VA}{IA_{TR}} = X_{1d} + X_{2d} + \frac{(X_{10} + X_{30} + 3X_n)}{2}$	$\frac{VA - VC}{IA_{TR} - IC_{TR}} = X_{1d} + X_{2d} + \frac{(X_{10} + 3X_n)}{2}$
Three-phase fault	$\frac{VA}{IA_{TR}} = X_{1d} + X_{2d}$ or $\frac{VA - VB}{IA_{TR} - IB_{TR}} = X_{1d} + X_{2d}$	$\frac{VA}{IA_{TR}} = X_{1d} + X_{2d}$ or $\frac{VA - VB}{IA_{TR} - IB_{TR}} = X_{1d} + X_{2d}$
Phase-to-phase fault (BC)	$\frac{VB - VC}{IB_{TR} - IC_{TR}} = X_{1d} + X_{2d}$	$\frac{VB}{IB_{TR}} = X_{1d} + X_{2d}$
Phase-to-phase-to-ground fault (BC to ground)	$\frac{VB - VC}{IB_{TR} - IC_{TR}} = X_{1d} + X_{2d}$	$\frac{VB}{IB_{TR}} = X_{1d} + X_{2d}$

Table 2-2: Formulae for Dy1 Transformer (Cigré 2008)

	Dy1 Transformer
Phase-to-ground fault (A)	$\frac{VA - VB}{IA_{TR} - IB_{TR}} = X_{1d} + X_{2d} + \frac{(X_G)}{2}$ Where: X_G = Value of the zero-sequence Impedance on delta HV side
Three-phase fault	$\frac{VA}{IA_{TR}} = X_{1d} + X_{2d}$ or $\frac{VA - VB}{IA_{TR} - IB_{TR}} = X_{1d} + X_{2d}$
Phase-to-phase fault (BC)	$\frac{VC}{IC_{TR}} = X_{1d} + X_{2d}$
Phase-to-phase-to-ground fault (BC to ground)	$\frac{VC}{IC_{TR}} = X_{1d} + X_{2d}$

From Tables 2-1 and 2-2 it can be concluded that only for the fault types (phase-to-phase, 3-phase and phase-to-phase-to-ground) where the formulae equates to $X_{1d} + X_{2d}$ can a correct distance to fault calculation be performed by the relay. For the single-phase-to-ground fault the relay measures a value different from X_T .

Accurate measurements of distance to fault through star/delta transformers are only possible for phase to phase loops (Ziegler 2008). The angle between the short-circuit current and the voltage in the faulted phase is close to 90° , since the transformer is mainly reactive. Correct distance measurement is possible through star/star transformers and autotransformers (Ziegler 2008).

In a GE D20 line distance relay the voltage and current applied to the phase distance element when reaching through delta/star or star/delta transformers is modified according to the vector group of the transformer. This results in accurate measurement through the transformer for phase-to-phase faults. If the transformer in Figure 2-1 had the vector group Yd1 and if the GE D30 relay was employed to provide Zone 1 protection as indicated, then the voltage transformer connection and the current transformer connection is set to Yd1. By implementing the Yd1 setting the currents and voltages shown in Table 2-3 are used in the phase distance element (GE Multilin 2011). Therefore, for a phase-to-phase fault on the secondary side of the transformer in Figure 2-1 the relay will calculate the apparent distance to fault using the equation 2.11.

$$Z_{\text{measured}} = \frac{\sqrt{3}V_A}{\frac{1}{\sqrt{3}}(2I_A - I_B - I_C)} \quad (2.11)$$

Table 2-3: Phase distance element input for Yd1 and Dy1 transformer (GE Multilin 2011)

Transformer Connection	Loop	Current Transformation	Voltage Transformation
Yd1	AB	$I_{AB_21P} = \frac{1}{\sqrt{3}}(2I_A - I_B - I_C)$	$V_{AB_21P} = \sqrt{3}V_A$
	BC	$I_{BC_21P} = \frac{1}{\sqrt{3}}(2I_B - I_A - I_C)$	$V_{BC_21P} = \sqrt{3}V_B$

	CA	$I_{CA_21P} = \frac{1}{\sqrt{3}}(2I_C - I_A - I_B)$	$V_{CA_21P} = \sqrt{3}V_C$
Dy1	AB	$\sqrt{3}I_A$	$\frac{1}{\sqrt{3}}(V_{AB} - V_{CA})$
	BC	$\sqrt{3}I_B$	$\frac{1}{\sqrt{3}}(V_{BC} - V_{AB})$
	CA	$\sqrt{3}I_C$	$\frac{1}{\sqrt{3}}(V_{CA} - V_{BC})$

Zimmerman and Roth (2005) have concluded that phase distance elements based on the Compensator Distance Element (not traditional phase element using phase-pairs) can accurately measure positive sequence impedance through star/delta and delta/star transformers. In this research investigation, single-line to ground faults were not simulated since a delta connection does not allow for the flow of zero sequence currents.

2.5 Zero Sequence Impedance of Transformers

Positive and negative sequence impedance values of transformers (which are static plant) are the same for three phase transformers. However the zero sequence impedance of a three phase transformer depends on the core construction of the transformer and the presence or absence of a delta winding (Heathcote 1998). In a star/delta transformer where the star winding is earthed, zero sequence currents can flow in the star winding and compensated circulating current flows in the delta winding (IEC 1997-10). In YNyn and auto transformers zero sequence currents are transformed through the transformer by the ampere-turn balance of the transformer (IEC 1997-10). In a 3-limb YNyn transformer the zero sequence impedance of the transformer is 90% to 95% of its positive sequence impedance. If the YNyn transformer had a 5-limb core, shell core or comprised of three single phase units then its zero sequence impedance will be equal to its positive sequence impedance. In a 3-limb core the construction does not provide an iron path for zero sequence flux. In these transformers the returning zero sequence flux path is through the air and tank (Heathcote 1998). In a 5-limb transformer the unwound outer limbs provide an iron path for zero sequence flux. Zero sequence flux produced by zero sequence current in each phase is co-phasal and therefore adds up at the bottom of the core. The flux produced by positive and negative sequence currents are balanced and summate to zero at the bottom of the core. Appendix 1 shows typical values of zero sequence impedances of transformers.

Autotransformers have lower series impedance than a conventional transformer (EPRI 2009). Appendix 4 shows the positive sequence impedance of transformers used in Eskom.

2.6 Tap-Changer and Transformer Inrush Currents

2.6.1 Transformer Magnetising Inrush Currents

A transformer is an inductive reactive electrical apparatus where the flux Φ should lag the voltage by 90 degrees. Therefore if the transformer is energised at the point where the voltage is zero then the flux should have been at -90 degrees and since $\sin(-90) = -1$ the flux should have been at its maximum negative value (Blackburn & Domin 2007). However let's assume that the transformer has no residual flux. At the end of the first half wave of the voltage the flux must be at its maximum positive value. Therefore the flux must start at zero and reach 2Φ in the first half wave of the voltage. To achieve this, the transformer draws a large magnetising inrush current. The magnitude on the inrush current can be up to 40 times the full load current of the transformer (Short 2005). If the transformer was previously energised then it should have residual flux Φ_R . This residual flux can have a positive or negative value. If the residual flux is positive then higher magnetising current is required to achieve $2\Phi + \Phi_R$ (Blackburn & Domin 2007). If the transformer was energised when the voltage was at its maximum point then the flux required at that moment would have been zero and no transient magnetising current will flow. Transformer magnetising inrush current occurs randomly and its prediction is almost impossible (Guzman, Altuve & Tziouvaras 2005). Various factors affect the value of the magnetising current apart from whether the transformer was energised at a point where the voltage was at its maximum value. Magnetising inrush can manifest itself during the following conditions ((Blackburn & Domin 2007):

1. Initial – Transformer is switched on after being disconnected.
2. Recovery – After a voltage dip the transformer draws a transient magnetising current when the voltage recovers to its normal value. The magnitude of the magnetising current depends on the severity of the voltage dip.
3. Sympathetic – Inrush current can flow in an energised transformer when a transformer in parallel is switched on.

The magnetising current has a high second harmonic content with respect to the fundamental frequency as shown in Table 2.4.

Table 2-4: Harmonics of the magnetising inrush current (Horowitz, Phadke & Niemira 2008)

Harmonic	$a_n I_{a1}$		
	$\alpha = 60^0$	$\alpha = 90^0$	$\alpha = 120^0$
2	0.705	0.424	0.171
3	0.352	0.000	0.086
4	0.070	0.085	0.017
5	0.070	0.000	0.017
6	0.080	0.036	0.019
7	0.025	0.000	0.006
8	0.025	0.029	0.006
9	0.035	0.000	0.008
10	0.013	0.013	0.003
11	0.013	0.000	0.003
12	0.020	0.009	0.005
13	0.008	0.000	0.002

When a transformer is energised from its primary side the transient magnetising inrush current appears only on the primary side which can result in differential protection for the transformer operating. Modern relays use second harmonic blocking/restraining methods to prevent the differential relay from operating (Zocholl, Guzman & Benmouyal. 2000). Differential relays use the percentage magnitude of 2nd harmonic current to differentiate between fault and transformer inrush conditions (GE 2014b). However the minimum percentage of second harmonic current in the inrush current decreases at higher flux density values. In other words since the core of new transformers is made from high grain orientated steel which can operate at high flux densities the percentage of second harmonic current in the inrush current will decrease (Mekic *et al.* 2006). For transformers operating at low flux densities 15% to 20% second harmonic restraint is used. For modern transformers operating at high flux densities 5% to 12% second harmonic restraint should be used (Mekic *et al.* 2006). Relays using 2nd harmonic blocking prevent operation of the differential element if the percentage of the 2nd harmonic current in the inrush current is greater than the setting (Basler Electric 2007). The magnetising inrush current phenomenon is not a fault condition and therefore distance relays applied for transformer protection must be stable during the inrush condition.

2.6.2 Distance Relay Response and Solutions to Inrush Currents

According to Mason (1956) the effect of magnetising inrush currents of transformers located at the remote ends of feeders has not affected performance of distance relays. Instantaneous forward reaching zones for line distance protection are not applied to overreach remote transformers. If zones with an intended delay are used to overreach remote transformers then the delay ensures that the magnitude of the inrush current has decreased below the pickup value of the distance relay (Masson 1956). However when a number of transformers are energised from the same line a line distance relay can operate due to the combined inrush currents (Perera & Kasztenny 2014).

According to Cigré (2008) distance elements overreaching transformers should be supervised with an undervoltage element set to 75-80% of the normal system voltage. In other words the distance element is only released when the voltage is below 75-80% of the normal system voltage. During inrush conditions the voltage does not collapse as much as when there is a solid fault. Distance relays that have inrush stabilisation capabilities will assess the value of the 2nd harmonic current to the fundamental and block/release the distance function. If the instantaneous zone is applied for transformer protection then the distance element should be supervised by an overcurrent element that is set higher than the maximum inrush current (Cigré 2008).

In Eskom the effects of transformer inrush conditions were not considered for distance relay settings (Teffo 2013). In Eskom an impedance relay located in the control room of the HV yard at power stations provides backup impedance protection for the generator transformer, generator and unit transformers. This relay needs to respond to Switch-On-To-Fault (SOTF) and Switch-on-to-Standstill (SOTSS) conditions. A SOTF condition will occur if earths used to create an equipotential zone during maintenance are left connected between line and earth. A SOTSS condition arises when the generator is energised from the HV yard. For generator-transformer distance applications the impedance setting in ohms for the relay to see through the transformer is large since the transformation ratio is large. The transformation ratio is typically 400kV/22kV for generator transformers. Teffo (2013) has shown that this high impedance setting results in the relay seeing an inrush condition in Zone 2 and therefore the relay needs to distinguish between SOTF, SOTSS and inrush conditions. However since the relay employed to provide backup distance protection for the generator transformer unit has harmonic filtering, 2nd harmonic current blocking will be used to prevent the distance

function from operating during inrush conditions. Teffo (2013) has also shown that in line bank applications the more transformers that are simultaneously energised the smaller will be the impedance seen by a line distance relay due to the inrush currents of all the transformers that were energised. In this case the distance relay used must have inrush stabilisation capabilities. According to Teffo (2013) the application of distance relays that do not have inrush stabilisation capabilities for generator transformer backup protection and line bank protection with many transformers in parallel should be studied.

Mooney and Samineni (2007) have stated that the filtering circuits in modern distance relays remove the harmonic currents from the CT and VT inputs before they are processed by the measuring elements. Therefore this filtering provides security for these relays from the 2nd harmonic current present during transformer exciting inrush currents. The 3rd harmonic content in inrush currents is too low to cause the operation of earth elements in distance relays (Mooney & Samineni 2007). Therefore only phase-to-phase distance elements can respond to transformer magnetising inrush currents. Recognition of inrush currents in numerical relays is advanced (Herrmann 2005).

Mooney and Samineni (2007) made the following recommendations when setting distance relays for transformer protection:

- a) If the instantaneous Zone 1 is employed then its reach should be reduced. Cigré (2008) suggests 70% of transformer impedance for the instantaneous Zone 1 protection.
- b) The distance elements should be supervised by overcurrent and under-voltage elements.

2.6.3 On-Load Tap-Changers

All power transformers used on the Eskom transmission and distribution systems incorporate a tap-changer. An on-load tap-changer adjusts the voltage ratio of the transformer by adding or removing tapping turns (ABB 2004). Tap-changers regulate the output voltage of the transformer depending on the system conditions. As the loading of the transformer increases the output voltage of the transformer decreases. If the loading of the transformer decreases the output voltage of the transformer increases. This is because a transformer has a volt drop (IX_T) which is determined by the current (I) passing through its windings and its leakage reactance (X_T). The primary voltage of the transformer will also fluctuate according to the

system conditions. Therefore the purpose of a tap-changer is to maintain constant secondary voltage as the primary voltage and its loading changes.

Three categories for voltage variation in transformers with tapplings are defined in IEC 60076-1 (IEC 1997-10). The three categories are as follows:

1. Constant flux voltage variation (CFVV).
2. Variable flux voltage variation (VFVV).
3. Combined voltage variation (CbVV).

In a tap-changer with CFVV the change in the HV tapping ensures that the volts per turn is kept constant as the HV voltage changes. Therefore as the HV voltage increases more turns are added to keep volts per turn constant. Also as the HV voltage decreases turns are removed to keep volts per turn constant (Heathcote 1998).

2.7 Conclusion

This chapter has shown how distance protection can be applied to power transformers. The position and ratio of the instrument transformers affects the settings. Fault current distribution is not the same on both sides of star/delta transformers. Therefore a phase-to-phase fault on one side of a power transformer can be measured accurately by an earth element located on the other side of the transformer. This will be shown in Chapter 4. The zero sequence impedance of a 3 phase transformer depends on whether the core construction is 3 limb or 5 limb. The phenomenon of transformer inrush current and the response of distance relays to inrush current were discussed. The subject of tap-changers was introduced. The effects of the tap-changer on settings for transformer distance protection are discussed in Section 3.3.

3 METHODOLOGY AND APPLICATION

3.1 Autotransformer basics and fault calculations

The current direction in the neutral of an autotransformer can reverse under certain conditions. The autotransformer zero sequence and positive sequence model can have a negative impedance. According to Zhang and Echeverria (n.d.) the negative impedance in the zero sequence affects the magnitude and direction of the current in the neutral of the autotransformer. Fault calculations are performed using the Z bus matrix method to calculate the voltages and currents at the relaying point for a phase-to-phase and a single-line-to-ground fault involving an autotransformer. These fault currents and voltages will be used in Section 3.2.

3.1.1 Autotransformers

The high voltage network in RSA (Republic of South Africa) is interconnected by the use of autotransformers. The system voltages that incorporate autotransformers in Eskom are 765kV, 400kV, 275kV and 220kV. In autotransformers a part of the high voltage winding is common with the medium voltage winding. Autotransformers are solidly earthed and have a tertiary delta connected winding. The purpose of the delta connected winding is to provide a low impedance path for third harmonic/zero sequence/earth fault currents or, in other words, a low reluctance path for third harmonic flux (Heathcote 1998). By providing a path for zero sequence currents to flow during unbalanced loading conditions the output voltage of the autotransformer becomes free of a third harmonic component. The tertiary delta connected winding is also called a stabilising winding. The tertiary delta connected winding is used to supply:

- Auxiliary transformers (example 22kV/400V);
- Compensation equipment;
- Rural feeders (at 22kV or 33kV).

The use of delta connected tertiary winding to supply rural feeders is not desirable since it extends the tertiary bay. A fault on the tertiary bay results in the HV and MV breakers opening in order to clear the fault. Where three single phase transformers are connected to form a three phase autotransformer, the delta connection is accomplished by the use of

cables. In these cases a Neutral Earthing Compensator (NEC) is employed. The rating of the tertiary winding must be adequate to carry the maximum circulating current during an earth fault on the secondary winding. The tertiary winding is commonly rated 1/3 of the primary and secondary windings (Heathcote 1998). The autotransformer consists of a series and common winding. The common winding is common to both the HV and MV winding as shown in Figure 3-1.

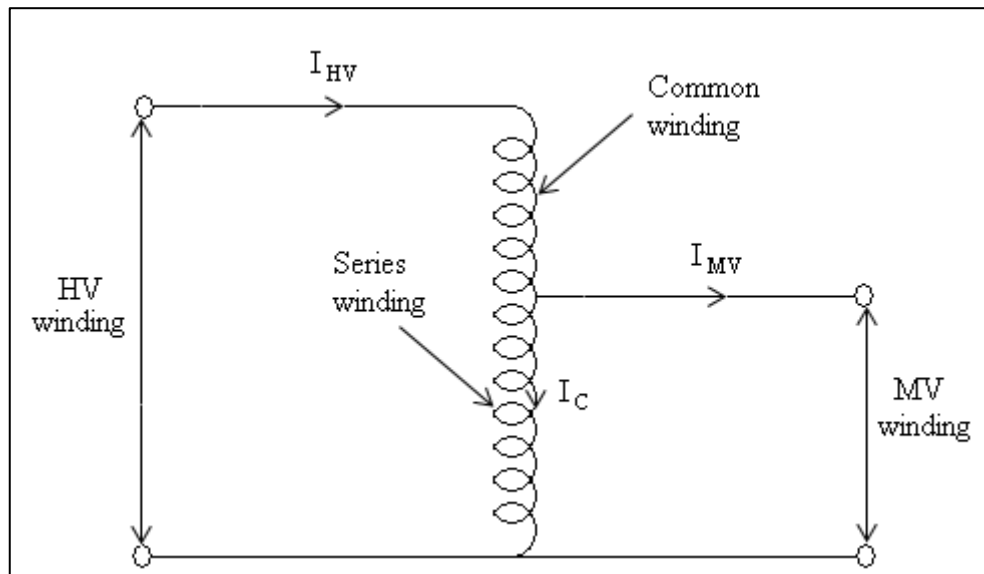


Figure 3-1: Schematic drawing of autotransformer (EPRI 2009)

Autotransformers can be constructed as a boosting autotransformer or a bucking autotransformer. In a bucking autotransformer the series winding opposes/bucks the output voltage and in the boosting autotransformer the series winding boosts the output voltage (Winders 2002).

From the short circuit impedance tests for an autotransformer we get Z_{ps} which is the impedance between the primary and secondary windings of the autotransformer.

$$Z_{ps} = Z_p + Z_s \quad (3.1)$$

This value is obtained by injecting the primary winding with a 3-phase voltage and with the secondary winding being short circuited. The delta tertiary winding is left open circuited.

With a voltmeter and ammeter connected to the supply voltage, Z_{ps} is calculated as follows:-

$$Z_{ps} = \frac{V_{\text{test}} \text{MVA}_P}{\sqrt{3} I_{\text{test}} \text{kV}_P^2} \times 100 \quad (3.2)$$

Where:

MVA_P – MVA of primary winding

kV_P – kV rating of primary winding

Similarly Z_{pt} and Z_{st} can be obtained, where:-

$$Z_{pt} = Z_p + Z_t = \frac{V_{\text{test}} \text{MVA}_P}{\sqrt{3} I_{\text{test}} \text{kV}_P^2} \times 100 \quad (3.3)$$

$$Z_{st} = Z_s + Z_t = \frac{V_{\text{test}} \text{MVA}_P}{\sqrt{3} I_{\text{test}} \text{kV}_P^2} \times 100 \quad (3.4)$$

All the above calculated values must then be converted to a common base. Case-Study-Example 3, Chapter 5 illustrates how Z_p , Z_s and Z_t are calculated from the short circuit test results of an autotransformer.

The values Z_p , Z_s and Z_t calculated in Case-Study-Example 3 are the positive sequence impedances of the auto transformer. Figure 3-2 shows the equivalent positive sequence impedance diagram of the autotransformer, where the respective impedance values have been converted to per unit values.

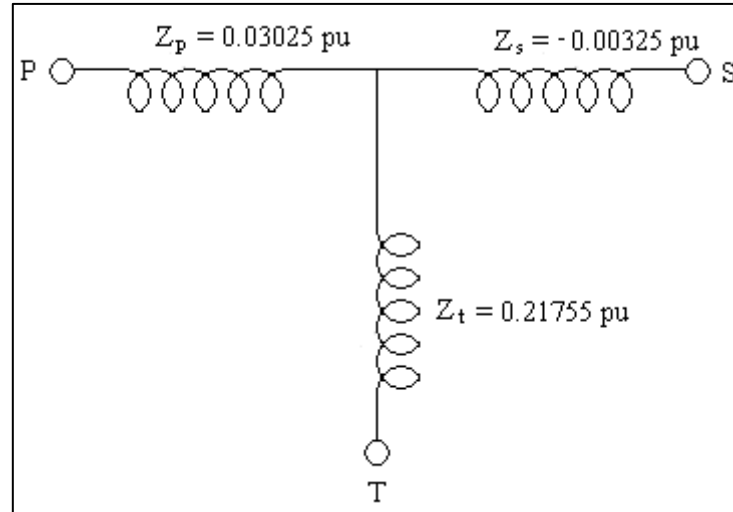


Figure 3-2: Equivalent positive sequence impedance diagram

The zero sequence tests for the transformer in Case-Study-Example 3 yielded the following results when converted to the 100MVA base:-

$$Z_{pt0} = 0.2383 \text{ pu} = Z_{p0} + Z_{t0}$$

$$Z_{st0} = 0.2038 \text{ pu} = Z_{s0} + Z_{t0}$$

$$Z_{ps0} = 0.027 \text{ pu} = Z_{p0} + Z_{s0} // Z_{t0}$$

Z_{pt0} - primary to tertiary zero sequence impedance

Z_{st0} - secondary to tertiary zero sequence impedance

Z_{ps0} - primary to secondary zero sequence impedance

Z_{p0} - primary winding zero sequence impedance

Z_{s0} - secondary winding zero sequence impedance

Z_{t0} - tertiary winding zero sequence impedance

From the above 3 equations it can be shown that (WSU 2014):-

$$\begin{aligned} Z_{t0} &= \sqrt{Z_{st0}(Z_{pt0} - Z_{ps0})} & (3.5) \\ &= \sqrt{0.2038(0.2383 - 0.027)} \\ &= 0.20752 \text{ pu} \end{aligned}$$

$$\begin{aligned}
 Z_{p0} &= Z_{pt0} - Z_{t0} & (3.6) \\
 &= 0.2383 - 0.20752 \\
 &= 0.03078\text{pu}
 \end{aligned}$$

$$\begin{aligned}
 Z_{s0} &= Z_{st0} - Z_{t0} & (3.7) \\
 &= 0.2038 - 0.20752 \\
 &= -0.00372\text{pu}
 \end{aligned}$$

Figure 3-3 shows the zero sequence equivalent circuit of an autotransformer.

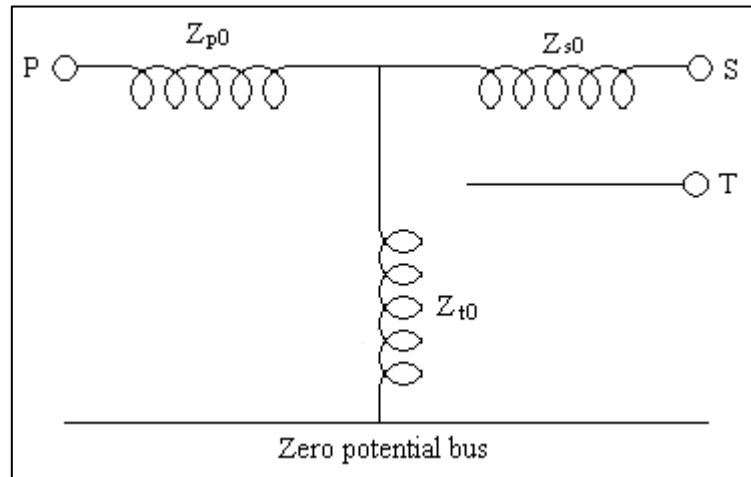


Figure 3-3: Zero sequence equivalent circuit of an autotransformer (GEC Alsthom Measurements Limited 1987)

Figure 3-4 shows the zero sequence model of a three winding transformer (GEC Alsthom Measurements Limited 1987). The link “a” is closed when the winding (primary, secondary or tertiary) is a star connection with its neutral earthed. The link “b” is closed when the winding (primary, secondary or tertiary) is a delta connection.

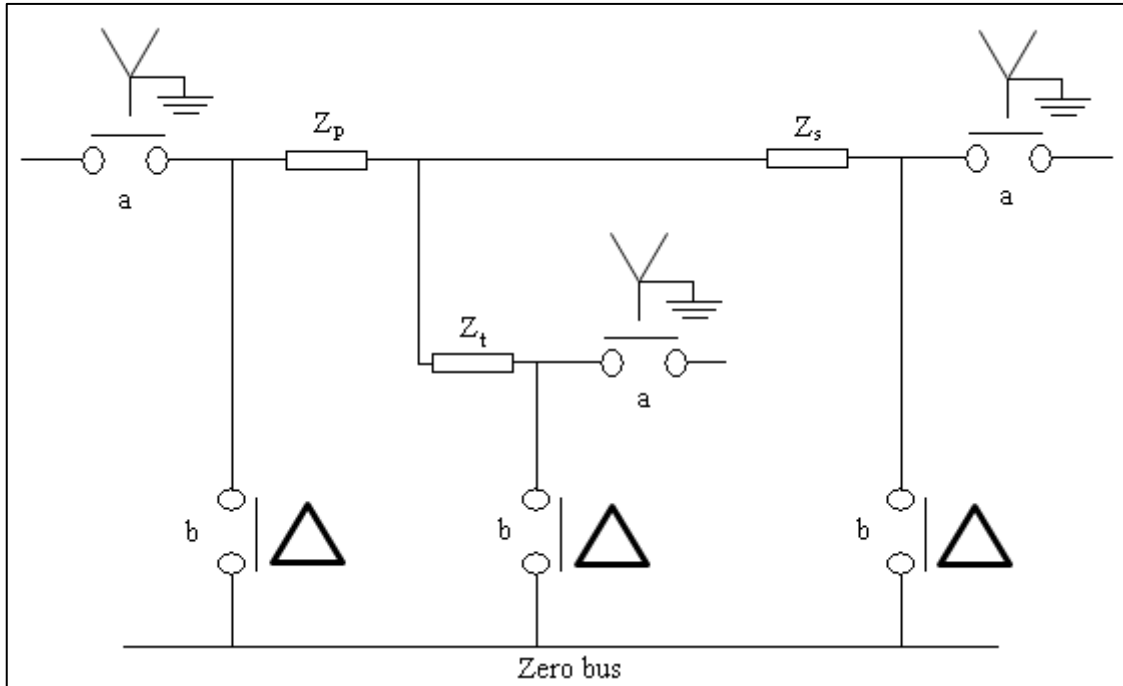


Figure 3-4: Zero sequence model of a 3 winding transformer (GEC Alsthom Measurements Limited 1987)

3.1.2 Review of zero sequence currents

According to Dr. C. L Fortescue (1918) any unbalanced 3-phase system can be resolved into two sets of balanced vectors (displaced by 120°) and one set of co-phasal vectors called symmetrical components. The positive sequence set consists of 3 vectors that are balanced and equal in magnitude and has a phase rotation which is the same as the original vectors. The negative sequence set consists of 3 vectors that are balanced and equal in magnitude and has a phase rotation which is opposite to that of the positive sequence set. The zero sequence set consists of three vectors that that are equal in magnitude (Grainger & Stevenson 1994). However there is a zero phase displacement between I_0 of the red, white and blue phase. Consequently zero sequence components can only exists in a four wire system where $3I_0$ flows from the unbalance into earth and returns via the neutral of any generator or transformer. When zero sequence currents flow up the neutral of a star/delta transformer, ampere turn balance is maintained by zero sequence currents circulating within the delta. When zero sequence currents (I_{r0} , I_{w0} , and I_{b0}) flow within a delta connected winding as part of the delta phase currents, they cannot exist in the line currents of the delta winding. The

following equations show how a delta winding traps zero sequence currents. The operator “a” is defined as follows:

$$a = 1 \angle 120^\circ$$

$$\begin{aligned}
 I_R &= I_r - I_w && \text{line current of delta winding} \\
 &= (I_{r_1} + I_{r_2} + I_{r_0}) - (I_{w_1} + I_{w_2} + I_{w_0}) \\
 &= I_{r_1} + I_{r_2} + I_{r_0} - I_{w_1} - I_{w_2} - I_{w_0} \\
 &= I_{r_1} + I_{r_2} - a^2 I_{r_1} - a I_{r_2} && I_{r_0} = I_{w_0} = I_{b_0}, I_{w_1} = a^2 I_{r_1} \text{ and } I_{w_2} = a I_{r_2} \\
 &= I_{r_1} (1 - a^2) + I_{r_2} (1 - a) && (3.8)
 \end{aligned}$$

From the above it is evident that the line currents of a delta connected winding do not contain zero sequence components when zero sequence currents flow within the delta.

3.1.3 Fault Calculation - Autotransformer (Line to Ground - MV side)

Case-Study-Example 4, Chapter 5 shows how fault calculation is performed for a single-line-to-ground fault located on the MV side of an autotransformer.

3.1.4 Fault Calculation - Autotransformer (Line to Ground - HV side)

Case-Study-Example 5, Chapter 5 shows how fault calculation is performed for a single-line-to-ground fault located on the HV side of an autotransformer.

For faults on the HV side of autotransformers, the direction of the current in the neutral of the autotransformer will reverse if the MV winding zero sequence reactance, which has a negative value, has a greater magnitude than the MV network zero sequence source reactance magnitude (absolute). Therefore the neutral current of an autotransformer is not appropriate for polarising (Blackburn & Domin 2007). Figure 5-8 shows the autotransformer from Case-Study-Example 3 incorporated in a network where the source impedances are converted to the 100MVA base for both the 400kV and 132kV sides. However in Case-Study-Example 5 the fault calculation is performed for a HV fault and the MV network zero sequence source reactance is lower in magnitude (absolute) than the MV winding zero sequence reactance.

3.1.5 Z Bus Method - Autotransformer (Line to Line Fault - MV side)

Case-Study-Example 6, Chapter 5 shows how fault calculation is performed for a line-to-line-fault located on the MV side of an autotransformer, using the Z bus method.

3.1.6 Z Bus Method - Autotransformer (Line to Ground Fault - MV side)

Case-Study-Example 7, Chapter 5 shows how fault calculation is performed for a single-line-to-ground fault located on the MV side of an autotransformer, using the Z bus method.

3.2 Distance Relays

In this subsection a brief introduction is given to the mho and quadrilateral characteristics employed in distance relays. The equations that conventional protection relays use to calculate the measured line impedance are also discussed. The voltages and currents calculated in subsections 3.1.5 and 3.1.6 are used to calculate the measured impedance seen by the distance relay.

3.2.1 Mho Characteristic

The most well known characteristic used in distance relays is the mho characteristic. The mho characteristic is a circle where the circumference passes through the origin of the X-R diagram and is therefore inherently directional. Figure 3-5 below shows the impedance diagram of a self-polarised mho. A self-polarised mho is a characteristic where the voltage of the faulted phase is used for polarisation.

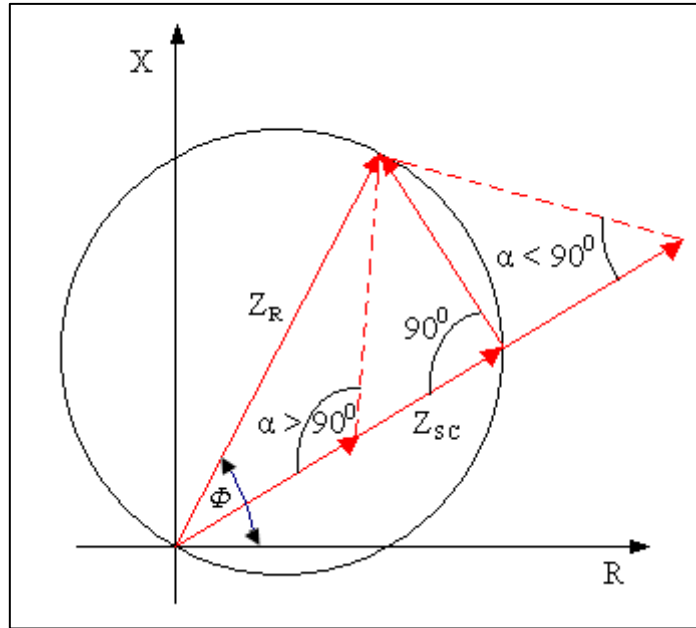


Figure 3-5: Self-polarised mho-impedance diagram (Ziegler 2008)

In Figure 3-5 Z_R is the line replica impedance which is the relay setting in secondary ohms. It determines the zone reach settings and is the diameter of the mho characteristic (Ziegler 2008). The angle Φ is the relay characteristic angle (RCA), which is usually the impedance angle of the protected line.

$\Phi = \tan^{-1} X/R$ (GE 2014a), Where X and R are the line reactance and line resistance respectively. Therefore Z_R matches the line impedance and is consequently called the line replica impedance.

Z_{SC} is the measured impedance from the relay location to the point of fault. Z_{SC} is also called the apparent impedance. Based on the six fault loops, numerical distance relays calculate Z_{SC} according to Table 3-1 (Perez 2006).

Table 3-1: Apparent impedance seen by self-polarised distance relays

Fault	Apparent Impedance (Z_{SC})
A-B	$(V_A - V_B) / I_A - I_B$
B-C	$(V_B - V_C) / I_B - I_C$
C-A	$(V_C - V_A) / I_C - I_A$
A-E	$V_A / (I_A + k_0 \cdot I_{res})$
B-E	$V_B / (I_B + k_0 \cdot I_{res})$
C-E	$V_C / (I_C + k_0 \cdot I_{res})$

A distance relay under-reaches when the apparent impedance seen by the relay is greater than the actual impedance to fault (Alstom 2011). A distance relay over-reaches when the apparent impedance seen by the relay is smaller than the actual impedance to fault (Alstom 2011).

k_0 is a relay setting called the residual compensation factor

I_{res} is the residual current, $I_{res} = (I_A + I_B + I_C)$ (3.9)

$$k_0 = \frac{Z_0 \text{ LINE} - Z_1 \text{ LINE}}{K \times Z_1 \text{ LINE}} \quad (3.10)$$

$K = 1$ or 3 , which is determined by the relay manufacturer (Andrichak & Alexander n.d.).

Relays measure the positive sequence impedance of the line. During a single line to earth fault, current flows through earth. Without residual current compensation the relay will measure the complete loop impedance i.e. from the relaying point to the fault and back to the relay via earth. Therefore, in order for the relay to measure the positive sequence impedance from its location to the fault, residual current compensation is required. Different relay manufacturers have named this residual current compensation factor differently, for example, K_N , K_0 , K_E , K_G , K_{ZN} , RE/RL, XE/XL and Z0/Z1 (Verzosa n.d.). In some relays the k_0 factor can be set independently for each zone.

The voltage diagram shown in Figure 3-6 is the result of the vectors in the impedance diagram being multiplied by I_{sc} .

For Phase to Phase faults:

$$I_{sc} = I_{ph1} - I_{ph2} \quad (3.11)$$

For single line to ground faults:

$$I_{sc} = I_{ph1} - k_0 \cdot I_{res} \quad (3.12)$$

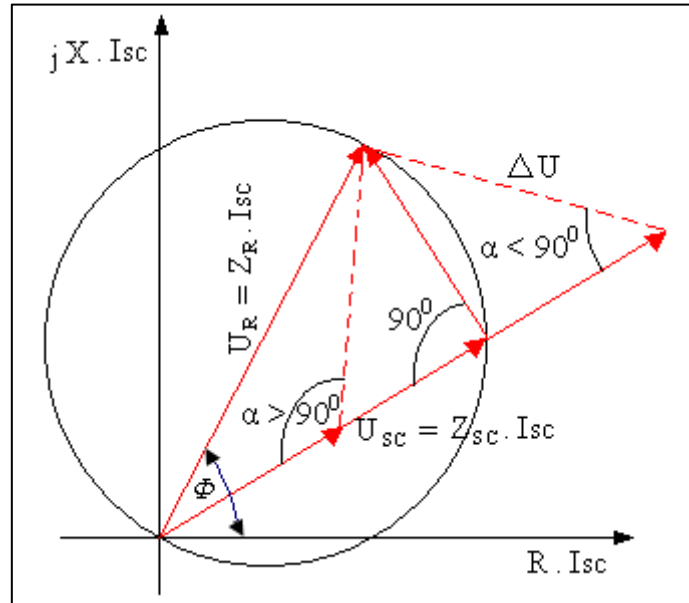


Figure 3-6: Self-polarised mho-voltage diagram (Ziegler 2008)

The numerical subtraction of the vectors U_R and U_{sc} results in the difference voltage ΔU . The points on the voltage diagram where the angle between ΔU and U_{sc} equals to 90° results in a circular characteristic. For points within the circle α is greater than or equal to 90° . Points within the circle corresponds to internal faults or, in other words, faults within the zone reach setting of the mho characteristic. External faults will have an angle α that is less than 90° (Ziegler 2008).

The mho characteristic is usually implemented using an angle comparator. In Figure 3-7 S1 is the operating quantity and S2 is the polarising or reference quantity. The operating quantity (S1) is ΔU and the polarising quantity (S2) is the voltage measured across the faulted phase (V_{pol}) (Perez 2006). For the mho characteristic a cosine comparator is used since $\cos 90^\circ = 0$ (Schweitzer & Roberts 1993). The operating quantity (S1) and the complex conjugate of the polarising quantity (S2) are applied to the phase comparator. If the real part of $S1 \cdot S2^*$ is equal to zero then the point is on the circular characteristic. If the real part of $S1 \cdot S2^*$ is greater than zero then the point is inside the circular characteristic. If the real part

of $S1.S2^*$ is less than zero then the point is outside the circular characteristic (Schweitzer & Roberts 1993). This relationship is shown below.

Let $S1 = A \angle \varepsilon$

and $S2 = B \angle \beta$

Then $\text{Re}(S1S2^*) = |A||B|\cos(\varepsilon - \beta)$

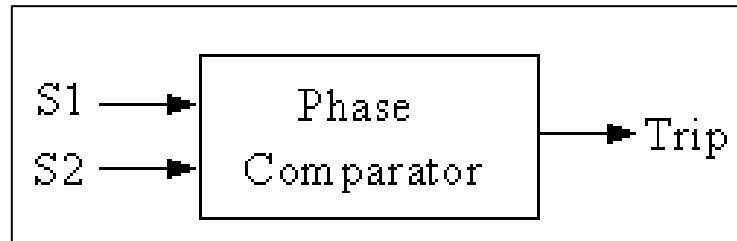


Figure 3-7: Circular phase comparator (Perez 2006)

Table 3-2 shows ΔU and V_{pol} for a self-polarised mho characteristic

Table 3-2: ΔU and V_{pol} for a self-polarised mho characteristic

Fault	ΔU	V_{pol}
A-B	$(I_A - I_B).Z_R - (V_A - V_B)$	$V_A - V_B$
B-C	$(I_B - I_C).Z_R - (V_B - V_C)$	$V_B - V_C$
C-A	$(I_C - I_A).Z_R - (V_C - V_A)$	$V_C - V_A$
A-E	$(I_A + k_0 \cdot I_{res}) Z_R - V_A$	V_A
B-E	$(I_B + k_0 \cdot I_{res}) Z_R - V_B$	V_B
C-E	$(I_C + k_0 \cdot I_{res}) Z_R - V_C$	V_C

From Table 3-2 above one can clearly see that for a close-in-fault $V_{pol} = 0$. The self-polarised mho characteristic therefore has a dead zone, since the characteristic passes the origin in the impedance diagram (Ziegler 2008). During zero-volt fault or faults with very low short-circuit voltage it is not possible for the self-polarised mho to securely determine whether the fault is in the forward or reverse direction. Since the low short-circuit voltage is close to the boundary of the characteristic, the pick-up time of the relay increases as the relay continues to measure repeatedly in order to make the decision whether to trip or not (Ziegler 2008).

Cross-polarised relays add a percentage of a healthy phase voltage to the faulted phase in order to make the directional decision for close-in-faults. Table 3-3 shows the inputs to a fully cross-polarised mho relay, where the faulted phase is not used for polarisation in each of the six measurement loops.

Table 3-3: Inputs for cross-polarised distance relay

Fault	ΔU	V_{pol}
A-B	$(I_A - I_B) \cdot Z_R - (k_c \cdot V_C)$	$k_c \cdot V_C$
B-C	$(I_B - I_C) \cdot Z_R - (k_a \cdot V_A)$	$k_a \cdot V_A$
C-A	$(I_C - I_A) \cdot Z_R - (k_b \cdot V_B)$	$k_b \cdot V_B$
A-E	$(I_A + k_0 \cdot I_{res}) Z_R - k_{bc} \cdot (V_B - V_C)$	$k_{bc} \cdot (V_B - V_C)$
B-E	$(I_B + k_0 \cdot I_{res}) Z_R - k_{ca} \cdot (V_C - V_A)$	$k_{ca} \cdot (V_C - V_A)$
C-E	$(I_C + k_0 \cdot I_{res}) Z_R - k_{ab} \cdot (V_A - V_B)$	$k_{ab} \cdot (V_A - V_B)$

k_0 is the residual compensation factor, I_{res} is the residual current k_a, k_b , etc. Are relay design constants. (Perez 2006)

The voltages used for polarising in Table 3-3 are similar to the 90° quadrature connection employed in overcurrent directional relays. For the fault loop A-B, the magnitude and phase angle of V_C is modified so that it equals $V_A - V_B$ prior to a fault occurring in that particular loop (Ziegler 2008). Similarly, V_{pol} for the other measurement loops are calculated. The effect of cross-polarisation on mho characteristics results in the circle enclosing the origin for forward faults and therefore has more resistive reach than a self-polarised mho. The cross-polarised mho characteristic does not expand for reverse faults (GEC Alstom Measurements Limited 1987).

3.2.2 Quadrilateral Characteristic

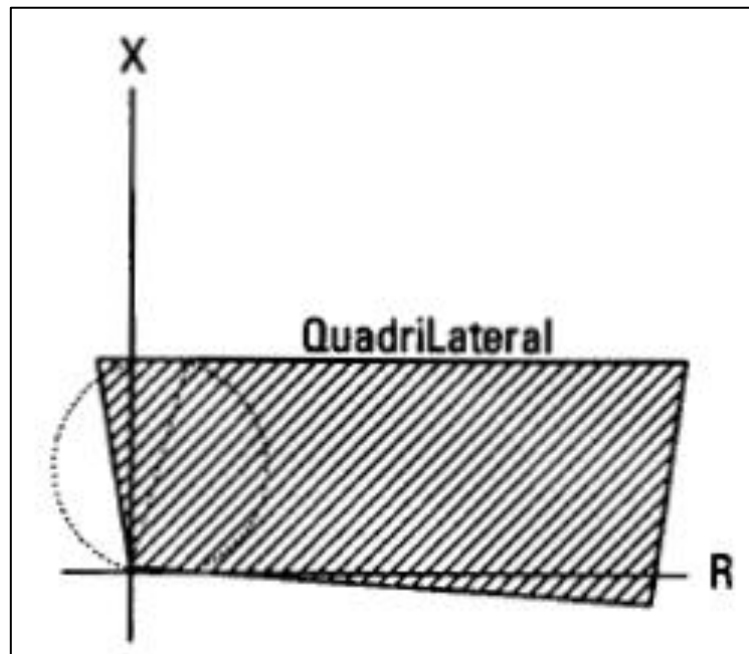


Figure 3-8: Quadrilateral characteristic (Andrichak & Alexander n.d.)

The quadrilateral characteristic requires four tests (Schweitzer & Roberts 1993):

- Reactance test (top line);
- Positive and negative resistance test (sides);
- Directional test (bottom).

Therefore four separate comparators are used to create the quadrilateral characteristic. A quadrilateral characteristic is shown in Figure 3-8. This characteristic is frequently used for single line to ground faults. The resistance and reactance reaches can be set independently (Ziegler 2008).

3.2.3 Impedance Measurement – Phase to Phase Fault

During phase to phase and 3-phase faults, impedance measurement to fault from the relay point is achieved by providing each phase-to-phase element with its corresponding phase to phase voltage and difference in phase currents (GEC Alsthom Measurements Limited 1987). This approach eliminates the dependence of the measured value on the source impedance.

The following derivation with the aid of Figure 3-9 shows how measurement for 3-phase and phase-to-phase faults is achieved.

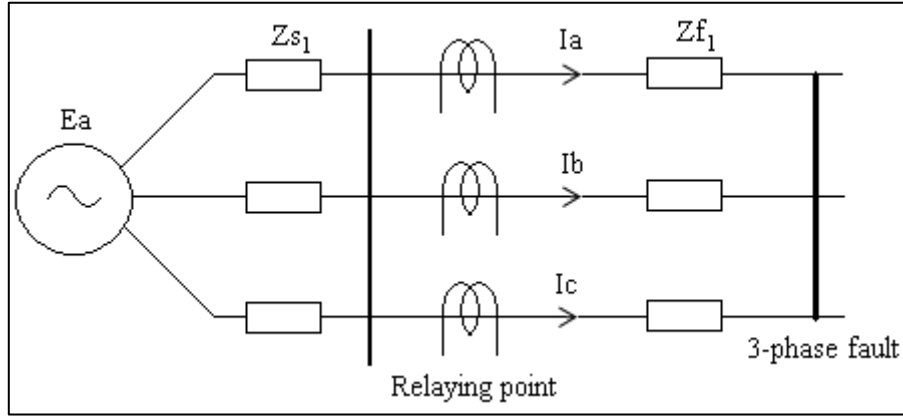


Figure 3-9: Impedance measurement – 3-phase fault (Alworthy 1999)

A 3-phase fault is a symmetrical fault and consists only of positive sequence components.

$$I_a = I_{a1} \quad (3.13)$$

$$V_{ab} = V_a - V_b = V_a - a^2 V_a = V_a(1 - a^2) \quad (3.14)$$

$$Z_{\text{measured}} = \frac{V_{ab}}{I_{\text{measured}}} = Z_{f1} \quad (3.15)$$

$$\begin{aligned} I_{\text{measured}} &= \frac{V_{ab}}{Z_{f1}} = \frac{V_a(1 - a^2)}{Z_{\text{measured}}} & (3.16) \\ &= \frac{(1 - a^2)(E_a - Z_{s1}I_a)}{Z_{f1}} \\ &= \frac{(1 - a^2)(I_a(Z_{s1} + Z_{f1}) - Z_{s1}I_a)}{Z_{f1}} \\ &= \frac{(1 - a^2)(I_a Z_{s1} + I_a Z_{f1} - Z_{s1}I_a)}{Z_{f1}} \\ &= \frac{(1 - a^2)(I_a Z_{f1})}{Z_{f1}} \\ &= I_a(1 - a^2) \\ &= I_a - I_b \end{aligned}$$

Therefore, $Z_{\text{measured}} = \frac{V_a - V_b}{I_a - I_b}$ (this also applies for phase to phase faults)

The impedance measured by a phase to phase element of a distance relay using the above equation can be proven using the currents and voltages calculated for Bus 2 in Case-Study-Example 6 of Section 3.1.5. Figure 3-14 shows the fault at Bus 4 and if the relaying point was at Bus 2 then the relay will measure the following impedance:-

$$\begin{aligned}
 Z_{\text{measured}} &= \frac{V_b - V_c}{I_b - I_c} & (3.17) \\
 &= \frac{(135.562 \angle -148.34^\circ)kV - (135.562 \angle 148.34^\circ)kV}{(1644.829 \angle 180^\circ) - (1644.829 \angle 0^\circ)} \\
 &= (43.26 \angle 90^\circ)\Omega
 \end{aligned}$$

From Case-Study-Example 3 the percentage impedance of the autotransformer is 13.48%.

$$\begin{aligned}
 Z_{\text{ps_actual}} &= 0.1348 \times \frac{400^2}{500} & (3.18) \\
 &= 43.14 \Omega
 \end{aligned}$$

Therefore the relay will measure the correct distance to fault.

3.2.4 Impedance Measurement – Single-Line-to-Ground Fault

During a single-line-to-ground fault, the voltage drop from the relaying point to the fault is not a simple product of the phase current and the line impedance (GEC Alstom Measurements Limited 1987). This is because the value of the fault current is affected by the number of earthed star points, type of earthing, and the positive, negative and zero sequence impedances of the fault loop. The voltage drop from the relaying point to the fault is the sum of the positive, negative and zero sequence voltages (GEC Alstom Measurements Limited 1987). The following derivation shows the impedance measured by a distance relay for a single-line-to-ground fault.

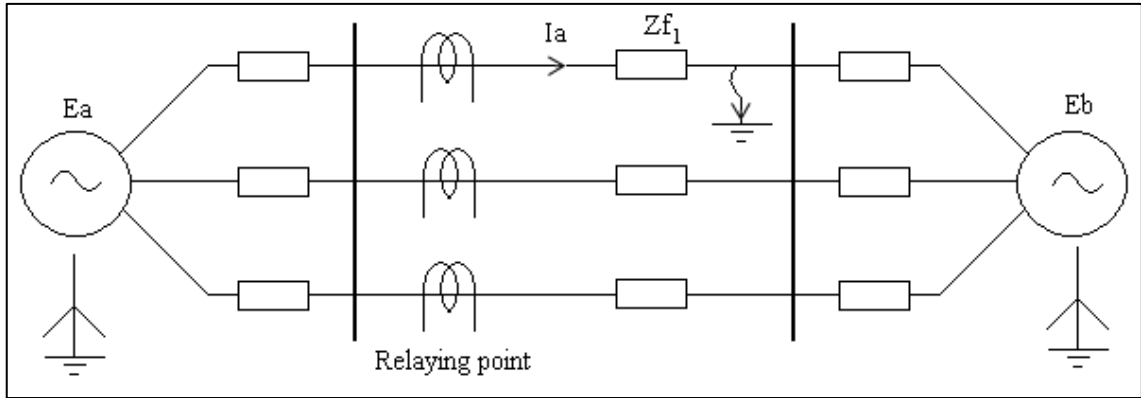


Figure 3-10: Impedance measurement – single-line-to-ground fault (Alworthy 1999)

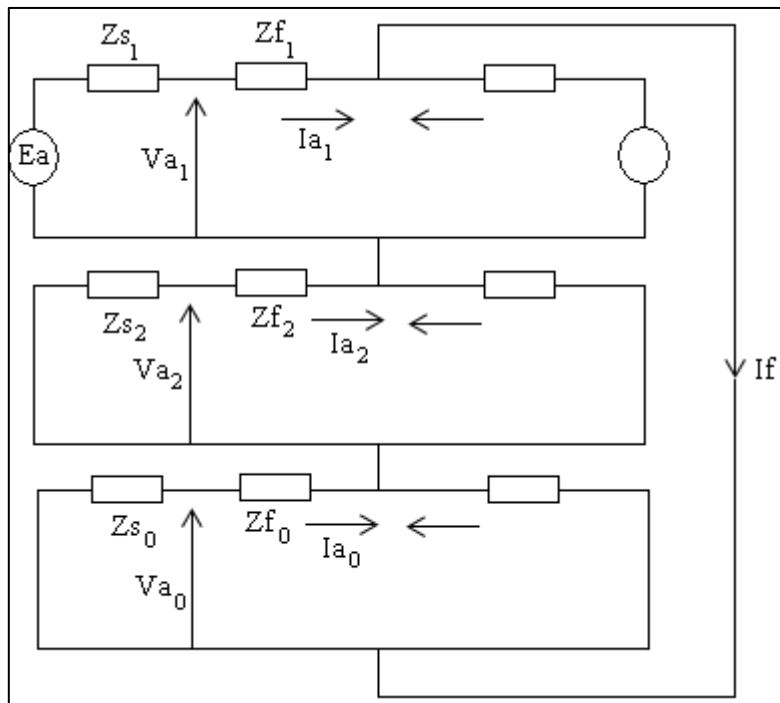


Figure 3-11: Impedance measurement – single-line-to-ground fault sequence diagram (Alworthy 1999)

For Figure 3-10 the voltage at the fault is zero. Positive, negative and zero sequence currents also flow from the right hand side source (E_b) into the fault. The values of these currents can be calculated, which has been shown in Section 3.1. For the fault loop shown in Figure 3-11 and by using Kirchoff's voltage law the following equation is obtained (Alworthy 1999).

Z_{f1} , Z_{f2} and Z_{f0} are the positive, negative and zero sequence impedances respectively of the line.

$$V_{a1} - I_{a1}Z_{f1} + V_{a0} - I_{a0}Z_{f0} + V_{a2} - I_{a2}Z_{f2} = 0$$

$$V_{a1} + V_{a2} + V_{a0} = V_a = Z_{f1} \left(I_{a1} + I_{a2} + I_{a0} \frac{Z_{f0}}{Z_{f1}} \right) \quad Z_{f1} = Z_{f2} \text{ for lines}$$

$$I_{a1} + I_{a2} + I_{a0} = I_a \text{ or } I_{a1} + I_{a2} = I_a - I_{a0}$$

$$\begin{aligned} V_a &= Z_{f1} \left(I_a - I_{a0} + I_{a0} + I_{a0} \left(\frac{Z_{f0}}{Z_{f1}} - 1 \right) \right) \quad (3.19) \\ &= Z_{f1} \left(I_a + I_{a0} \left(\frac{Z_{f0}}{Z_{f1}} - 1 \right) \right) \end{aligned}$$

The relay's neutral element will measure the residual current (I_r), since this element is situated in the residual connection of the current transformers. Figure 3-12 below shows the residual connection of CT's to a digital relay. I_r in Figure 3-12 is the residual current. The 'a' phase element of the relay will measure the current I_a .

$$\text{Now, } I_r = 3I_{a0} \quad (3.20)$$

$$V_a = Z_{f1} \left(I_a + \frac{I_r}{3} \left(\frac{Z_{f0}}{Z_{f1}} - 1 \right) \right) \quad (3.21)$$

$$k_0 = \frac{1}{3} \left(\frac{Z_{f0}}{Z_{f1}} - 1 \right) = \frac{Z_{f0} - Z_{f1}}{3Z_{f1}} \quad (3.22)$$

k_0 is called the residual compensation factor or 'k' factor.

$$V_a = Z_{f1} (I_a + I_r k_0) \quad (3.23)$$

$$\text{Therefore, } Z_{\text{measured}} = \frac{V_a}{I_a + I_r k_0} \quad (3.24)$$

According to ABB (2011b) the phase to earth loop impedance can also be calculated, using the following equation:-

$$Z_{\text{measured}} = \frac{V_a}{I_a} \quad (3.25)$$

This equation was also suggested for impedance measurement through transformers in Tables 2-1 and 2-2.

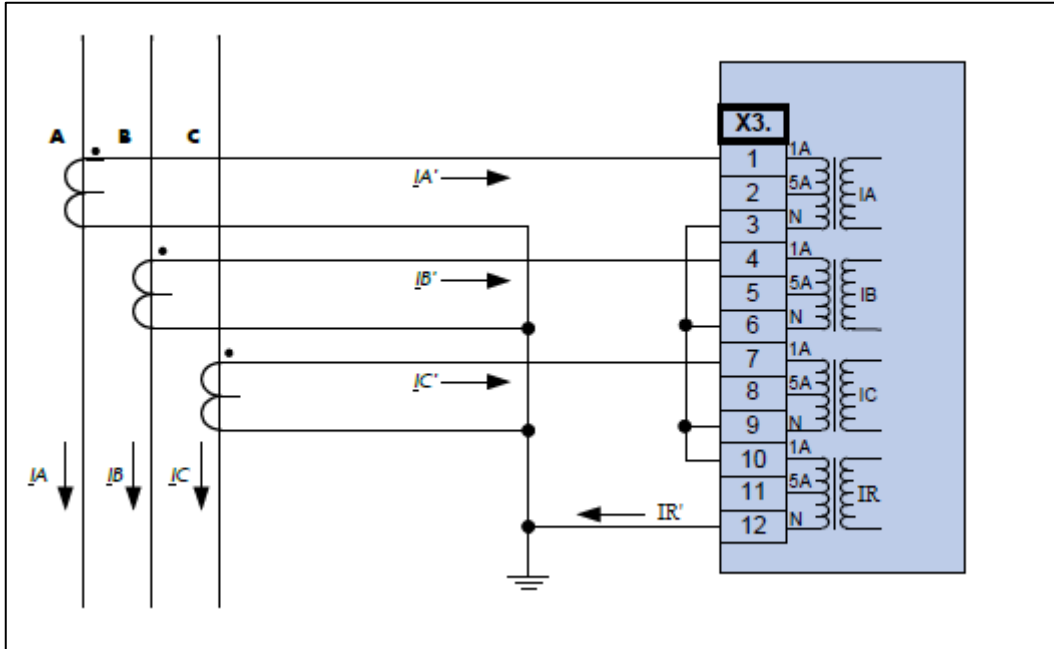


Figure 3-12: Residual connection of CTs (Eaton 2014)

3.2.5 Impedance Measurement – Line-to-Ground Fault through Autotransformer

The equation for the residual compensation factor or ‘k’ factor that measures the autotransformer’s positive sequence impedance Z_{Tps} for a single line to ground fault through the autotransformer is shown below (Ziegler 2011):-

$$k_0 = \frac{Z_{0 \text{ total}} - (Z_{Tps} + Z_{1 \text{ line}})}{3 \times Z_{Tps}} \quad (3.26)$$

$Z_{1 \text{ line}}$ is the positive sequence impedance of the line on the secondary side of the transformer.

$$Z_{0 \text{ total}} = Z_{p0} + \frac{Z_{s0} (Z_{1 \text{ Source}} + Z_{p0} + Z_{t0})}{Z_{t0}} \quad (3.27)$$

Where $Z_{1 \text{ Source}}$ is the total positive sequence source impedance up to the autotransformer. Therefore $Z_{0 \text{ total}}$ depends on the source impedance.

The impedance measured by a phase to ground element of a distance relay using the above equations can be proved using the currents and voltages calculated for Bus 2 in Case-Study-Example 7 of Section 3.1.6. Figure 5-17 shows the fault at Bus 4 and if the relaying point was at Bus 2 then the relay will measure the following impedance:-

$$\begin{aligned} Z_{0 \text{ total}} &= 0.03078 + \frac{-0.00372(0.033 + 0.016 + 0.03078 + 0.20752)}{0.20752} \quad (3.28) \\ &= 0.02563 \end{aligned}$$

Figure 5-15 and Figure 5-18 show the values used in the above equation.

$$\begin{aligned} k_0 &= \frac{0.02563 - 0.027}{3 \times 0.027} \quad (3.29) \\ &= -0.01691 \end{aligned}$$

Note that in the above equation the positive sequence impedance of the line is not included since in this case study the intention is to provide 100% protection for the autotransformer only.

$$\begin{aligned} \text{Therefore, } Z_{\text{measured}} &= \frac{V_a}{I_a + I_r k_0} \quad (3.30) \\ &= \frac{70206}{1725.668 \angle -90^\circ + 1725.668 \angle -90^\circ (-0.01691)} \\ &= 41.38 \Omega \end{aligned}$$

In the equation above I_r is assumed to be equal to I_a since only fault current is assumed to flow. However if the relay connection points 10 and 12 in Figure 3-12 are swapped then the residual element will measure $I_r = 1725 \angle 90^\circ$. In this case:-

$$Z_{\text{measured}} = \frac{V_a}{I_a - I_r k_0} \quad (3.31)$$

However every relay manual will indicate how the CT's should be connected, based on the algorithm it uses.

3.2.6 Distance Relay Settings

In the Eskom network Zone 1 is usually set to 80% of the line's positive sequence reactance. For distance relays employed on lines the Zone 1 tripping is instantaneous. Zone 1 can be set lower than 80% in certain conditions such as series compensated lines, teed lines, traction feeders, etc. Zone 1 is the under-reaching zone and Zone 2 is the over-reaching zone. Zone 2 has a minimum setting of 120% of the lines' positive sequence reactance. Zone 2 must not over-reach transformers in parallel at the remote substation and the Zone 1 setting of the shortest line at the remote substation. The delay for Zone 2 operation is usually set at 400ms. Zones 3, 4 and 5 are applied as backup zones of protection. The number of backup zones depends on the type of relay. Zone 1 and Zone 2 are forward reaching zones. Zone 3 can be set as a forward or reverse zone. Zone 3 is set with a standard delay time of 1s. However in order to achieve coordination the Zone 3 time can be set to 5s. The reverse reaching Zone 3 element of local HV feeders are sometimes employed to provide backup for the MV buszone protection. In certain areas of the network where the fault level is low, and many transformers are connected in parallel, the overcurrent protection of the transformer does not respond to un-cleared MV multiphase busbar faults since the current contribution to the fault by each transformer is lower than its overcurrent setting. Note that in Eskom Transmission the overcurrent setting is twice the full load current of the transformer. This condition is shown in Figure 3-13 below. Note that if the transformer's protection relay had distance functions it could be used to backup the MV busbar protection.

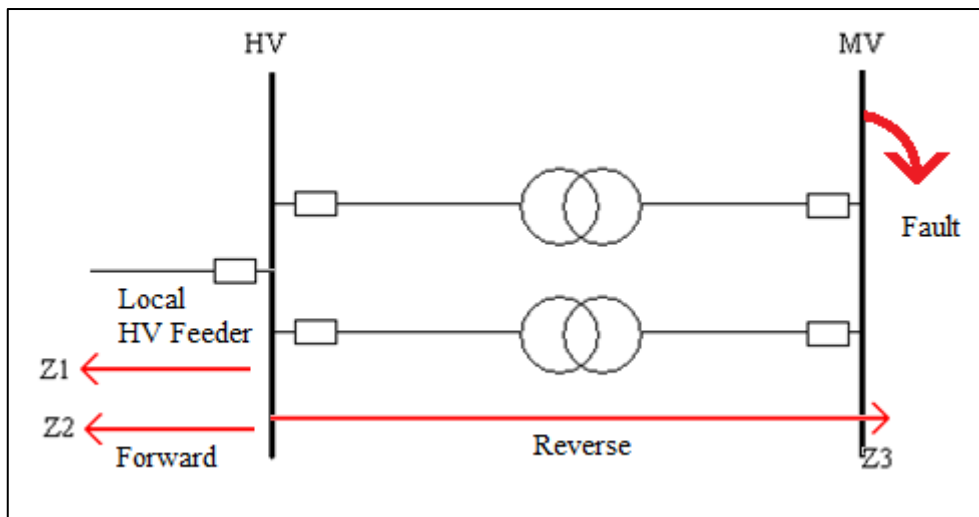


Figure 3-13: Zone 3 for local HV feeder

With regards to local backup for the HV Busbar protection (Figure 3-13), Jewalika (2008) has suggested using a reversing reaching zone at the HV feeder to trip the HV bus-section or HV bus coupler before the remote end feeder trips in Zone 2 time. The opening of the bus-section/coupler will prevent a total shutdown in the event of HV busbar protection failure.

Shukri, Hairi & Mohd Zin (2005) have recommended the following settings when applying distance protection for an autotransformer:

- a) Zone 1 should set to 80% of the transformer's impedance.
- b) Zone 2 should be set to 120% of the transformer's impedance.
- c) Forward reaching Zone 3 should be set to 120% of the longest adjacent line in order to provide backup for all remote busbars.
- d) Reverse reaching Zone 3 of transformer IED should be set to 20% of the transformer's impedance to provide backup for the local busbar.
- e) The transformer's impedance should take into account the effect of the tap-changer.

3.3 Effects of Tap-Changer on Settings for Transformer Distance Protection

The impedance of a transformer will change based on its tap position (Heathcote 1998). The minimum impedance for a 400/132/22kV transformer is specified as 13% in Eskom (see Appendix 4). The maximum and minimum deviation for the percentage impedance of Eskom transformers is also specified as shown in Table 3-4. The maximum impedance specified for the 400/132/22kV autotransformer which has a voltage ratio above 2.5 is 14.25%. The actual percentage impedances and ohmic values at Taps 1 and 13 of an actual 400/132/22kV transformer are shown in Table 3-5.

Table 3-4: HV/MV transformer impedance ranges (Goosen, (2004))

Impedance Range (%)	Auto Transformers With Ratios			Double-wound Transformers With Ratios	
	Up to 1.5	Between 1.5 and 2.5	2.5 and above	On Load Tap Changer	Off Circuit Tap Switch
Minimum	1.00	1.00	1.00	1.00	1.00
Maximum	1.35	1.30	1.25	1.25	1.40

Table 3-5: Eros S/S - Transformer 1

Transformer 1 - Eros S/S	
MVA	500
Vector group	YNa0d1
Voltage (HV/MV/LV)	400/132/22kV
$Z_{1(H-M)}$ (Tap 1) %	13.5
$Z_{1(H-M)}$ (Tap 1) Ω	43.2
$Z_{1(H-M)}$ (Tap 13) %	14.1
$Z_{1(H-M)}$ (Tap 13) Ω	45.12
Z_{ps} (on 100MVA) Tap 1	0.027pu
Z_{ps} (on 100MVA) Tap 13	0.0282pu
Z_{p0} (on 100MVA)	0.02363pu
Z_{s0} (on 100MVA)	0.00183pu
Z_{t0} (on 100MVA)	0.05597pu
Z_{source} (Up to 400kV B/B excluding Transformer on 400kV side, based on 100 MVA)	(0.082461 \angle 89.58 $^{\circ}$)

As shown above the actual variation in impedances between maximum and minimum taps for Eskom transformers is very small. For Transformer 1 at Eros S/S the difference is only 1.92 Ω . For Zone 1 protection the relay (located on the EHV (400kV) side) can be set to 70% of the transformers maximum impedance.

$$\text{Zone 1} = 0.7 \times 45.12\Omega = 31.58\Omega$$

This will provide 70% instantaneous coverage for the transformer at Tap 13 and 73% instantaneous coverage for the transformer at Tap 1.

For Zone 1 k_0 is calculated as follows (Ziegler 2011):-

$$k_0 = \frac{Z_0 \text{ total} - (Z_{Tps})}{3 \times Z_{Tps}} \quad (3.32)$$

$$Z_{0 \text{ total}} = Z_{p0} + \frac{Z_{s0} (Z_{1 \text{ Source}} + Z_{p0} + Z_{t0})}{Z_{t0}} \quad (3.33)$$

$$\begin{aligned} Z_{0 \text{ total}} &= j0.02363 + \frac{j0.00183(0.082461 \angle 89.58^\circ + j0.02363 + j0.05597)}{j0.05597} \quad (3.34) \\ &= 0.028929 \angle 89.96^\circ \end{aligned}$$

$$\begin{aligned} k_0 &= \frac{0.028929 - 0.027}{3 \times 0.027} \quad (3.35) \\ &= 0.0238 \end{aligned}$$

In order to provide backup protection for the MV (132kV) busbar, Zone 2 can be set to 120% of the transformer's minimum impedance.

$$\begin{aligned} \text{Zone 2} &= 1.2 \times 43.2\Omega = 51.84\Omega \\ k_0 &= 0.0238 \text{ (same as Zone 1)} \end{aligned}$$

This will provide 120% time delayed coverage for the transformer and MV busbar at Tap 1 and 115% time delayed coverage for the transformer at Tap 13.

If backup protection for the remote HV busbar is required then Zone 3 can be set to cover 120% of the transformer's maximum impedance and the line impedance.

Let's assume that the 132kV HV line has the following data:-

$$\begin{aligned} Z_1 &= (18 \angle 87^\circ)\Omega \\ Z_1 &= (0.103306 \angle 87^\circ)\text{pu (100MVA base)} \end{aligned}$$

Transferring the impedance of the line to the 400kV side at Tap 13 yields the following results:-

$$\begin{aligned} Z_L &= (18 \angle 87^\circ) \times \left(\frac{V_p}{V_s} \right)_{\min}^2 \quad (3.36) \\ &= (18 \angle 87^\circ) \times \left(\frac{400 \times 0.85}{132} \right)^2 \\ &= 125.19\Omega \end{aligned}$$

$$\text{Zone 3} = 1.2 \times (Z_{1(\text{H-M})} + Z_L) = 1.2 \times (45.12 + 125.19) = 204.38\Omega$$

For Zone 3 k_0 is calculated as follows (Ziegler 2011):-

$$k_0 = \frac{Z_{0 \text{ total}} - (Z_{\text{TPs}} + Z_{1 \text{ line}})}{3 \times Z_{\text{TPs}}} \quad (3.37)$$

$$\begin{aligned} Z_{0 \text{ total}} &= Z_{p0} + \frac{Z_{s0} (Z_{1 \text{ Source}} + Z_{p0} + Z_{t0})}{Z_{t0}} & (3.38) \\ &= j0.02363 + \frac{j0.00183(0.082461\angle 89.58^\circ + j0.02363 + j0.05597)}{j0.05597} \\ &= 0.028929\angle 89.96^\circ \end{aligned}$$

$$\begin{aligned} k_0 &= \frac{0.028929 - (0.027 + 0.103306)}{3 \times 0.027} & (3.39) \\ &= -1.25 \end{aligned}$$

The tripping time for Zone 3 should be co-ordinated with other relays.

If backup is required for the local 400kV busbar protection then the reverse reaching Zone 4 can be set to 20% of the transformer's minimum impedance.

$$\text{Zone 4} = 0.2 \times (Z_{1(\text{H-M})}) = 0.2 \times (43.2) = 8.64\Omega$$

3.4 Conclusion

In Case-Study-Example 4 it was shown that the current flows up the neutral of the autotransformer for a MV single-line-to-ground fault. In Case-Study-Example 5 it was shown that the current flows down the neutral of the autotransformer for a HV single-line-to-ground fault. This occurs when the absolute value of the MV winding zero sequence reactance, which has a negative value, is greater than the MV network zero sequence source reactance in magnitude. Case-Study-Examples 6 and 7 have shown how the voltages during faults can be calculated using the Z Bus Matrix method. The voltages and current values calculated in Case-Study-Examples 6 and 7 were used in Section 3.2 to calculate distance to fault through the autotransformer. Since neutral current can change directions care must be

taken when applying neutral current for polarisation and overcurrent protection (Zhang & Echeverria n.d.).

The actual impedance of the autotransformer used in the calculations of Sections 3.2.3 and 3.2.5 is 43.26Ω . The values measured in Section 3.2.3 by the distance elements are not identical to the actual impedance of the transformer for the phase-to-phase fault. However, the percentage error is only 0.28%. This error is due to manual calculations. In reality if 100% coverage of the transformer is required the relay setting will be calculated at 120% and set with a time delay for tripping. Setting calculations in Eskom incorporate a 20% measurement error. This 20% caters for errors in measurement due to instrument transformer measurement error, relay measurement error and incorrect transformer impedance data. For the single-line-to-ground fault both the source impedance and infeed from the 132kV network affect the distance measured by the relay. However, with the results obtained being slightly less than the actual impedance of the transformer, the distance relay will perform correctly if Zone 1 is set to protect the entire transformer.

In Section 3.3 it was shown how setting calculations can be performed for a transformer that has a tap-changer.

4 FAULT SIMULATIONS

DigSilent Power Factory software version 15.0.2 was used in the modelling and simulation of faults.

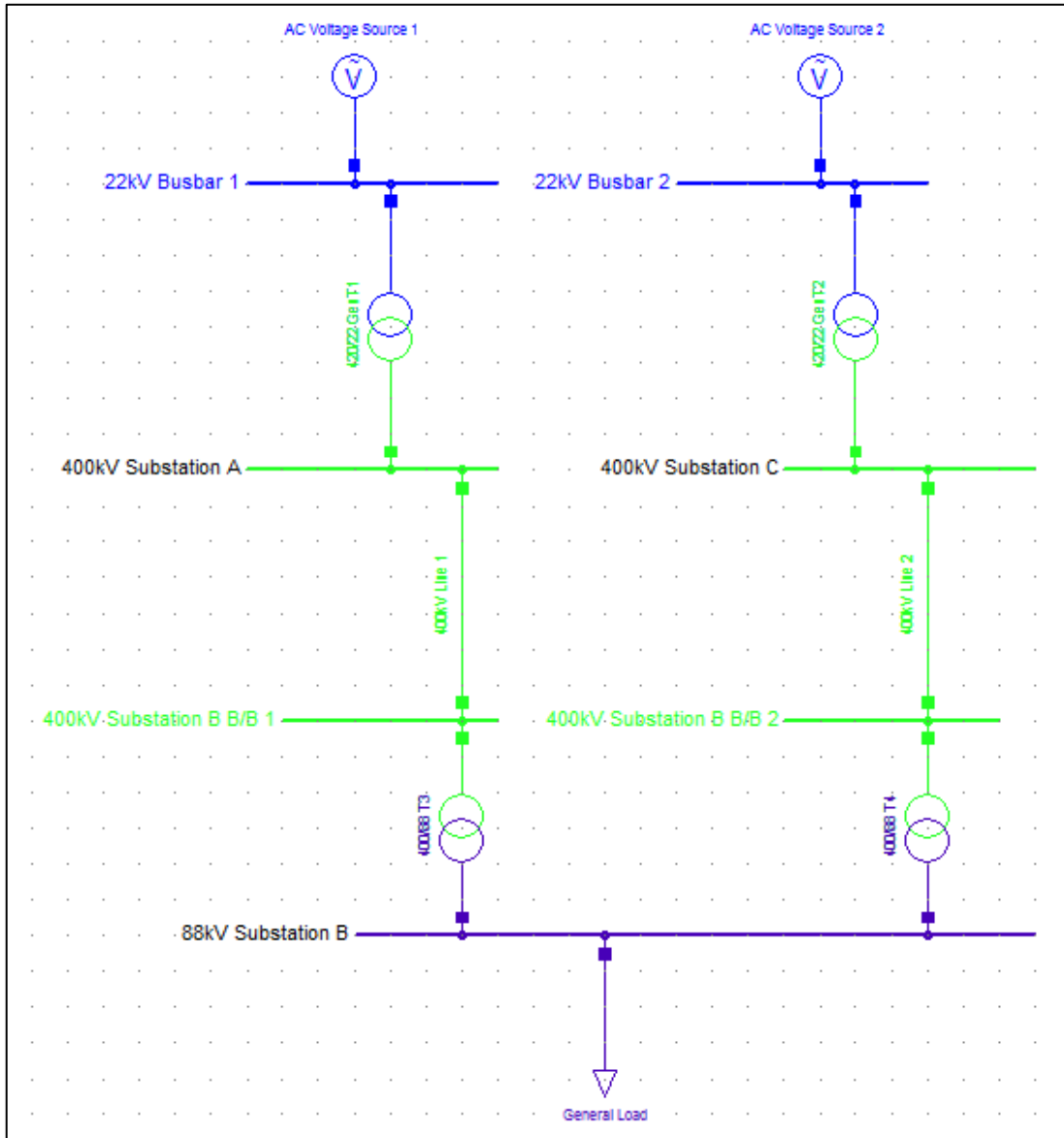


Figure 4-1: Network diagram for fault simulations

Faults were simulated on one side of power transformers having varying vector groups. Voltages and currents were then recorded on the other side of these transformers. These values were inserted into equations for measurement of apparent distance. Figure 4-1 shows the general network diagram for the fault simulations.

The data for the equipment depicted in Figure 4-1 are shown in Tables 4-1 to Tables 4-5.

Table 4-1: AC Voltage Source 1 & 2 data

Positive sequence reactance, X_1	0.219 Ω
Negative sequence reactance, X_2	0.219 Ω
Zero sequence reactance, X_0	0.219 Ω
Voltage	22kV
Type	3-phase voltage source

Table 4-2: 420/22kV Generator Transformers T1 and T2 data

MVA	795
HV Voltage	420kV
LV Voltage	22kV
Vector group	YNd1
Positive sequence impedance	13.7%
Zero sequence impedance	13.7%

Table 4-3: 400kV Line 1 data

Positive sequence impedance, Z_1	17.831 Ω
Positive sequence impedance, Angle	86.98 $^\circ$
Zero sequence resistance, R_0	22.202 Ω
Zero sequence reactance, X_0	71.843 Ω
Length of line	64.43km

Table 4-4: 400kV Line 2 data

Positive sequence impedance, Z_1	21.864 Ω
Positive sequence impedance, Angle	86.98 $^\circ$
Zero sequence resistance, R_0	27.223 Ω
Zero sequence reactance, X_0	88.09 Ω
Length of line	69km

Table 4-5: General Load data

Active Power	160MW
Power Factor	0.8 lagging
Type	3 phase, balanced

4.1 Star/Star Transformer Fault Simulation and Analysis

Figure 4-1 shows a network diagram where the vector group of the 400/88kV transformers T3 and T4 are YNyn. The data for Transformers T3 and T4 are shown in Table 4-6. Symmetrical and asymmetrical faults were placed on the 88kV Busbar at Substation B. Voltages were recorded at the 400kV Busbar 1 and currents were recorded on the EHV (400kV) side of Transformer 3 at substation B. The results are shown in Tables 4-7 and 4-8.

Table 4-6: 400/88 TX3 and TX4 data

MVA	160
HV Voltage	400kV
LV Voltage	88kV
Vector group	YNyn
Positive sequence impedance	9.38%
Positive sequence impedance (actual)	93.8 Ω
Zero sequence impedance	8.44%
Zero sequence impedance (actual)	84.4 Ω

Table 4-7: Fault currents - Star/Star Transformer

	I_A	I_B	I_C
3-phase	$(1.1093\angle-59.76^0)\text{kA}$	$(1.1093\angle-179.76^0)\text{kA}$	$(1.1093\angle60.24^0)\text{kA}$
Single-line-to-ground (A-G)	$(1.1745\angle-57.95^0)\text{kA}$	$(0.1307\angle-110.58^0)\text{kA}$	$(0.1212\angle88.04^0)\text{kA}$
Phase-to-phase (B-C)	$(0.1435\angle-11.62^0)\text{kA}$	$(1.0153\angle-152.46^0)\text{kA}$	$(0.9085\angle33.26^0)\text{kA}$
Phase-to-phase-to-ground (B-C-G)	$(0.0908\angle-8.68^0)\text{kA}$	$(1.1763\angle178.39^0)\text{kA}$	$(1.1117\angle64.18^0)\text{kA}$

Table 4-8: Fault Voltages - Star/Star Transformer

	V_A	V_B	V_C
3-phase	$(104.0508\angle30.24^0)\text{kV}$	$(104.0508\angle-89.76^0)\text{kV}$	$(104.0508\angle150.24^0)\text{kV}$
Single-line-to-ground (A-G)	$(106.6192\angle32.11^0)\text{kV}$	$(231.7164\angle-92.66^0)\text{kV}$	$(238.8967\angle144.93^0)\text{kV}$
Phase-to-phase (B-C)	$(238.1392\angle26.61^0)\text{kV}$	$(144.6990\angle-114.97^0)\text{kV}$	$(153.8089\angle170.83^0)\text{kV}$
Phase-to-phase-to-ground (B-C-G)	$(232.2563\angle25.56^0)\text{kV}$	$(108.4328\angle-89.99^0)\text{kV}$	$(102.3091\angle152.48^0)\text{kV}$

4.1.1 Star/Star Transformer - 3-Phase Fault

Simulation-Example 1, Chapter 5 shows the results of the six fault loop calculations that will be performed by a distance relay located on the EHV side of Transformer 3 (YNyn) during the 3-phase fault on the HV 88kV busbar.

The positive sequence impedance of TX3 is 93.8Ω . From the results of Simulation-Example 1 it can be seen that all fault measuring loops will measure the correct distance to fault in the right direction during the 3-phase fault on the HV 88kV busbar. The algorithm V_p/I_p yielded accurate results since $I_r = 0$.

4.1.2 Star/Star Transformer – Single-Line-to-Ground Fault

Simulation-Example 2, Chapter 5 shows the results of the ground measuring elements that will be performed by a distance relay located on the EHV side of Transformer 3(YNyn) during the single-line-to-ground fault (phase A) on the HV 88kV busbar.

From the results of Simulation-Example 2 it can be seen the 'A' phase to ground element using the traditional algorithm will measure the correct distance to fault through the transformer. The other ground elements will under-reach. The algorithm V_p/I_p slightly over-reaches since this equation does not have zero sequence compensation and $I_r \neq 0$. The phase-to-phase elements will also under-reach for this fault and yield very high impedances.

4.1.3 Star/Star Transformer – Phase-to-Phase Fault

Simulation-Example 3, Chapter 5 shows the results of the phase-to-phase distance element calculations that will be performed by a distance relay located on the EHV side of Transformer 3 (YNyn) during the phase-to-phase fault (phase B & C) on the HV 88kV busbar.

From the results of Simulation-Example 3 it can be seen that the BC phase-to-phase element will measure the correct distance to fault through the star/star transformer. The other phase-to-phase elements will under-reach.

4.1.4 Star/Star Transformer – Phase-to-Phase-to-Ground Fault

Simulation-Example 4, Chapter 5 shows the results of the phase measuring elements that will be performed by a distance relay located on the EHV side of Transformer 3 (YNyn) during the phase-to-phase-to-ground fault (phase B & C & G) on the HV 88kV busbar.

From the results of Simulation-Example 4 it can be seen that the BC phase-to-phase element, B phase earth element, and C phase earth element will measure the correct distance to fault through the star/star transformer. The other phase-to-phase and earth elements will under-reach.

4.2 Star/Delta (YNd1) Transformer Fault Simulation and Analysis

Figure 4-2 shows a network diagram where the vector group of the 400/88kV transformers T3 and T4 are YNd1. The data for Transformers T3 and T4 are similar to Table 4-6, except that the vector group has changed. Transformer T5 is also connected to the 88kV busbar at substation B. The data for Transformer T5 is shown in Table 4-9. The purpose of TX5 is to provide an earth on the 88kV network, thereby allowing the flow of zero sequence currents during earth faults. The data for the rest of the equipment depicted in Figure 4-2 are shown in Tables 4-1 to Tables 4-5. Symmetrical and asymmetrical faults were simulated on the 88kV busbar at Substation B. The resulting voltages and currents were recorded at the 400kV Busbar 1 and Transformer 3 at Substation B for both the symmetrical and asymmetrical faults. The results are shown in Tables 4-10 and 4-11.

Table 4-9: 88/6.6 TX5 data

MVA	5
HV Voltage	88kV
LV Voltage	6.6kV
Vector group	YNd1
Positive sequence impedance	9.1%
Positive sequence impedance (actual)	140.94 Ω
Zero sequence impedance	8.64%
Zero sequence impedance (actual)	133.82 Ω

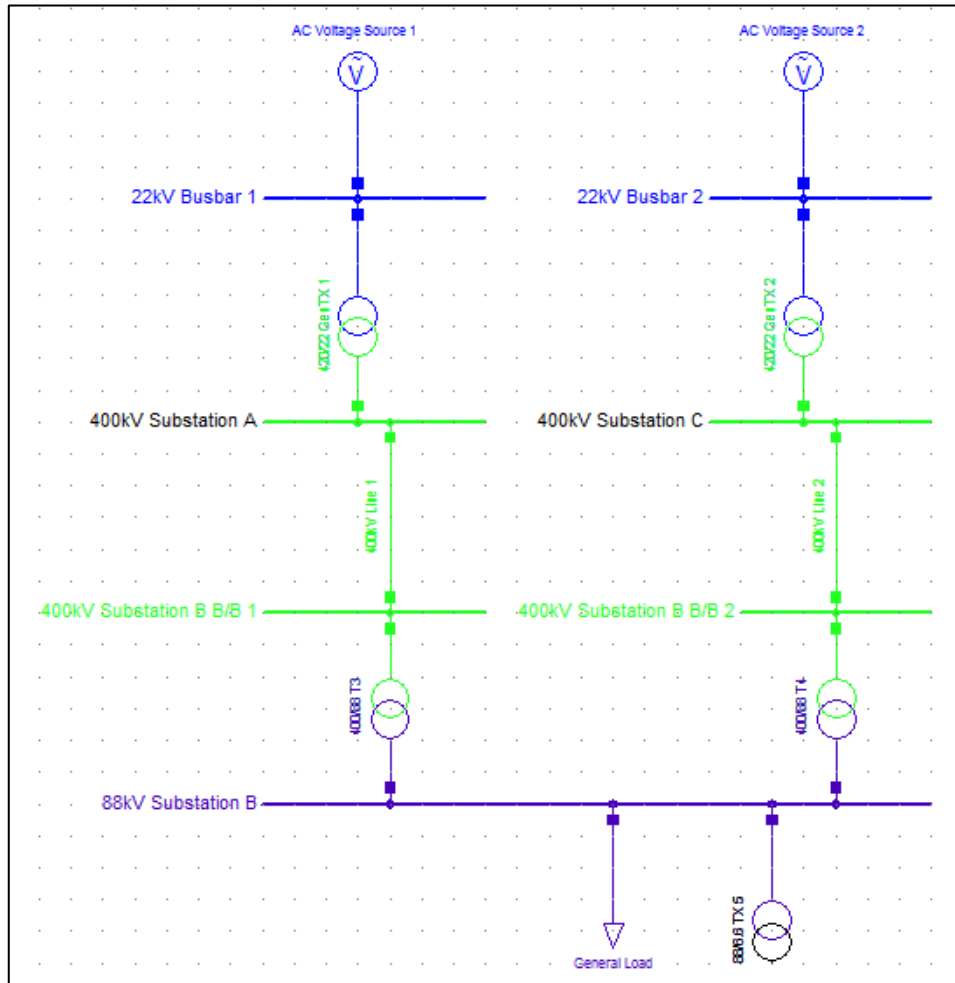


Figure 4-2: Network diagram for fault simulations - YNd1

Table 4-10: Fault currents - star/delta transformer

	I_A	I_B	I_C
3-phase	$(1.1093 \angle -59.76^0) \text{kA}$	$(1.1093 \angle -179.76^0) \text{kA}$	$(1.1093 \angle 60.24^0) \text{kA}$
Single-line-to-ground (A-G)	$(0.1564 \angle -34.99^0) \text{kA}$	$(0.1435 \angle -131.62^0) \text{kA}$	$(0.1997 \angle 99.44^0) \text{kA}$
Phase-to phase (B-C)	$(0.6525 \angle -7.06^0) \text{kA}$	$(1.1093 \angle -179.76^0) \text{kA}$	$(0.4694 \angle 10.42^0) \text{kA}$
Phase-to-phase-to-ground (B-C-G)	$(0.6513 \angle -8.5^0) \text{kA}$	$(1.1093 \angle -179.76^0) \text{kA}$	$(0.4759 \angle 12.24^0) \text{kA}$

Table 4-11: Fault voltages - star/delta transformer

	V _A	V _B	V _C
3-phase	(104.0508∠30.24 ⁰)kV	(104.0508∠-89.76 ⁰)kV	(104.0508∠150.24 ⁰)kV
Single-line-to-ground (A-G)	(231.8061∠27.87 ⁰)kV	(238.1392∠-93.39 ⁰)kV	(230.5368∠145.87 ⁰)kV
Phase-to-phase (B-C)	(209.4747∠10.96 ⁰)kV	(104.0508∠-89.76 ⁰)kV	(215.8681∠162.69 ⁰)kV
Phase-to-phase-to-ground (B-C-G)	(207.4943∠11.19 ⁰)kV	(104.0508∠-89.76 ⁰)kV	(213.7173∠162.64 ⁰)kV

4.2.1 Star/Delta Transformer – 3-Phase Fault

Since the star/delta transformer has the same positive sequence impedance of the star/star transformer in Section 4.1.1 the results for the voltages and currents are the same at the 400kV Busbar 1 and Transformer 3 at Substation B for a 3-phase fault compared to the star/star transformer. TX5 is not on load. Therefore all fault measuring loops will measure the correct distance to fault in the right direction during the 3-phase fault on the HV 88kV busbar similar to Section 4.1.1

4.2.2 Star/Delta Transformer – Single Line-to-Ground Fault

Simulation-Example 5 show the results of the measuring element calculations that will be performed by a distance relay located on the EHV 400kV side of Transformer 3 (YNd1) during the single-line-to-ground fault (A & G) on the HV 88kV busbar.

From the results of Simulation-Example 5 it can be seen that for the A-G fault on the delta side of the transformer, all the phase and earth measuring elements on the star side will under-reach. The zero sequence current on the delta side of the power transformer is not

transformed to the star side. Therefore the traditional algorithms for distance elements would not measure the distance to fault through a star/delta transformer, during a single-line-to-ground fault on the delta side.

4.2.3 Star/Delta Transformer – Phase-to-Phase Fault

Simulation-Example 6 shows the results of the measuring elements that will be performed by a distance relay located on the EHV 400kV side of Transformer 3 (YNd1) during the phase-to-phase fault (phase B & C) on the HV 88kV busbar.

From the results of Simulation-Example 6 it can be seen that for the B-C (phase-to-phase) fault on the delta side of the transformer, all the phase measuring elements on the star side will under-reach. $3I_0$ on the star side of the transformer equals to zero.

$$\begin{aligned}
 3I_0 = I_r &= (I_A + I_B + I_C) && (4.1) \\
 &= (0.6525\angle-7.06^\circ + 1.1093\angle-179.76^\circ + 0.4694\angle10.42^\circ)\text{kA} \\
 &= (0)\text{A}
 \end{aligned}$$

Only the B-G earth element will measure the correct distance to the phase-to-phase fault through the YNd1 transformer. The other two earth elements will also under-reach. The algorithm that the GE D20 line distance relay employs (Table 2-3) will also measure the correct distance to the phase-to-phase fault through the YNd1 transformer, as shown below.

$$\begin{aligned}
 Z_{BC} &= \frac{\sqrt{3}V_B}{\frac{1}{\sqrt{3}}(2I_B - I_A - I_C)} && (4.2) \\
 &= \frac{\sqrt{3}(104.0508\angle-89.76^\circ)\text{kV}}{\frac{1}{\sqrt{3}}(2(1.1093\angle-179.76^\circ) - 0.6525\angle-7.06^\circ - 0.4694\angle10.42^\circ)} \\
 &= (93.8\angle90^\circ)\Omega
 \end{aligned}$$

4.2.4 Star/Delta Transformer – Phase-to-Phase-to-Ground Fault

Simulation-Example 7 shows the results of the measuring elements that will be performed by a distance relay located on the EHV 400kV side of Transformer 3 (YNd1) during the phase-to-phase-to-ground fault (phase B & C & G) on the HV 88kV busbar.

From the results of Simulation-Example 7 it can be seen that for the B-C-G fault on the delta side of the transformer, all the phase measuring elements on the star side will under-reach. $3I_0$ on the star side of the transformer equals to zero.

$$\begin{aligned} 3I_0 &= I_r = (I_A + I_B + I_C) & (4.3) \\ &= (0.6513\angle-8.5^\circ + 1.1093\angle-179.76^\circ + 0.4759\angle12.24^\circ)\text{kA} \\ &= (0)\text{A} \end{aligned}$$

Only the B-G earth element will measure the correct distance to the phase-to-phase-to-ground fault through the YNd1 transformer. The other two earth elements will also under-reach. The algorithm that the GE D20 line distance relay employs (Table 2-3) will also measure the correct distance to the phase-to-phase-to-ground fault through the YNd1 transformer, as shown below.

$$\begin{aligned} Z_{BC} &= \frac{\sqrt{3}V_B}{\frac{1}{\sqrt{3}}(2I_B - I_A - I_C)} & (4.4) \\ &= \frac{\sqrt{3}(104.0508\angle-89.76^\circ)\text{kV}}{\frac{1}{\sqrt{3}}(2(1.1093\angle-179.76^\circ) - 0.6513\angle-8.5^\circ - 0.4759\angle12.24^\circ)} \\ &= (93.8\angle90^\circ)\Omega \end{aligned}$$

4.3 Delta/Star (Dyn1) Transformer Fault Simulation and Analysis

Figure 4-1 shows a network diagram where the vector group of the 400/88kV transformers T3 and T4 are now Dyn1. The data for Transformers T3 and T4 are similar to Table 4-6, except that the vector group has changed. The data for the rest of the equipment depicted in Figure 4-1 are shown in Tables 4-1 to Tables 4-5. Symmetrical and asymmetrical faults were simulated on the 88kV busbar at Substation B. The resulting voltages and currents were

recorded at the 400kV Busbar 1 and Transformer 3 at Substation B for both the symmetrical and asymmetrical faults. The results are shown in Tables 4-12 and 4-13. The phase-to-phase fault simulated on the 88kV busbar at Substation B is shown in Appendix 2.

Table 4-12: Fault currents - delta/star transformer

	I_A	I_B	I_C
3-phase	$(1.1093\angle-59.76^0)\text{kA}$	$(1.1093\angle-179.76^0)\text{kA}$	$(1.1093\angle60.24^0)\text{kA}$
Single Line-to-ground (A-G)	$(0.7604\angle-86^0)\text{kA}$	$(0.1435\angle-131.62^0)\text{kA}$	$(0.8669\angle87.21^0)\text{kA}$
Phase-to-phase (B-C)	$(0.6525\angle-7.06^0)\text{kA}$	$(1.1093\angle-179.76^0)\text{kA}$	$(0.4694\angle10.42^0)\text{kA}$
Phase-to-phase-to-ground (B-C-G)	$(0.8048\angle-44.45^0)\text{kA}$	$(1.1093\angle-179.76^0)\text{kA}$	$(0.7803\angle46.74^0)\text{kA}$

Table 4-13: Fault voltages – delta/star transformer

	V_A	V_B	V_C
3-phase	$(104.0508\angle30.24^0)\text{kV}$	$(104.0508\angle-89.76^0)\text{kV}$	$(104.0508\angle150.24^0)\text{kV}$
Single-line-to-ground (A-G)	$(166.6363\angle45.53^0)\text{kV}$	$(238.1392\angle-93.39^0)\text{kV}$	$(157.0144\angle130.82^0)\text{kV}$
Phase-to-phase (B-C)	$(209.4747\angle10.96^0)\text{kV}$	$(104.0508\angle-89.76^0)\text{kV}$	$(215.8681\angle162.69^0)\text{kV}$
Phase-to-phase-to-ground (B-C-G)	$(150.4786\angle19.38^0)\text{kV}$	$(104.0508\angle-89.76^0)\text{kV}$	$(152.3302\angle159.19^0)\text{kV}$

4.3.1 Delta/Star Transformer – 3-Phase Fault

Since the delta/star transformer has the same positive sequence impedance of the star/star transformer in Section 4.1.1 the results for the voltages and currents are the same at the

400kV Busbar 1 and Transformer 3 at Substation B for a 3-phase fault compared to the star/star transformer. Therefore all fault measuring loops will measure the correct distance to fault in the right direction during the 3 phase fault on the HV 88kV busbar similar to Section 4.1.1.

4.3.2 Delta/Star Transformer – Single-Line-to-Ground Fault

Simulation-Example 8 shows the results of the measuring elements computations that will be performed by a distance relay located on the EHV (400kV) side of Transformer 3 (Dyn1) during a single-line-to-ground fault (A & G) on the HV (88kV) busbar.

From the results of Simulation-Example 8 it can be seen that for a single-line-to-ground-fault on the star side of the transformer, all the phase and earth measuring elements on the delta side will under-reach. The zero sequence current on the star side of the power transformer is not transformed to the delta side. Therefore the traditional algorithms for distance elements would not measure the distance to fault through a delta/star transformer, during a single-line-to-ground fault on the star side.

4.3.3 Delta/Star Transformer – Phase-to-Phase Fault

The resulting voltages and currents on the EHV 400kV side of Transformer 3 (Dyn1) during the phase-to-phase fault (phase B & C) on the HV 88kV busbar are similar for the YNd1 Transformer in Section 4.2.3

Therefore only the B-G earth element will measure the correct distance to the phase-to-phase fault through the Dyn1 transformer. The other two earth elements and all the phase elements will under-reach. The algorithm that the GE D20 line distance relay employs (Table 2-3) will also measure the correct distance to the phase-to-phase fault through the Dyn1 transformer, as shown below.

$$\begin{aligned}
Z_{BC} &= \frac{1}{\sqrt{3}} \frac{(V_{BC} - V_{AB})}{\sqrt{3I_B}} & (4.5) \\
&= \frac{1}{\sqrt{3}} \frac{((V_B - V_C) - (V_A - V_B))}{\sqrt{3I_B}} \\
&= \frac{1}{\sqrt{3}} \frac{((104.0508\angle-89.76^\circ - 215.8681\angle162.69^\circ) - (209.4747\angle10.96^\circ - 104.0508\angle-89.76^\circ))}{\sqrt{3}(1.1093\angle-179.76^\circ)\text{kA}} \\
&= (93.8\angle90^\circ)\Omega
\end{aligned}$$

4.3.4 Delta\Star Transformer – Phase-to-Phase-to-Ground Fault

Simulation-Example 9 shows the results of the measuring elements that will be performed by a distance relay located on the EHV 400kV side of Transformer 3 (Dyn1) during the phase-to-phase-to-ground fault (phase B & C & G) on the HV 88kV busbar.

From the results of Simulation-Example 9 it can be seen that for the B-C-G fault on the star side of the transformer, all the phase measuring elements on the delta side will under-reach. $3I_0$ on the delta side of the transformer equals to zero.

$$\begin{aligned}
3I_0 = I_r &= (I_A + I_B + I_C) & (4.6) \\
&= (0.8048\angle-44.45^\circ + 1.1093\angle-179.76^\circ + 0.7803\angle46.74^\circ)\text{kA} \\
&= (0)\text{A}
\end{aligned}$$

Only the B-G earth element will measure the correct distance to the phase-to-phase-to-ground fault through the Dyn1 transformer. The other two earth elements will also under-reach. The algorithm that the GE D20 line distance relay employs (Table 2-3) will also measure the correct distance to the phase-to-phase-to-ground fault through the Dyn1 transformer, as shown below.

$$\begin{aligned}
Z_{BC} &= \frac{1}{\sqrt{3}} \frac{(V_{BC} - V_{AB})}{\sqrt{3I_B}} & (4.7) \\
&= \frac{1}{\sqrt{3}} \frac{((V_B - V_C) - (V_A - V_B))}{\sqrt{3I_B}} \\
&= \frac{1}{\sqrt{3}} \frac{((104.0508\angle-89.76^\circ) - (152.3302\angle159.19^\circ) - (150.4786\angle19.38^\circ - 104.0508\angle-89.76^\circ))}{\sqrt{3}(1.1093\angle-179.76^\circ)\text{kA}} \\
&= (93.8\angle90^\circ)\Omega
\end{aligned}$$

4.4 Star/Star/Delta (YNynd1) Transformer Fault Simulation and Analysis

Figure 4-3 shows a network diagram where the vector group of the 400/88/22kV transformers T3 and T4 are YNyd1. The data for Transformers T3 and T4 are shown in Table 4-14. The data for Transformers T3 and T4 that was implemented in DigSilent Power Factory is shown in Appendix 3, where it can be seen that any impedance involving the LV (tertiary) winding is based on 40MVA. The data for the rest of the equipment depicted in Figure 4-3 are shown in Tables 4-1 to Tables 4-5. Symmetrical and asymmetrical faults were simulated on the 88kV busbar at Substation B. The resulting voltages and currents were recorded at the 400kV Busbar 1 and Transformer 3 at Substation B for both the symmetrical and asymmetrical faults. The results are shown in Tables 4-15 and 4-16.

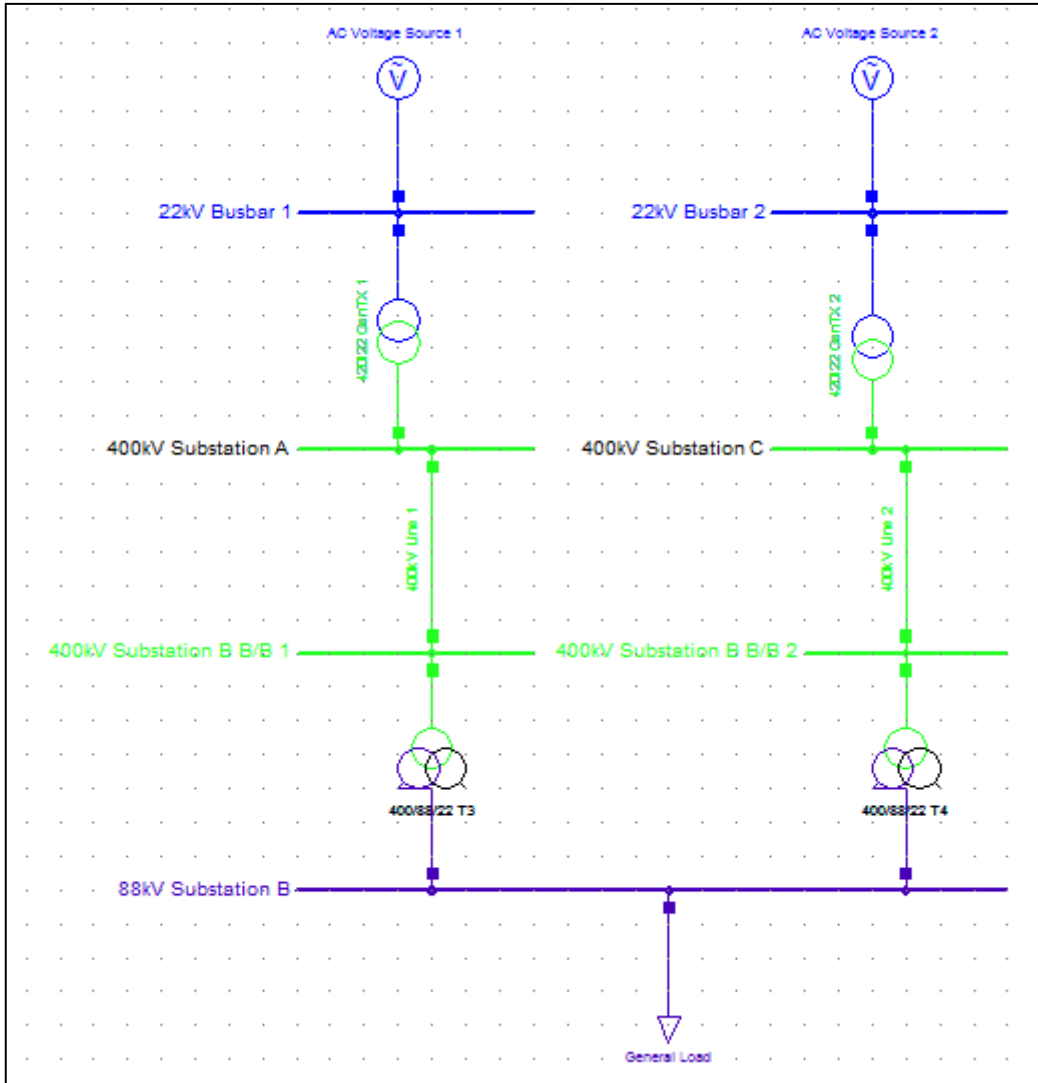


Figure 4-3: Network diagram for fault simulations - YNyd1

Table 4-14: 400/88/22 TX3 and TX4 data

MVA (HV and MV)	315
MVA (LV)	40
HV Voltage (Primary)	400kV
MV Voltage (Secondary)	88kV
LV Voltage (Tertiary)	22kV
Vector group	YNyd1
Z_{ps} (on 315MVA)	13.5%
Z_{pt} (on 315MVA)	80.17%
Z_{st} (on 315MVA)	64.81%

Z_{ps} (on 100MVA)	0.042857pu
Positive sequence impedance Z_{ps} (actual)	68.57 Ω
Z_{ps0} (on 100MVA)	0.042063pu
Z_{pt0} (on 100MVA)	0.241079pu
Z_{st0} (on 100MVA)	0.188508pu
Z_{p0} (on 100MVA)	0.047388pu
Z_{s0} (on 100MVA)	-0.005183pu
Z_{t0} (on 100MVA)	0.193691pu
Z_{source} (Up to 400kV Substation B B/B1 excluding Transformer TX3 on 400kV side, based on 100MVA)	(0.082461 \angle 89.58 $^{\circ}$)pu

Table 4-15: Fault currents - star/star/delta transformer

	I_A	I_B	I_C
3-phase	(1.2489 \angle -59.73 $^{\circ}$)kA	(1.2489 \angle -179.73 $^{\circ}$)kA	(1.2489 \angle 60.27 $^{\circ}$)kA
Single-line-to-ground (A-G)	(1.3023 \angle -58.18 $^{\circ}$)kA	(0.1185 \angle 161.92 $^{\circ}$)kA	(0.2859 \angle 103.56 $^{\circ}$)kA
Phase-to phase (B-C)	(0.1417 \angle -10.69 $^{\circ}$)kA	(1.1360 \angle -152.07 $^{\circ}$)kA	(1.0291 \angle 32.86 $^{\circ}$)kA
Phase-to-phase-to-ground (B-C-G)	(0.2569 \angle -50.63 $^{\circ}$)kA	(1.3174 \angle 178.80 $^{\circ}$)kA	(1.2465 \angle 63.76 $^{\circ}$)kA

Table 4-16: Fault voltages - star/star/delta transformer

	V_A	V_B	V_C
3-phase	(85.6359 \angle 30.27 $^{\circ}$)kV	(85.6359 \angle -89.73 $^{\circ}$)kV	(85.6359 \angle 150.27 $^{\circ}$)kV
Single-line-to-ground (A-G)	(87.3827 \angle 31.93 $^{\circ}$)kV	(225.1888 \angle -87.74 $^{\circ}$)kV	(227.7635 \angle 140.66 $^{\circ}$)kV

Phase-to-phase (B-C)	$(238.5276 \angle 26.61^{\circ})\text{kV}$	$(136.3586 \angle -120.52^{\circ})\text{kV}$	$(144.4102 \angle 175.78^{\circ})\text{kV}$
Phase-to-phase-to-ground (B-C-G)	$(206.9766 \angle 26.16^{\circ})\text{kV}$	$(89.2765 \angle -89.90^{\circ})\text{kV}$	$(84.1099 \angle 152.51^{\circ})\text{kV}$

4.4.1 Star/Star/Delta Transformer – 3-Phase Fault

Simulation-Example 10 shows the results of the six fault loop calculations that will be performed by a distance relay located on the EHV side of Transformer 3 during the 3 phase fault on the HV 88kV busbar.

The positive sequence impedance of the three winding transformer TX3 is 68.57Ω . From the results of Simulation-Example 10 it can be seen that all fault measuring loops will measure the correct distance to fault in the right direction during the 3 phase fault on the HV 88kV busbar.

4.4.2 Star/Star/Delta Transformer – Single-Line-to-Ground Fault

Simulation-Example 11 shows the results of the calculations that will be performed by a distance relay located on the EHV side of Transformer 3 during the single-line-to-ground fault (phase A) on the HV 88kV busbar.

The actual series impedance of the 3 winding transformer is 68.57Ω . From the results of Simulation-Example 11 it can be seen that using Ziegler's 'k' factor for an autotransformer yields the most accurate result.

4.4.3 Star/Star/Delta Transformer – Phase-to-Phase Fault

Simulation-Example 12, Chapter 5 shows the results of the phase-to-phase distance element calculations that will be performed by a distance relay located on the EHV side of Transformer 3 during the phase-to-phase fault (phase B & C) on the HV 88kV busbar.

From the results of Simulation-Example 12 it can be seen that the BC phase-to-phase element will measure the correct distance to fault through the star/star/delta 3 winding transformer. The other phase-to-phase elements will under-reach.

4.4.4 Star/Star/Delta Transformer – Phase-to-Phase-to-Ground Fault

Simulation-Example 13 shows the results of the phase and ground measuring elements that will be performed by a distance relay located on the EHV side of Transformer 3 (YNYnd1) during the phase-to-phase-to-ground fault (phase B & C & G) on the HV 88kV busbar.

From the results of Simulation-Example 13 it can be seen that the BC phase-to-phase element, B phase earth element, and C phase earth element will measure the correct distance to fault through the star/star transformer. The other phase-to-phase and earth elements will under-reach. The earth elements without zero sequence compensation result in slight over-reaching.

4.5 Autotransformer (YNa0d1) Fault Simulation and Analysis

An autotransformer is smaller in physical size and has lower impedances than a conventional two winding magnetically coupled only transformer that has the same power rating (IS 2009). A conventional transformer has no electrical connection like an autotransformer between the primary and secondary windings. The saving in copper is greater the closer the ratio between the primary and secondary windings approaches 1. The lower impedance of an autotransformer results in higher short circuit currents compared to an equivalent conventional transformer. However an autotransformer can be specified with impedances that match a conventional transformer. The 3 winding model for transformers apply to conventional 3 winding transformers and autotransformers that have a delta tertiary. When

the 3 winding transformer (YNyNd1) described in Section 4.4 is simulated as having an autotransformer connection between its 400kV and 88kV windings, the results for the fault simulations were identical. Similar results were expected since the impedances of the transformer, MVA rating and voltage ratings were not changed for the autotransformer.

The current in the neutral of an autotransformer can change direction and therefore care must be taken when applying the neutral current for polarisation. This has been discussed in Chapter 3.

The results for the response of the autotransformer to various faults during simulations are similar to Sections 4.4.1, 4.4.2, 4.4.3 and 4.4.4.

4.6 Conclusion

Tables 4-17 and 4-18 indicate the measurement loops that will calculate the fault impedance through transformers having varying vector groups. Some fault loops will measure the precise distance to fault through the transformer and some loops will measure the distance to fault with a slight error. It was shown that the error in measurement is insignificant. Distance protection for transformers is applied with a time delay for over-reaching zones. Therefore the slight error in measurement for some loops will not produce any relay maloperations. In Tables 4-17 and 4-18 the fault is located on the LV side of the transformer and the relay measurement is performed on the HV side of the transformer.

Table 4-17: Formulae for distance measurement through YNyn and YNd1 transformer

	YNyn	YNd1
3 phase fault (A-B-C)	All six measuring loops (precise measurement)	All six measuring loops (precise measurement)
1-phase-to-ground (A-G)	$Z_A = \frac{V_A}{I_A + I_r k_0}$ (fairly accurate)	Not possible with traditional algorithms
Phase-to-phase (B-C)	$Z_{BC} = \frac{V_B - V_C}{I_B - I_C}$ (precise measurement)	$Z_B = \frac{V_B}{I_B + I_r k_0}$ (precise measurement, $I_r = 0$) $Z_{BC} = \frac{\sqrt{3}V_B}{\frac{1}{\sqrt{3}}(2I_B - I_A - I_C)}$ (precise measurement)
Phase-to-phase-to ground (B-C-G)	$Z_{BC} = \frac{V_B - V_C}{I_B - I_C}$ (precise measurement) $Z_B = \frac{V_B}{I_B + I_r k_0}$ (fairly accurate) $Z_C = \frac{V_C}{I_C + I_r k_0}$ (fairly accurate)	$Z_B = \frac{V_B}{I_B + I_r k_0}$ (precise measurement, $I_r = 0$) $Z_{BC} = \frac{\sqrt{3}V_B}{\frac{1}{\sqrt{3}}(2I_B - I_A - I_C)}$ (precise measurement)

Table 4-18: Formulae for distance measurement through Dyn1 and 3 winding transformers

	Dyn1	YNynd1 or YNa0d1
3 phase fault (A-B-C)	All six measuring loops (precise measurement)	All six measuring loops (precise measurement)
1-phase-to-ground (A-G)	Not possible with traditional algorithms	$Z_A = \frac{V_A}{I_A + I_r k_0}$ <p>Where,</p> $k_0 = \frac{Z_{0 \text{ total}} - (Z_{Tps} + Z_{1 \text{ line}})}{3 \times Z_{Tps}}$ <p>(most accurate)</p> $k_0 = \frac{Z_0 - Z_1}{3Z_1}$ <p>(fairly accurate)</p>
Phase-to-phase (B-C)	$Z_B = \frac{V_B}{I_B + I_r k_0}$ <p>(precise measurement, $I_r = 0$)</p> $Z_{BC} = \frac{\frac{1}{\sqrt{3}}(V_{BC} - V_{AB})}{\sqrt{3}I_B}$ <p>(precise measurement)</p>	$Z_{BC} = \frac{V_B - V_C}{I_B - I_C}$ <p>(precise measurement)</p>
Phase-to-phase-to ground (B-C-G)	$Z_B = \frac{V_B}{I_B + I_r k_0}$ <p>(precise measurement, $I_r = 0$)</p> $Z_{BC} = \frac{\frac{1}{\sqrt{3}}(V_{BC} - V_{AB})}{\sqrt{3}I_B}$ <p>(precise measurement)</p>	$Z_{BC} = \frac{V_B - V_C}{I_B - I_C}$ <p>(precise measurement)</p> $Z_B = \frac{V_B}{I_B + I_r k_0}$ <p>(fairly accurate)</p> $Z_C = \frac{V_C}{I_C + I_r k_0}$ <p>(fairly accurate)</p>

5 CASE STUDIES AND SIMULATIONS

5.1 Case-Study-Example 1

In Figure 2.1 let the transformer and line have the following parameters:

500MVA, 400/132kV, $X_T = 13.48\%$, YNa0d1

Triple Kingbird, $X_L = 0.28681 \Omega/\text{km}$, Line length = 25km

$HV_{CT\text{RATIO}} = 1000/1$

$$HV_{VT\text{RATIO}} = \frac{400000/\sqrt{3}}{110/\sqrt{3}} \quad (5.1)$$

$$\begin{aligned} X_{T\text{actual}} &= X_{T\text{pu}} \times X_{T\text{base}} \quad (5.2) \\ &= (0.1348) \times \frac{kV^2}{MVA_{\text{base}}} \\ &= (0.1348) \times \frac{400^2}{500} \\ &= 43.136\Omega \end{aligned}$$

Now transferring the reactance of the line to the 400kV side:-

$$\begin{aligned} X_L &= (0.28681 \times 25) \times \left(\frac{400}{132}\right)^2 \quad (5.3) \\ &= 65.843\Omega \end{aligned}$$

If the first zone of the transformer feeder is set to 80% then:-

$$\begin{aligned} X_{1\text{pri}} &= 0.8(X_T + X_L) \quad (5.4) \\ &= 0.8(43.136 + 65.843) \\ &= 87.183\Omega \end{aligned}$$

Now percentage of the line protected by Zone 1:-

$$\begin{aligned}
 &= \frac{X_1 - X_T}{X_L} & (5.5) \\
 &= \frac{87.183 - 43.136}{65.843} \\
 &= 66.9\%
 \end{aligned}$$

The Zone 1 setting in secondary ohms is calculated as follows:-

$$\begin{aligned}
 X_{1_{\text{sec}}} &= X_{1_{\text{pri}}} \times \frac{CT_{\text{RATIO}}}{VT_{\text{RATIO}}} & (5.6) \\
 &= 87.183 \times \frac{1000/1}{\frac{400000/\sqrt{3}}{110/\sqrt{3}}} \\
 &= 23.98\Omega
 \end{aligned}$$

However the voltage changes caused by the tap-changer should be considered (Cigré 2008). Now if we assume that the tap changer has a tapping range of -5% to +15% then at the highest tap:-

$$\begin{aligned}
 X_L &= (0.28681 \times 25) \times \left(\frac{V_p}{V_s}\right)_{\text{min}}^2 & (5.7) \\
 &= (0.28681 \times 25) \times \left(\frac{400 \times 0.85}{132}\right)^2 \\
 &= 47.571\Omega
 \end{aligned}$$

If the first zone of the transformer feeder is set to 80% then:-

$$\begin{aligned}
 X_{1_{\text{pri}}} &= 0.8(X_T + X_L) & (5.8) \\
 &= 0.8(43.136 + 47.571) \\
 &= 72.566\Omega
 \end{aligned}$$

It must be noted that the percentage reactance of the transformer also changes due to its tap settings. This has been neglected in this example, but will be considered in Section 3.3

Now the Zone 1 setting in secondary ohms at the highest tap is calculated as follows:-

$$\begin{aligned}
 X_{1\text{sec}} &= X_{1\text{pri}} \times \frac{CT_{\text{RATIO}}}{VT_{\text{RATIO}}} \quad (5.9) \\
 &= 72.566 \times \frac{1000/1}{\frac{400000/\sqrt{3}}{110/\sqrt{3}}} \\
 &= 19.956\Omega
 \end{aligned}$$

This demonstrates how the tap-changer influences the distance measured by the impedance relay.

5.2 Case-Study-Example 2

The objective of this Case-Study-Example is to show the setting calculation to protect the line on the secondary side of the transformer, which has an impedance of 10Ω. In Case 1 both the CT and VT will be located on the secondary side of the transformer. In Case 2 the CT will be located on the primary side and the VT will remain on the secondary side.

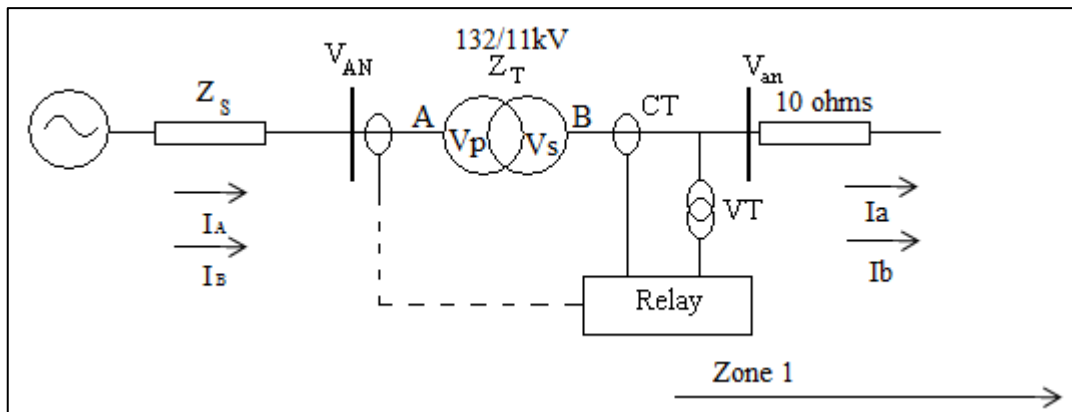


Figure 5-1: Network for Case-Study-Example 2

The parameters in Figure 5-1 are as follows:

Transformer vector group – Yd1

Transformer ratio (132/11kV) (Vp/Vs)

HV CT ratio = 200/1

MV CT ratio = 1000/1

$$Z_L = (10 \angle 75^\circ) \Omega$$

$$\text{HV VT ratio} = \frac{\frac{132000}{\sqrt{3}}}{\frac{110}{\sqrt{3}}}$$

$$\text{MV CT ratio} = \frac{\frac{11000}{\sqrt{3}}}{\frac{110}{\sqrt{3}}}$$

I_A and I_B are the A and B phase load currents on the 132kV side of the transformer and I_a and I_b are the A and B phase load currents on the 11kV side of the transformer. V_{AN} and V_{BN} are the A and B phase voltages on the 132kV side of the transformer and V_{an} and V_{bn} are the A and B phase voltages on the 11kV side of the transformer.

$$I_A = (100 \angle -30^\circ) \text{A}$$

$$I_B = (100 \angle -150^\circ) \text{A}$$

$$I_a = (1200 \angle -60^\circ) \text{A}$$

$$I_b = (1200 \angle -180^\circ) \text{A}$$

$$V_{AN} = \left(\frac{132}{\sqrt{3}} \angle 0^\circ \right) \text{kV}$$

$$V_{BN} = \left(\frac{132}{\sqrt{3}} \angle -120^\circ \right) \text{kV}$$

$$V_{an} = \left(\frac{11}{\sqrt{3}} \angle -30^\circ \right) \text{kV}$$

$$V_{bn} = \left(\frac{132}{\sqrt{3}} \angle -150^\circ \right) \text{kV}$$

In star/delta transformers there is a 30° phase shift between primary and secondary line voltages (Theraja & Theraja 2005).

Case 1

The secondary impedance which is the value in the relay setting is calculated as follows:-

$$\begin{aligned} Z_1 (\text{secondary}) &= Z_{L (\text{primary})} \times \frac{CT_{\text{ratio}}}{VT_{\text{ratio}}} & (5.10) \\ &= 10\angle 75^0 \times \frac{\frac{1000}{1}}{\frac{11000}{110}} \\ &= (100\angle 75^0)\Omega \end{aligned}$$

Case 2

The secondary impedance which is the value in the relay setting is calculated as follows:-

$$\begin{aligned} Z_1 (\text{secondary}) &= Z_{L (\text{primary})} \times \frac{CT_{\text{ratio}}}{VT_{\text{ratio}}} \times \frac{V_P}{V_S} & (5.11) \\ &= 10\angle 75^0 \times \frac{\frac{200}{1}}{\frac{132000}{110}} \times \frac{132000}{11000} \\ &= (240\angle 75^0)\Omega \end{aligned}$$

Note that the calculation for the setting in Case 2 has been multiplied by the factor V_p/V_s since the CT is located on the other side of the transformer compared to the VT and the direction of the zone.

In Case 1 the traditional phase-to-phase measuring loop will measure the following secondary value under the load conditions described:-

$$\begin{aligned} Z_{\text{measured}} &= \frac{V_{an} - V_{bn}}{I_a - I_b} & (5.12) \\ &= \frac{63.5\angle -30^0 - 63.5\angle -150^0}{1.2\angle -60^0 - 1.2\angle -180^0} \\ &= (52.917\angle 30^0)\Omega \end{aligned}$$

Now, percentage of the measured impedance compared to the Zone 1 setting is:-

$$\begin{aligned} &= \frac{52.917}{100} \times 100\% \\ &= 52.917\% \end{aligned}$$

In Case 2 the phase-to-phase measuring loop will measure the following secondary value under the load conditions described:-

$$\begin{aligned} Z_{\text{measured}} &= \frac{V_{\text{an}} - V_{\text{bn}}}{I_{\text{A}} - I_{\text{B}}} && (5.13) \\ &= \frac{63.5\angle-30^{\circ} - 63.5\angle-150^{\circ}}{0.5\angle-60^{\circ} - 0.5\angle-180^{\circ}} \\ &= (127\angle30^{\circ})\Omega \end{aligned}$$

Note that the CT currents have been compensated in the above equation. The CT secondary currents have been put through a Yd1 interposing transformer.

Now, percentage of the measured impedance compared to zone 1 setting:-

$$\begin{aligned} &= \frac{127}{240} \times 100\% \\ &= 52.917\% \end{aligned}$$

Therefore the percentage impedance measured is identical for both Case 1 and Case 2. This proves that the apparent distance measured by the relay is correct with respect to its settings when the instrument transformers connected to the distance relay are located on either side of the power transformer.

5.3 Case-Study-Example 3

The following results were obtained during the short circuit tests of a 400/132/22kV 500MVA autotransformer, which has the vector group YNa0d1.

$$Z_{\text{ps}} = 13.48\%$$

$$Z_{\text{pt}} = 123.88\%$$

$$Z_{st} = 107.13\%$$

Z_{ps} - primary to secondary positive sequence impedance

Z_{pt} - primary to tertiary positive sequence impedance

Z_{st} - secondary to tertiary positive sequence impedance

Z_p - primary winding positive sequence impedance

Z_s - secondary winding positive sequence impedance

Z_t - tertiary winding positive sequence impedance

Converting the impedance to the base MVA: 100MVA

$$\begin{aligned} Z_{ps} &= \frac{\text{Base MVA}}{\text{Rated MVA}} \times \text{percentage impedance at rated MVA} & (5.14) \\ &= \frac{100}{500} \times 13.48 \\ &= 2.7\% \end{aligned}$$

$$\begin{aligned} Z_{pt} &= \frac{\text{Base MVA}}{\text{Rated MVA}} \times \text{percentage impedance at rated MVA} & (5.15) \\ &= \frac{100}{500} \times 123.88 \\ &= 24.78\% \end{aligned}$$

$$\begin{aligned} Z_{st} &= \frac{\text{Base MVA}}{\text{Rated MVA}} \times \text{percentage impedance at rated MVA} & (5.16) \\ &= \frac{100}{500} \times 107.13 \\ &= 21.43\% \end{aligned}$$

Z_p , Z_s and Z_t can be calculated using the following equations (Winders 2002):-

$$\begin{aligned} Z_p &= \frac{1}{2} (Z_{ps} + Z_{pt} - Z_{st}) & (5.17) \\ &= \frac{1}{2} (2.7 + 24.78 - 21.43) \\ &= 3.025\% \end{aligned}$$

$$\begin{aligned}
 Z_s &= \frac{1}{2}(Z_{ps} + Z_{st} - Z_{pt}) & (5.18) \\
 &= \frac{1}{2}(2.7 + 21.43 - 24.78) \\
 &= -0.325\%
 \end{aligned}$$

$$\begin{aligned}
 Z_t &= \frac{1}{2}(Z_{pt} + Z_{st} - Z_{ps}) & (5.19) \\
 &= \frac{1}{2}(24.78 + 21.43 - 2.7) \\
 &= 21.755\%
 \end{aligned}$$

5.4 Case-Study-Example 4

Figure 5-2 shows the autotransformer from Case-Study-Example 3 incorporated into a network where the source impedances are converted to a 100MVA base for both the 400kV and 132kV sides.

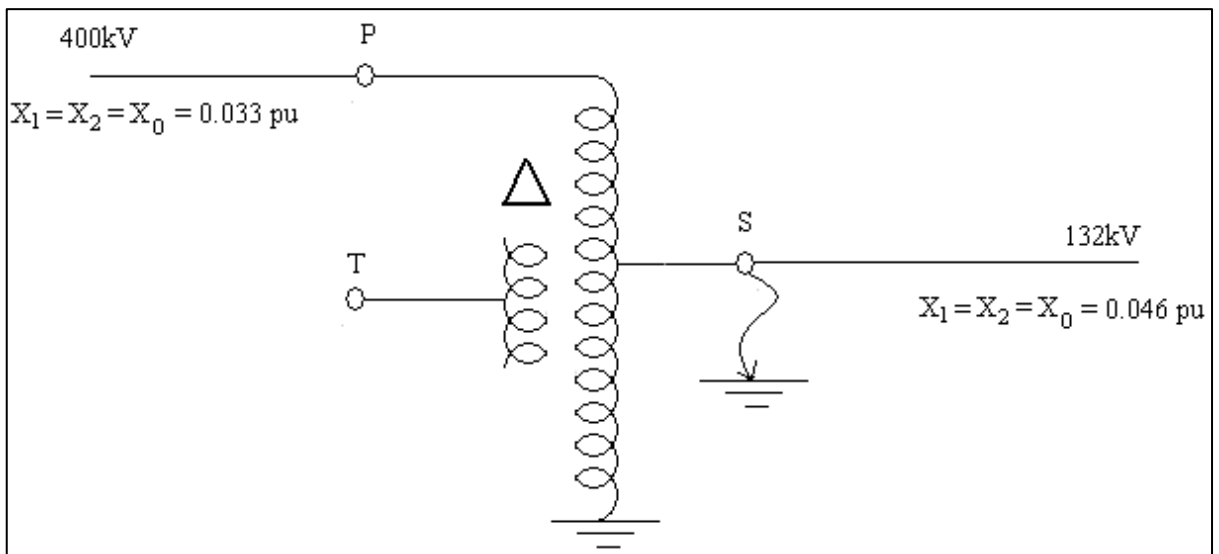


Figure 5-2: Network with an autotransformer – Case-Study-Example 4

According to Blackburn and Domin (2007) the procedure to calculate the distribution of currents within the autotransformer for a fault at S is as follows:

From Case-Study-Example 3 and section 3.1.1 the positive, negative and zero sequence impedances of the autotransformer converted to the 100MVA base are:

$$X_{p1} = X_{p2} = j0.03025$$

$$X_{s1} = X_{s2} = -j0.00325$$

$$X_{t1} = X_{t2} = j0.21755$$

$$X_{p0} = j0.03078$$

$$X_{s0} = -j0.00372$$

$$X_{i0} = j0.20752$$

Figures 5-3 and 5-4 show the positive sequence diagram and zero sequence diagram respectively for Case-Study-Example 3.

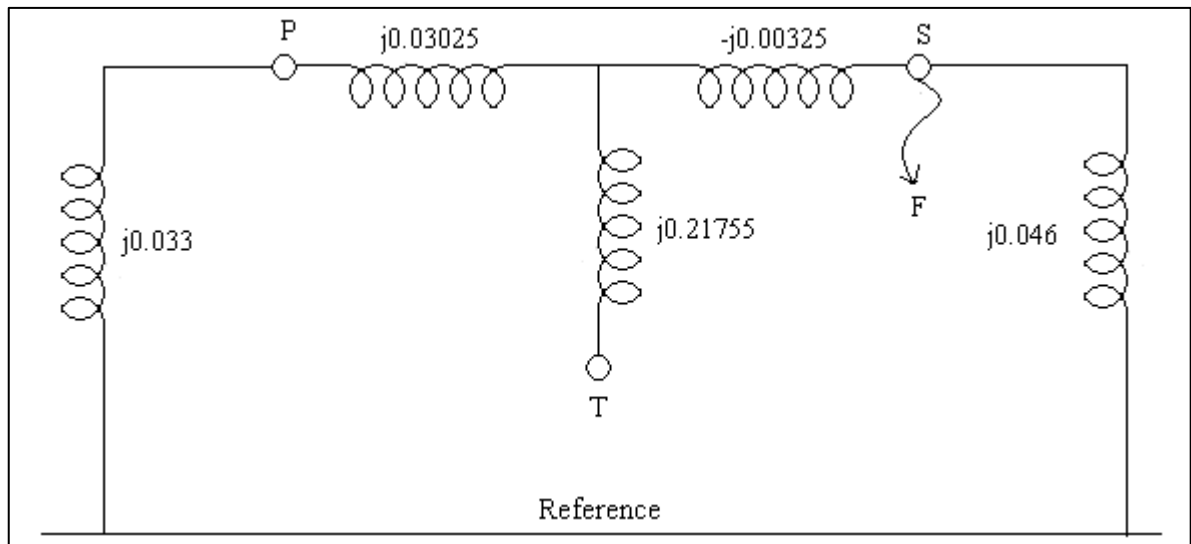


Figure 5-3: Positive sequence reactance diagram for Case-Study-Example 4

$$X_{th1} = X_{th2} = \frac{(0.033 + 0.03025 - 0.00325)(0.046)}{0.033 + 0.03025 + 0.046 - 0.00325} \quad (5.20)$$

$$= 0.026\text{pu}$$

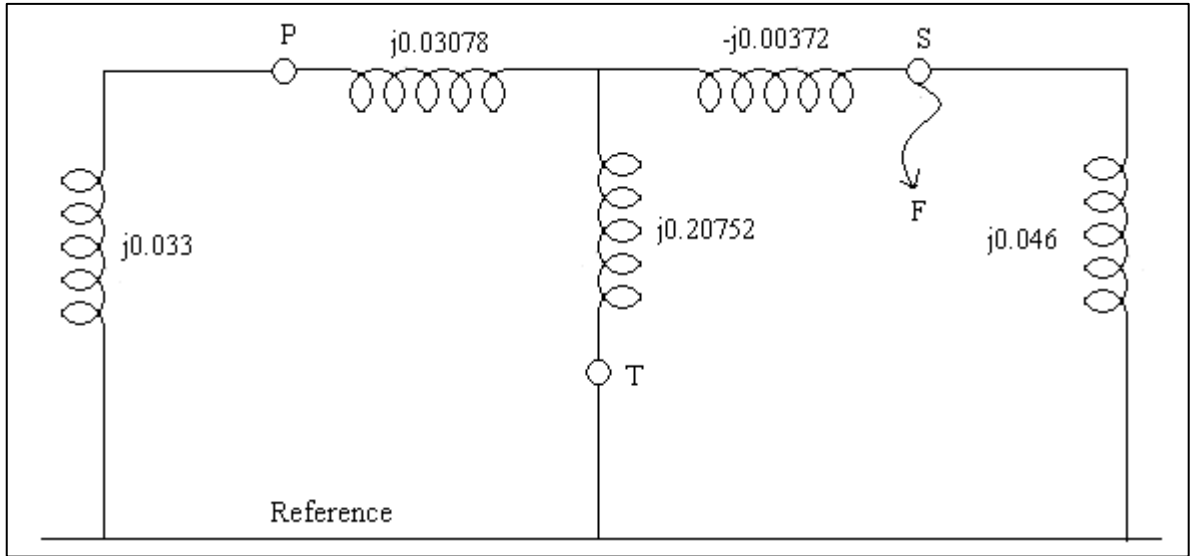


Figure 5-4: Zero sequence reactance diagram for Case-Study-Example 4

Solving initially the left hand side of the zero sequence diagram:-

$$\frac{(0.033 + 0.03078)(0.20752)}{0.033 + 0.03078 + 0.20752} = 0.0488\text{pu}$$

$$X_{\text{th0}} = \frac{(0.0488 - 0.00372)(0.046)}{0.0488 - 0.00372 + 0.046} \quad (5.21)$$

$$= 0.0288\text{pu}$$

The distribution of fault current in the zero sequence reactance diagram where $I_{\text{fault}} = 1\text{pu}$ is shown in Figure 5-5.

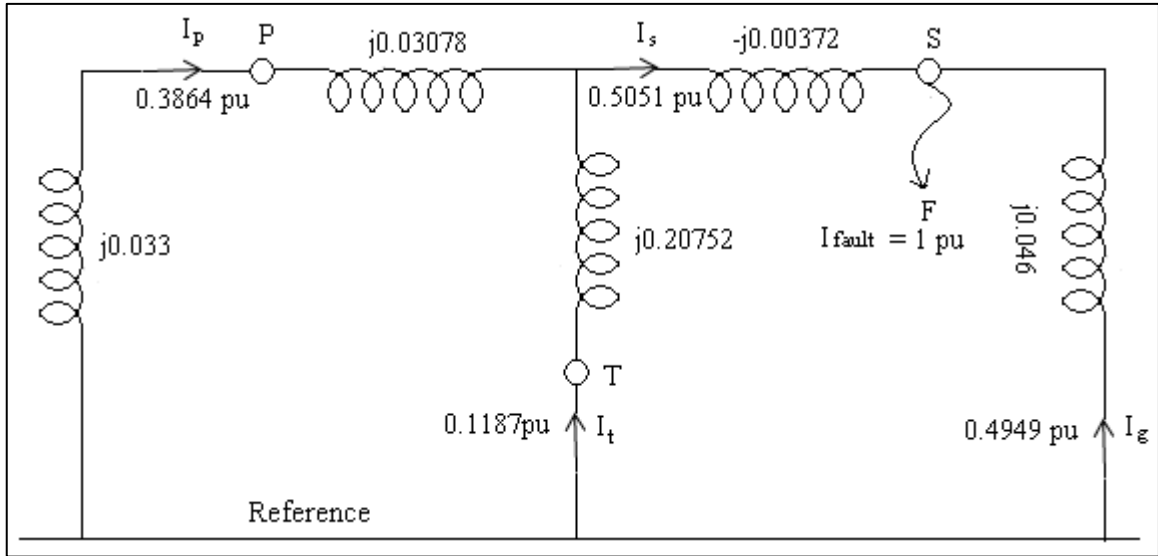


Figure 5-5: Distribution of fault current for zero sequence reactance diagram - Case-Study-Example 4

Using the current divider rule the distribution of currents for the zero sequence diagram is calculated as follows:-

$$I_s = \frac{0.046}{0.0488 - 0.00372 + 0.046} = 0.5051 \text{ pu} \quad (5.22)$$

$$I_g = \frac{0.0488 - 0.00372}{0.0488 - 0.00372 + 0.046} = 0.4949 \text{ pu} \quad (5.23)$$

$$I_t = 0.5051 \times \frac{0.033 + 0.03078}{0.033 + 0.03078 + 0.20752} = 0.1187 \text{ pu} \quad (5.24)$$

$$I_p = 0.5051 \times \frac{0.20752}{0.033 + 0.03078 + 0.20752} = 0.3864 \text{ pu} \quad (5.25)$$

The distribution of fault current in the positive/negative sequence reactance diagram where $I_{\text{fault}} = 1 \text{ pu}$, is shown in Figure 5-6.

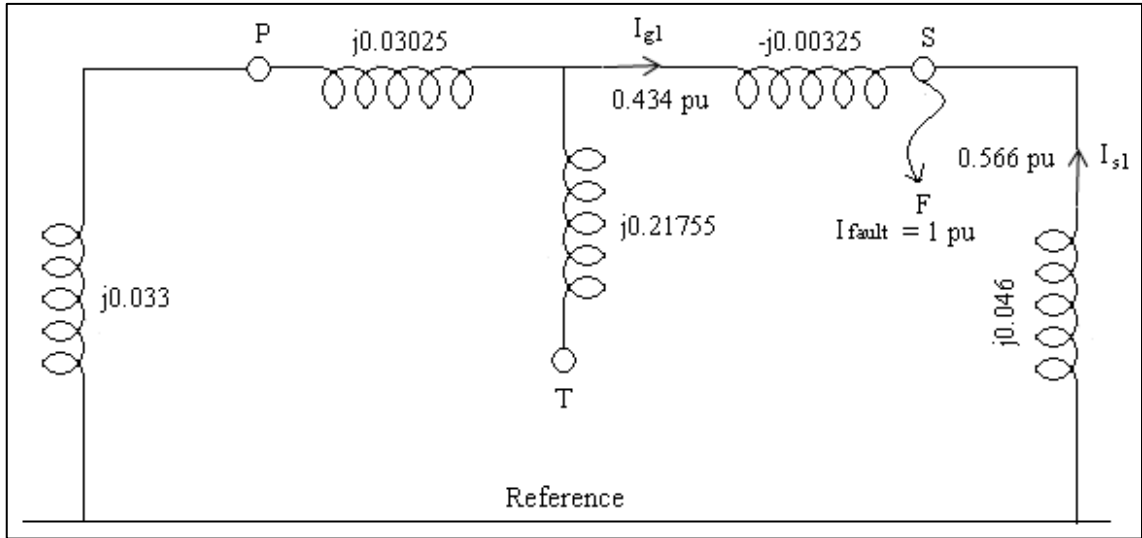


Figure 5-6: Distribution of fault current for the positive/negative sequence reactance diagram - Case-Study-Example 4

$$I_{g1} = \frac{0.046}{0.046 - 0.00325 + 0.03025 + 0.033} = 0.434 \text{ pu} \quad (5.26)$$

$$I_{s1} = \frac{0.03025 - 0.00325 + 0.033}{0.046 - 0.00325 + 0.03025 + 0.033} = 0.566 \text{ pu} \quad (5.27)$$

For the single line to ground fault current $I_0 = I_1 = I_2$:-

$$\begin{aligned} I_0 = I_1 = I_2 &= \frac{1}{X_{th1} + X_{th2} + X_{th0}} \quad (5.28) \\ &= \frac{1}{0.026 + 0.026 + 0.0228} \\ &= 13.369 \text{ pu} \end{aligned}$$

$$I_{f_{pu}} = 3I_0 = 40.107 \text{ pu} \quad (5.29)$$

$$I_{base} = \frac{100 \times 10^6}{\sqrt{3} \times 132000} = 437.387 \text{ A} \quad (5.30)$$

$$I_{actual} = I_{base} \times I_{f_{pu}} = 17542.242 \text{ A} \quad (5.31)$$

Figure 5-7 shows the magnitude and direction of the fault current distribution for the single line to ground fault occurring on the 132kV terminal of the autotransformer. The values of the currents shown in Figure 5-7 are calculated as follows:-

$$\begin{aligned} I_H &= I_{\text{base}} \left(\frac{132}{400} \right) [I_1(0.434) + I_2(0.434) + I_0(0.3864)] \quad (5.32) \\ &= 437.387 \times 13.369 \times 0.33(0.434 + 0.434 + 0.3864) \\ &= 2420.554\text{A} \end{aligned}$$

$$\begin{aligned} I_M &= I_{\text{base}} [I_1(0.434) + I_2(0.434) + I_0(0.5051)] \quad (5.33) \\ &= 437.387 \times 13.369(0.434 + 0.434 + 0.5051) \\ &= 8029.102\text{A} \end{aligned}$$

$$\begin{aligned} I_G &= I_{\text{base}} [I_1(0.566) + I_2(0.566) + I_0(0.4949)] \quad (5.34) \\ &= 437.387 \times 13.369(0.566 + 0.566 + 0.4949) \\ &= 9513.179\text{A} \end{aligned}$$

$$\begin{aligned} \text{Current up the 132 kV neutrals} &= 3I_0(0.4949)I_{\text{base}} \quad (5.35) \\ &= 3 \times (13.369)(0.4949) \times 437.387 \\ &= 8681.675\text{A} \end{aligned}$$

$$\begin{aligned} \text{Current up the 400 kV neutrals} &= 3I_0 \left(\frac{132}{400} \right) (0.3864) I_{\text{base}} \quad (5.36) \\ &= 3 \times (0.33)(13.369)(0.3864) \times 437.387 \\ &= 2236.851\text{A} \end{aligned}$$

$$\begin{aligned} \text{Current up the autotransformer neutral} &= 3I_0 I_{\text{base}} \left(0.5051 - 0.3864 \times \frac{132}{400} \right) \quad (5.37) \\ &= 3 \times 13.369 \times 437.387(0.5051 - 0.128) \\ &= 6623.755\text{A} \\ &= I_C \end{aligned}$$

$$I_F = I_{\text{base}} \times I_{f_{\text{pu}}} = 437.387 \times 40.107 = 17542.242\text{A} \quad (5.38)$$

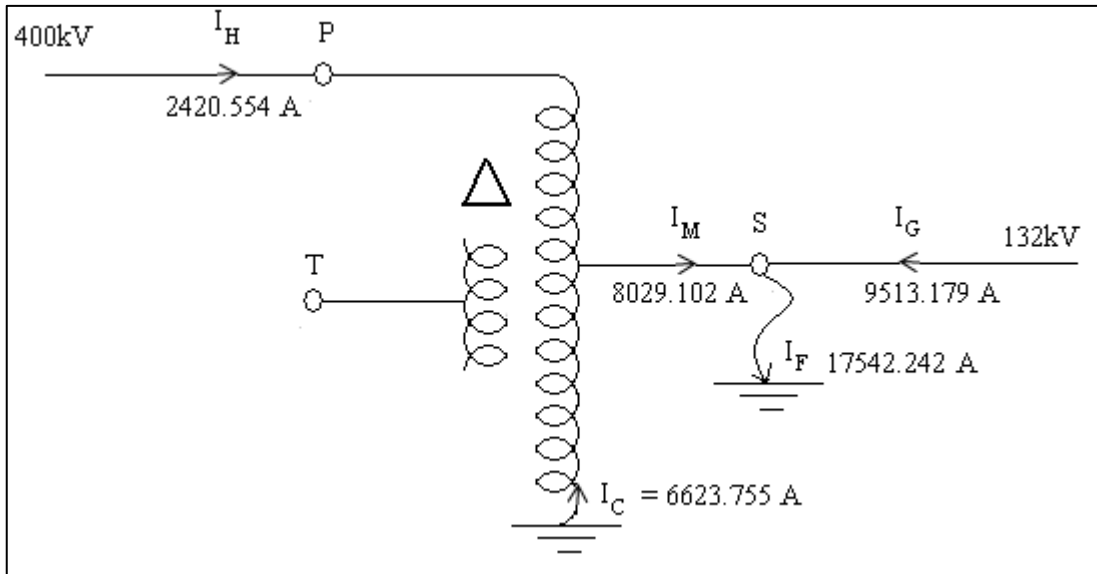


Figure 5-7: Network diagram for Case-Study-Example 4 showing fault current distribution

5.5 Case-Study-Example 5

Figures 5-8, 5-9 and 5-10 shows the positive sequence diagram, zero sequence diagram and network diagram respectively for Case-Study-Example 5.

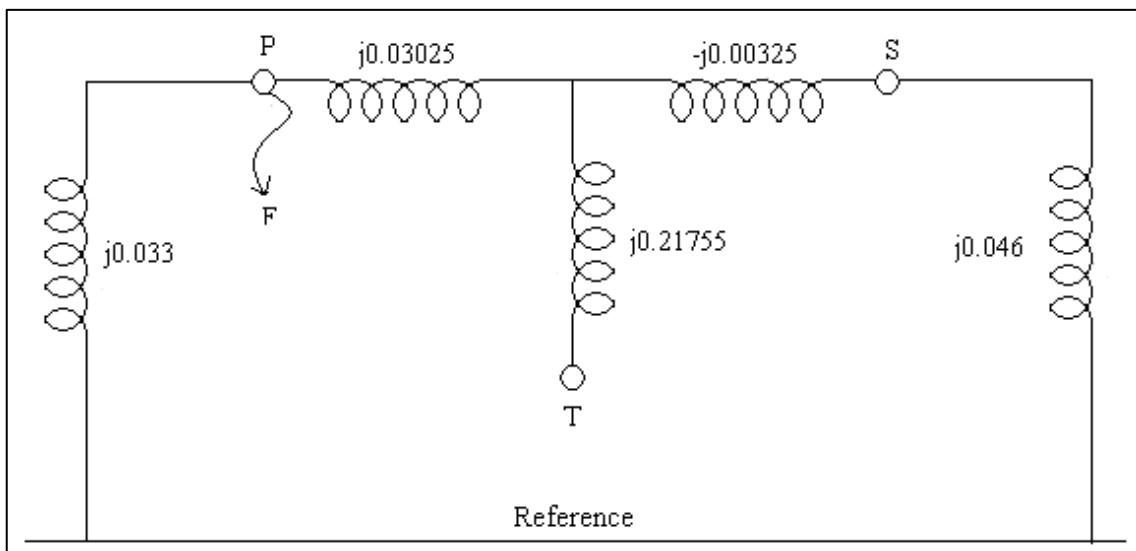


Figure 5-8: Positive sequence reactance diagram for Case-Study-Example 5

$$X_{th1} = X_{th2} = \frac{(0.033)(0.03025 - 0.00325 + 0.046)}{0.033 + 0.03025 + 0.046 - 0.00325} \quad (5.39)$$

$$= 0.0277\text{pu}$$

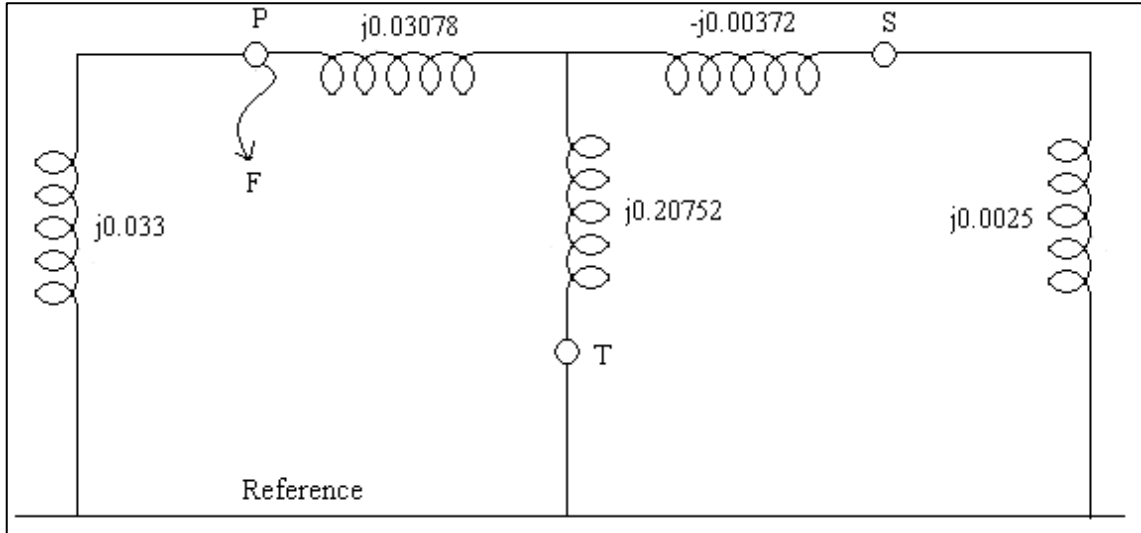


Figure 5-9: Zero sequence reactance diagram for Case-Study-Example 5

Solving initially the right hand side of the zero sequence diagram:-

$$\frac{(-0.00372 + 0.0025)(0.20752)}{0.0025 - 0.00372 + 0.20752} = -0.0012\text{pu}$$

$$X_{th0} = \frac{(0.03078 - 0.0012)(0.033)}{0.033 - 0.0012 + 0.03078} \quad (5.40)$$

$$= 0.0156\text{pu}$$

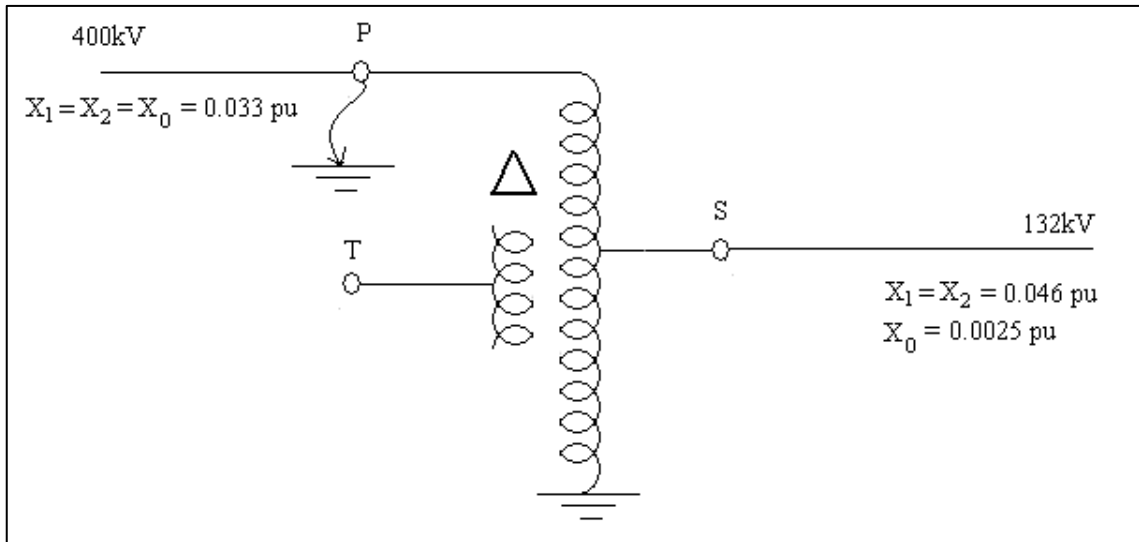


Figure 5-10: Network diagram for Case-Study-Example 5

The distribution of fault current in the zero sequence reactance diagram where $I_{\text{fault}} = 1 \text{ pu}$ is shown in Figure 5-11 below.

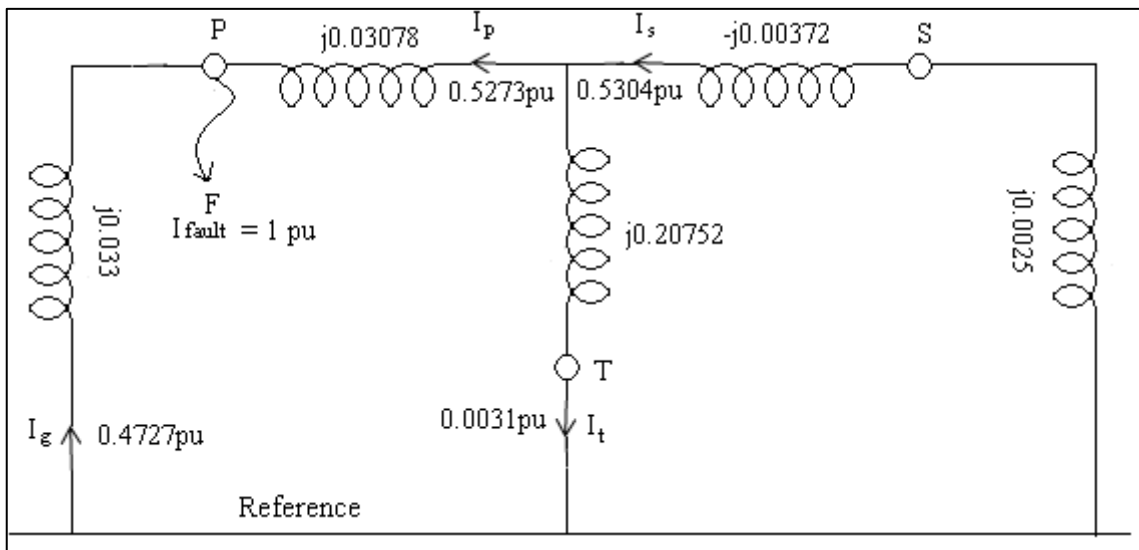


Figure 5-11: Distribution of fault current for zero sequence reactance diagram - Case-Study-Example 5

Using the current divider rule the distribution of currents for the zero sequence diagram is calculated as follows:-

$$I_p = \frac{0.033}{0.03078 - 0.0012 + 0.033} = 0.5273 \text{ pu} \quad (5.41)$$

$$I_g = \frac{0.03078 - 0.0012}{0.03078 - 0.0012 + 0.033} = 0.4727\text{pu} \quad (5.42)$$

$$I_t = 0.5273 \times \frac{0.0025 - 0.00372}{0.20752 - 0.00372 + 0.0025} = -0.0031\text{pu} \quad (5.43)$$

$$I_s = 0.5273 \times \frac{0.20752}{0.20752 - 0.00372 + 0.0025} = 0.5304\text{pu} \quad (5.44)$$

The distribution of fault current in the positive/negative sequence reactance diagram where $I_{\text{fault}} = 1\text{pu}$ is shown in Figure 5-12 below.

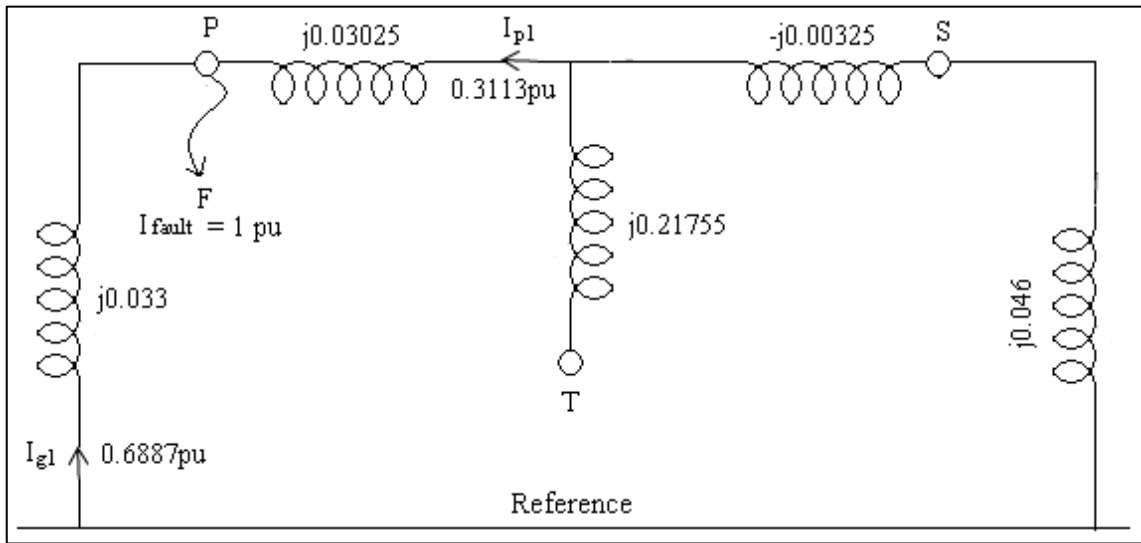


Figure 5-12: Distribution of fault current for the positive/negative sequence reactance diagram – Case-Study-Example 5

$$I_{p1} = \frac{0.033}{0.033 - 0.00325 + 0.03025 + 0.046} = 0.3113\text{pu} \quad (5.45)$$

$$I_{g1} = \frac{0.03025 - 0.00325 + 0.046}{0.046 - 0.00325 + 0.03025 + 0.033} = 0.6887\text{pu} \quad (5.46)$$

For the single line to ground fault current $I_0 = I_1 = I_2$:-

$$\begin{aligned} I_0 = I_1 = I_2 &= \frac{1}{X_{\text{th1}} + X_{\text{th2}} + X_{\text{th0}}} \quad (5.47) \\ &= \frac{1}{0.0277 + 0.0277 + 0.0156} \\ &= 14.085\text{pu} \end{aligned}$$

$$I_{f_{\text{pu}}} = 3I_0 = 42.255\text{pu} \quad (5.48)$$

$$I_{\text{base}} = \frac{100 \times 10^6}{\sqrt{3} \times 400000} = 144.338\text{A} \quad (5.49)$$

$$I_{\text{actual}} = I_{\text{base}} \times I_{\text{fpu}} = 6099.002\text{A} \quad (5.50)$$

Figure 5-13 shows the magnitude and direction of the fault current distribution for the single line to ground fault occurring on the 400kV terminal of the autotransformer. The values of the currents shown in Figure 5-13 are calculated as follows:-

$$\begin{aligned} I_{\text{H}} &= I_{\text{base}}[I_1(0.3113) + I_2(0.3113) + I_0(0.5273)] \quad (5.51) \\ &= 144.338 \times 14.085(0.3113 + 0.3113 + 0.5273) \\ &= 2337.748\text{A} \end{aligned}$$

$$\begin{aligned} I_{\text{M}} &= I_{\text{base}}\left(\frac{400}{132}\right)[I_1(0.3113) + I_2(0.3113) + I_0(0.5304)] \quad (5.52) \\ &= 144.338 \times 14.085 \times 3.03(0.3113 + 0.3113 + 0.5304) \\ &= 7103.181\text{A} \end{aligned}$$

$$\begin{aligned} I_{\text{G}} &= I_{\text{base}}[I_1(0.6887) + I_2(0.6887) + I_0(0.4727)] \quad (5.53) \\ &= 144.338 \times 14.085(0.6887 + 0.6887 + 0.4727) \\ &= 3761.255\text{A} \end{aligned}$$

$$\begin{aligned} \text{Current up the 132 kV neutrals} &= 3I_0\left(\frac{400}{132}\right)(0.5304)I_{\text{base}} \quad (5.54) \\ &= 3 \times (14.085)(3.03)(0.5304) \times 144.338 \\ &= 9802.76\text{A} \end{aligned}$$

$$\begin{aligned} \text{Current up the 400 kV neutrals} &= 3I_0(0.4727)I_{\text{base}} \quad (5.55) \\ &= 3 \times (14.085)(0.4727) \times 144.338 \\ &= 2882.998\text{A} \end{aligned}$$

$$\begin{aligned}
 \text{Current up the} & & & = 3I_0I_{\text{base}} \left(0.5273 - 0.5304 \times \left(\frac{400}{132} \right) \right) & (5.56) \\
 \text{autotransformer neutral} & & & = 3 \times 14.085 \times 144.338(0.5273 - 1.607) \\
 & & & = -6586.756\text{A} \\
 & & & = I_C
 \end{aligned}$$

I_C has a negative value which indicates that the current flows down the neutral of the transformer.

$$I_F = I_{\text{base}} \times I_{f_{\text{pu}}} = 144.338 \times 42.2535 = 6099.002\text{A} \quad (5.57)$$

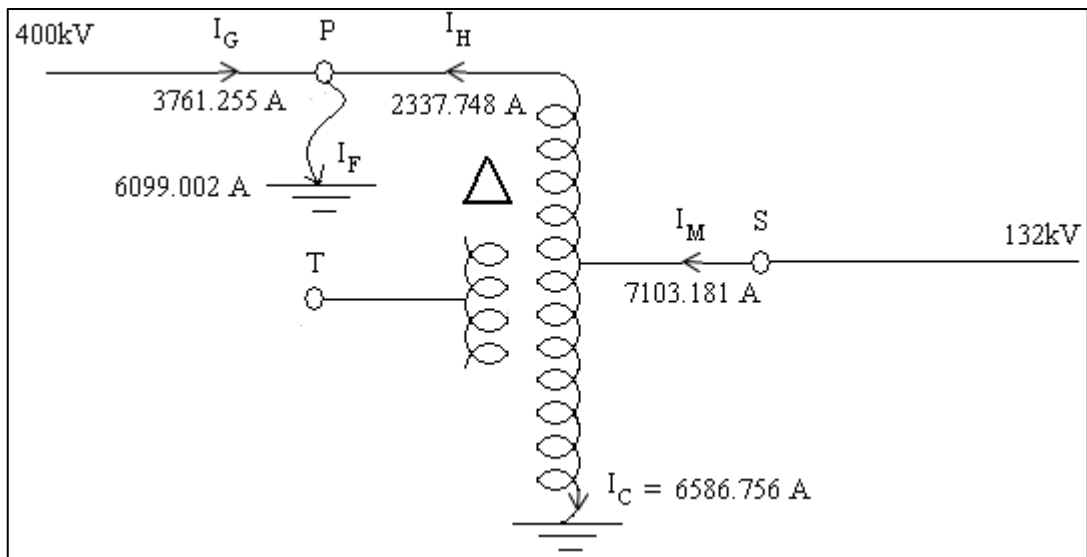


Figure 5-13: Network diagram for Case-Study-Example 5 showing fault current distribution

5.6 Case-Study-Example 6

Figure 5-14 shows the autotransformer from Case-Study-Example 3 incorporated in a network where all the impedances are converted to a 100MVA base.

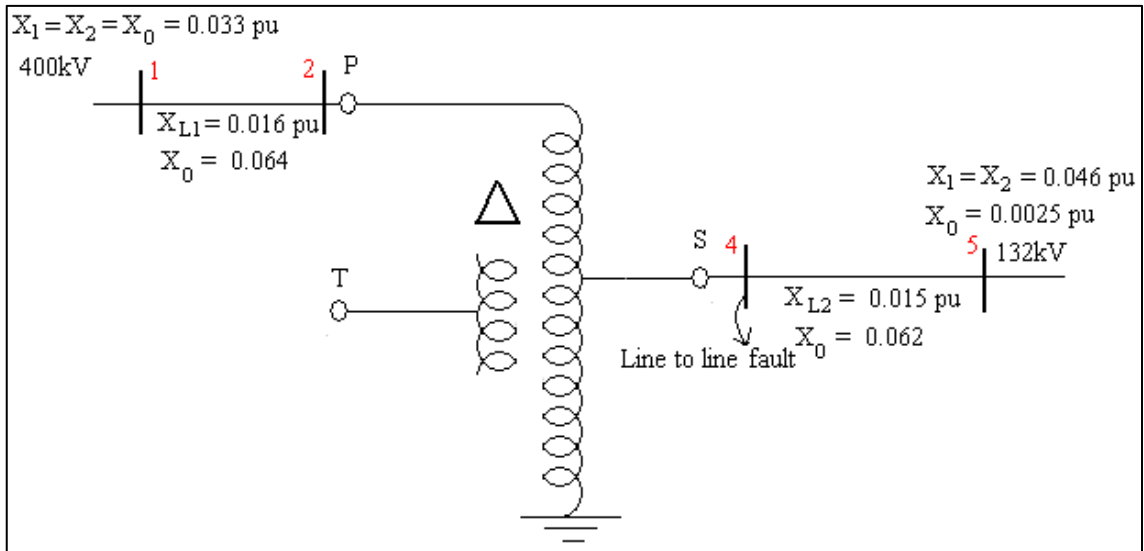


Figure 5-14: Network diagram for Case-Study-Example 6

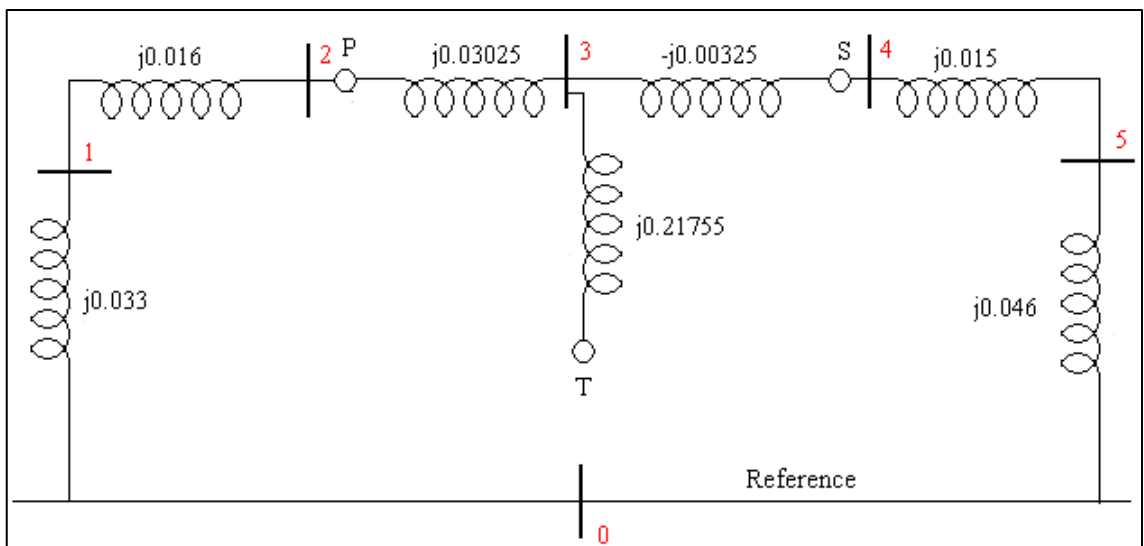


Figure 5-15: Positive and negative sequence reactance diagram for Case-Study-Example 6

Figure 5-15 shows the positive sequence reactance diagram for Case-Study-Example 6. Bus 3 in Figure 5-15 represents an imaginary node between the primary, secondary and tertiary windings of the autotransformer. The fault calculation for the line-to-line fault on bus 4 was solved using the Z_{bus} method (Grainger & Stevenson 1994).

$$Z_{bus,1} = [j0.033] \quad (5.58)$$

$$Z_{bus,2} = \begin{bmatrix} j0.033 & j0.033 \\ j0.033 & j0.049 \end{bmatrix} \quad (5.59)$$

$$Z_{bus,3} = \begin{bmatrix} j0.033 & j0.033 & j0.033 \\ j0.033 & j0.049 & j0.049 \\ j0.033 & j0.049 & j0.079 \end{bmatrix} \quad (5.60)$$

$$Z_{bus,4} = \begin{bmatrix} j0.033 & j0.033 & j0.033 & j0.033 \\ j0.033 & j0.049 & j0.049 & j0.049 \\ j0.033 & j0.049 & j0.079 & j0.079 \\ j0.033 & j0.049 & j0.079 & j0.076 \end{bmatrix} \quad (5.61)$$

$$Z_{bus,5} = \begin{bmatrix} j0.033 & j0.033 & j0.033 & j0.033 & j0.033 \\ j0.033 & j0.049 & j0.049 & j0.049 & j0.049 \\ j0.033 & j0.049 & j0.079 & j0.079 & j0.079 \\ j0.033 & j0.049 & j0.079 & j0.076 & j0.076 \\ j0.033 & j0.049 & j0.079 & j0.076 & j0.091 \end{bmatrix} \quad (5.62)$$

$$Z_{bus,6} = \begin{bmatrix} j0.033 & j0.033 & j0.033 & j0.033 & j0.033 & j0.033 \\ j0.033 & j0.049 & j0.049 & j0.049 & j0.049 & j0.049 \\ j0.033 & j0.049 & j0.079 & j0.079 & j0.079 & j0.079 \\ j0.033 & j0.049 & j0.079 & j0.076 & j0.076 & j0.076 \\ j0.033 & j0.049 & j0.079 & j0.076 & j0.091 & j0.091 \\ j0.033 & j0.049 & j0.079 & j0.076 & j0.091 & j0.137 \end{bmatrix} \quad (5.63)$$

The sixth row and column is eliminated by Kron reduction (Grainger & Stevenson 1994).

$$\begin{aligned} Z_{11}(\text{new}) &= Z_{11} - \frac{(Z_{16})(Z_{61})}{Z_{kk} + Z_b} & (5.64) \\ &= j0.033 - \frac{(j0.033)(j0.033)}{j0.137} \\ &= j0.02505 \end{aligned}$$

$$\begin{aligned} Z_{21}(\text{new}) &= Z_{12}(\text{new}) = Z_{21} - \frac{(Z_{26})(Z_{61})}{Z_{55} + Z_b} & (5.65) \\ &= j0.033 - \frac{(j0.049)(j0.033)}{j0.137} \\ &= j0.02120 \end{aligned}$$

$$\begin{aligned}
Z_{22}(\text{new}) &= Z_{22} - \frac{(Z_{26})(Z_{62})}{Z_{kk} + Z_b} & (5.66) \\
&= j0.049 - \frac{(j0.049)(j0.049)}{j0.137} \\
&= j0.03147
\end{aligned}$$

$$\begin{aligned}
Z_{31}(\text{new}) &= Z_{13}(\text{new}) = Z_{13} - \frac{(Z_{16})(Z_{63})}{Z_{66}} & (5.67) \\
&= j0.033 - \frac{(j0.033)(j0.079)}{0.137} \\
&= j0.01397
\end{aligned}$$

$$\begin{aligned}
Z_{41}(\text{new}) &= Z_{14}(\text{new}) = Z_{41} - \frac{(Z_{46})(Z_{61})}{Z_{kk} + Z_b} & (5.68) \\
&= j0.033 - \frac{(j0.076)(j0.033)}{0.137} \\
&= j0.01469
\end{aligned}$$

$$\begin{aligned}
Z_{32}(\text{new}) &= Z_{23}(\text{new}) = Z_{32} - \frac{(Z_{36})(Z_{62})}{Z_{kk} + Z_b} & (5.69) \\
&= j0.049 - \frac{(j0.079)(j0.049)}{0.137} \\
&= j0.02074
\end{aligned}$$

$$\begin{aligned}
Z_{42}(\text{new}) &= Z_{24}(\text{new}) = Z_{42} - \frac{(Z_{46})(Z_{62})}{Z_{kk} + Z_b} & (5.70) \\
&= j0.049 - \frac{(j0.076)(j0.049)}{0.137} \\
&= j0.02182
\end{aligned}$$

$$\begin{aligned}
Z_{43}(\text{new}) &= Z_{34}(\text{new}) = Z_{43} - \frac{(Z_{46})(Z_{63})}{Z_{kk} + Z_b} & (5.71) \\
&= j0.079 - \frac{(j0.076)(j0.079)}{0.137} \\
&= j0.03518
\end{aligned}$$

$$\begin{aligned}
Z_{33 \text{ (new)}} &= Z_{33} - \frac{(Z_{36})(Z_{63})}{Z_{kk} + Z_b} & (5.72) \\
&= j0.079 - \frac{(j0.079)(j0.079)}{j0.137} \\
&= j0.03345
\end{aligned}$$

$$\begin{aligned}
Z_{44 \text{ (new)}} &= Z_{44} - \frac{(Z_{46})(Z_{64})}{Z_{kk} + Z_b} & (5.73) \\
&= j0.076 - \frac{(j0.076)(j0.076)}{j0.137} \\
&= j0.03384
\end{aligned}$$

$$\begin{aligned}
Z_{51 \text{ (new)}} &= Z_{15 \text{ (new)}} = Z_{51} - \frac{(Z_{56})(Z_{61})}{Z_{kk} + Z_b} & (5.74) \\
&= j0.033 - \frac{(j0.091)(j0.033)}{0.137} \\
&= j0.01108
\end{aligned}$$

$$\begin{aligned}
Z_{52 \text{ (new)}} &= Z_{25 \text{ (new)}} = Z_{52} - \frac{(Z_{56})(Z_{62})}{Z_{kk} + Z_b} & (5.75) \\
&= j0.049 - \frac{(j0.091)(j0.049)}{0.137} \\
&= j0.01645
\end{aligned}$$

$$\begin{aligned}
Z_{53 \text{ (new)}} &= Z_{35 \text{ (new)}} = Z_{53} - \frac{(Z_{56})(Z_{63})}{Z_{kk} + Z_b} & (5.76) \\
&= j0.079 - \frac{(j0.091)(j0.079)}{0.137} \\
&= j0.02653
\end{aligned}$$

$$\begin{aligned}
Z_{54 \text{ (new)}} &= Z_{45 \text{ (new)}} = Z_{54} - \frac{(Z_{56})(Z_{64})}{Z_{kk} + Z_b} & (5.77) \\
&= j0.076 - \frac{(j0.091)(j0.076)}{0.137} \\
&= j0.02252
\end{aligned}$$

$$\begin{aligned}
Z_{55 \text{ (new)}} &= Z_{55} - \frac{(Z_{56})(Z_{65})}{Z_{kk} + Z_b} & (5.78) \\
&= j0.091 - \frac{(j0.091)(j0.091)}{j0.137} \\
&= j0.03055
\end{aligned}$$

$$Z_{\text{bus}}^1 = Z_{\text{bus}}^2 = \begin{bmatrix} j0.02505 & j0.02120 & j0.01397 & j0.01469 & j0.01108 \\ j0.02120 & j0.03147 & j0.02074 & j0.02182 & j0.01645 \\ j0.01397 & j0.02074 & j0.03345 & j0.03518 & j0.02653 \\ j0.01469 & j0.02182 & j0.03518 & j0.03348 & j0.02552 \\ j0.01108 & j0.01645 & j0.02653 & j0.02552 & j0.03055 \end{bmatrix} \quad (5.79)$$

For the line-to-line (yellow and blue phase) fault current at Bus 4 $I_0 = 0$ and $I_1 = -I_2$:-

$$\begin{aligned}
I_1 &= -I_2 = \frac{1}{Z_{44}^1 + Z_{44}^2} & (5.80) \\
&= \frac{1}{j0.03384 + j0.03384} \\
&= -j14.775\text{pu}
\end{aligned}$$

$$\begin{aligned}
I_{\text{fault}} &= I_Y = a^2 I_1 + a I_2 & (5.81) \\
&= (1\angle 240^\circ)(-j14.775) + (1\angle 120^\circ)(j14.775) \\
&= (25.59\angle 180^\circ)\text{pu}
\end{aligned}$$

$$\begin{aligned}
I_B &= a I_1 + a^2 I_2 & (5.82) \\
&= (1\angle 120^\circ)(-j14.775) + (1\angle 240^\circ)(j14.775) \\
&= 25.59\text{pu}
\end{aligned}$$

The distribution of fault current in the positive/negative sequence reactance diagram where $I_{\text{fault}} = 1\text{pu}$, is shown in Figure 5-16.

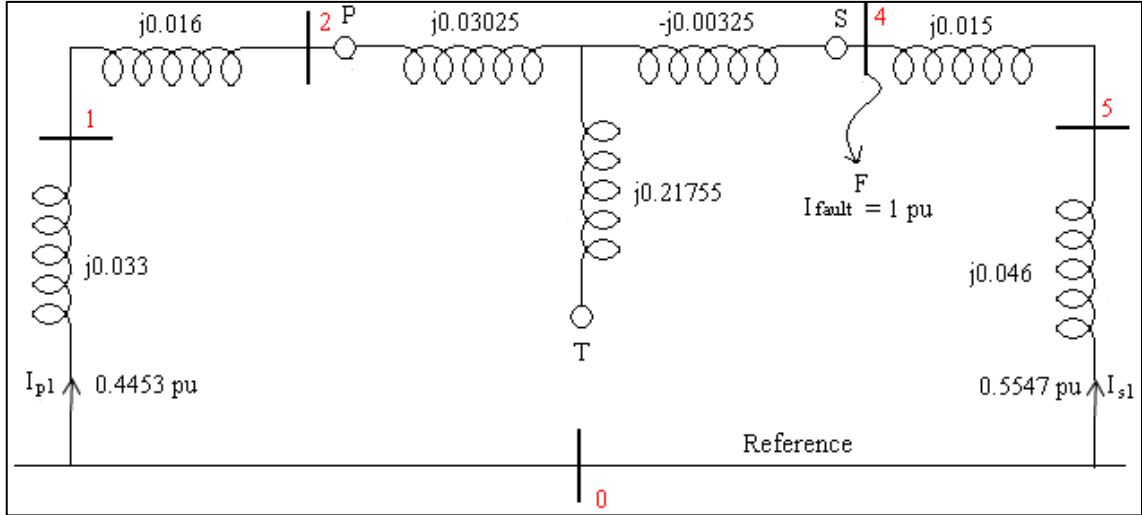


Figure 5-16: Distribution of fault current for the positive/negative sequence reactance diagram – Case-Study-Example 6 and 7

$$I_{p1} = \frac{0.015 + 0.046}{0.033 + 0.016 + 0.03035 - 0.00325 + 0.015 + 0.046} = 0.4453 \text{ pu} \quad (5.83)$$

$$I_{s1} = \frac{0.033 + 0.016 + 0.03025 - 0.00325}{0.033 + 0.016 + 0.03035 - 0.00325 + 0.015 + 0.046} = 0.5547 \text{ pu} \quad (5.84)$$

$$I_{\text{base}} = \frac{100 \times 10^6}{\sqrt{3} \times 132000} = 437.387 \text{ A} \quad (5.85)$$

$$I_{\text{actual}} = I_{\text{base}} \times I_{\text{pu}} = 11192.733 \text{ A} \quad (5.86)$$

The currents at Bus 2 are calculated as follows:-

$$\begin{aligned} I_{R_{\text{bus } 2}} &= [I_1(0.4453)I_{\text{base}} + I_2(0.4453)I_{\text{base}}]^{132/400} \quad (5.87) \\ &= [-j14.775(0.4453)437.387 + j14.775(0.4453)437.387]^{132/400} \\ &= 0 \text{ A} \end{aligned}$$

$$\begin{aligned} I_{Y_{\text{bus } 2}} &= [a^2 I_1(0.4453)I_{\text{base}} + a I_2(0.4453)I_{\text{base}}]^{132/400} \quad (5.88) \\ &= \left[\begin{aligned} &[(1 \angle 240^\circ)(-j14.775)(0.4453)437.387] \\ &+ [(1 \angle 120^\circ)(j14.775)(0.4453)437.387] \end{aligned} \right]^{132/400} \\ &= (1644.829 \angle 180^\circ) \text{ A} \end{aligned}$$

$$\begin{aligned}
I_{B_{bus\ 2}} &= [aI_1(0.4453)I_{base} + a^2I_2(0.4453)I_{base}]^{132/400} \quad (5.89) \\
&= \left[(1\angle 120^\circ)(-j14.775)(0.4453)437.387 \right. \\
&\quad \left. + (1\angle 240^\circ)(j14.775)(0.4453)437.387 \right]^{132/400} \\
&= (1644.829\angle 0^\circ)A
\end{aligned}$$

According to Grainger and Stevenson (1994), the voltages at Bus 2 for a fault at Bus 4 are calculated as follows:-

$$\begin{aligned}
V_{1_{bus\ 2}} &= V_f - Z_{24}^{(1)}I_1 \quad (5.90) \\
&= 1 - (j0.02182)(-j14.775) \\
&= 0.678pu
\end{aligned}$$

$$\begin{aligned}
V_{2_{bus\ 2}} &= -Z_{24}^{(2)}I_2 \quad (5.91) \\
&= (-j0.02182)(j14.775) \\
&= 0.322pu
\end{aligned}$$

$$\begin{aligned}
V_{R_{bus\ 2}} &= V_{1_{bus\ 2}} + V_{2_{bus\ 2}} \quad (5.92) \\
&= 0.678 + 0.322 \\
&= 1pu \\
&= 1 \times 400 / \sqrt{3} \\
&= 230.94kV
\end{aligned}$$

$$\begin{aligned}
V_{Y_{bus\ 2}} &= a^2V_{1_{bus\ 2}} + aV_{2_{bus\ 2}} \quad (5.93) \\
&= (1\angle 240^\circ)0.678 + (1\angle 120^\circ)0.322 \\
&= 0.587\angle -148.34^\circ pu \\
&= (0.587\angle -148.34^\circ) \times 400 / \sqrt{3} \\
&= (135.562\angle -148.34^\circ)kV
\end{aligned}$$

$$\begin{aligned}
V_{B_{bus\ 2}} &= aV_{1_{bus\ 2}} + a^2V_{2_{bus\ 2}} & (5.94) \\
&= (1\angle 120^\circ)0.678 + (1\angle 240^\circ)0.322 \\
&= 0.587\angle 148.34^\circ \text{ pu} \\
&= (0.587\angle 148.34^\circ) \times 400/\sqrt{3} \\
&= (135.562\angle 148.34^\circ)\text{kV}
\end{aligned}$$

$$\begin{aligned}
V_{Y_{B_{bus\ 2}}} &= V_{Y_{bus\ 2}} - V_{B_{bus\ 2}} & (5.95) \\
&= 135.562\angle -148.34^\circ - 135.562\angle 148.34^\circ \\
&= (142.307\angle -90^\circ)\text{kV}
\end{aligned}$$

5.7 Case-Study-Example 7

Figure 5-17 shows the network from Case-Study-Example 6 with a single line to ground fault at bus 4.

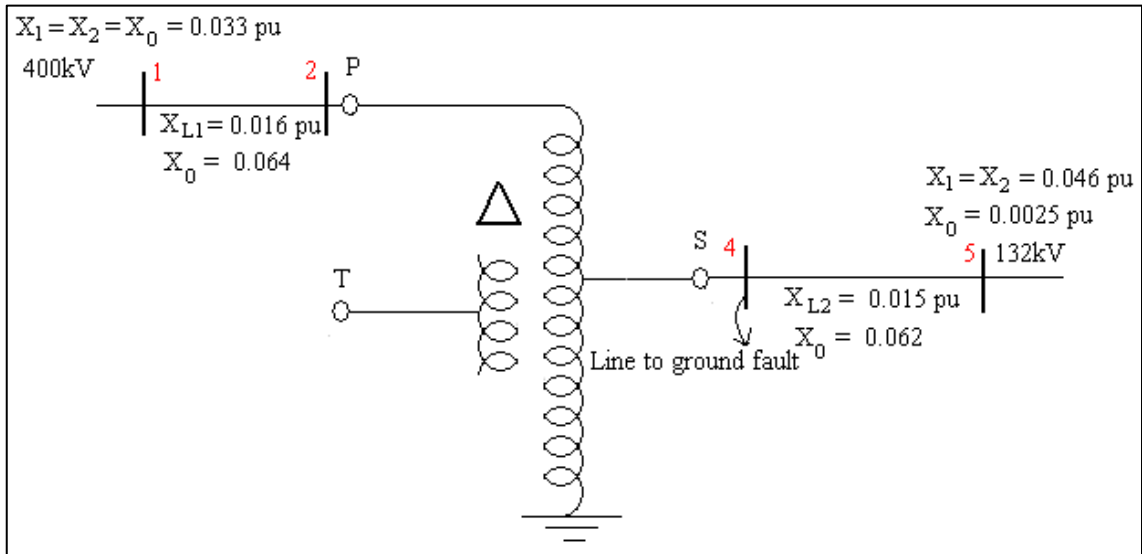


Figure 5-17: Network diagram for Case-Study-Example 7

From Case-Study-Example 6

$$Z_{\text{bus}}^1 = Z_{\text{bus}}^2 = \begin{bmatrix} j0.02505 & j0.02120 & j0.01397 & j0.01469 & j0.01108 \\ j0.02120 & j0.03147 & j0.02074 & j0.02182 & j0.01645 \\ j0.01397 & j0.02074 & j0.03345 & j0.03518 & j0.02653 \\ j0.01469 & j0.02182 & j0.03518 & j0.03348 & j0.02552 \\ j0.01108 & j0.01645 & j0.02653 & j0.02552 & j0.03055 \end{bmatrix} \quad (5.96)$$

Figure 5-18 shows the zero sequence diagram for the network in Figure 5-17.

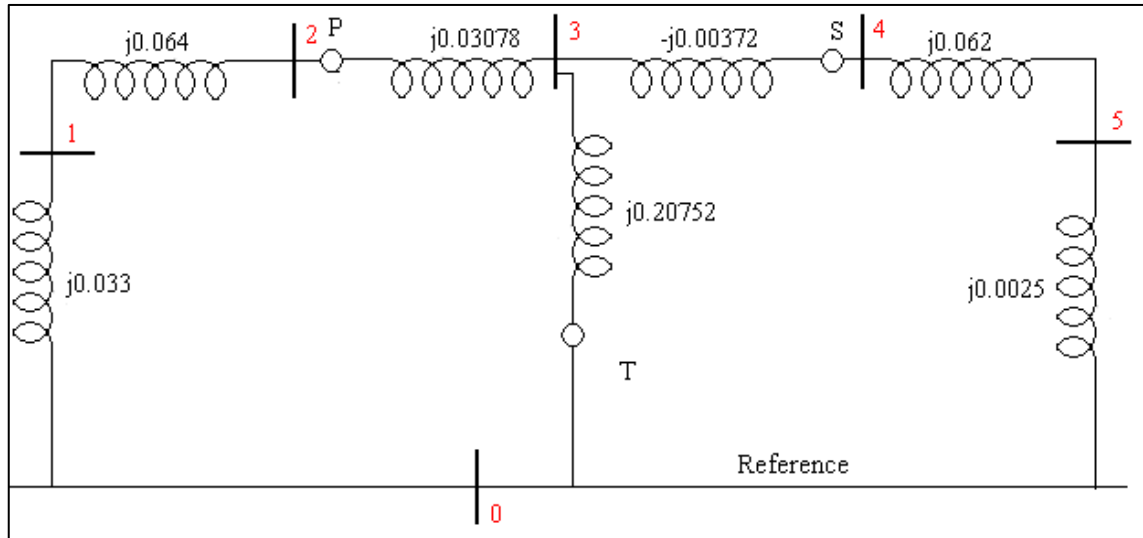


Figure 5-18: Zero sequence reactance diagram for Case-Study-Example 7

$$Z_{\text{bus},1} = [j0.033] \quad (5.97)$$

$$Z_{\text{bus},2} = \begin{bmatrix} j0.033 & j0.033 \\ j0.033 & j0.097 \end{bmatrix} \quad (5.98)$$

$$Z_{\text{bus},3} = \begin{bmatrix} j0.033 & j0.033 & j0.033 \\ j0.033 & j0.097 & j0.097 \\ j0.033 & j0.097 & j0.12778 \end{bmatrix} \quad (5.99)$$

$$Z_{\text{bus},4} = \begin{bmatrix} j0.033 & j0.033 & j0.033 & j0.033 \\ j0.033 & j0.097 & j0.097 & j0.097 \\ j0.033 & j0.097 & j0.12778 & j0.12778 \\ j0.033 & j0.097 & j0.12778 & j0.3353 \end{bmatrix} \quad (5.100)$$

The fourth row and column is eliminated by Kron reduction (Grainger & Stevenson 1994).

$$\begin{aligned}
 Z_{11} \text{ (new)} &= Z_{11} - \frac{(Z_{14})(Z_{41})}{Z_{kk} + Z_b} & (5.101) \\
 &= j0.033 - \frac{(j0.033)(j0.033)}{j0.3353} \\
 &= j0.02975
 \end{aligned}$$

$$\begin{aligned}
 Z_{21} \text{ (new)} &= Z_{12} \text{ (new)} = Z_{21} - \frac{(Z_{24})(Z_{41})}{Z_{33} + Z_b} & (5.102) \\
 &= j0.033 - \frac{(j0.097)(j0.033)}{j0.3353} \\
 &= j0.02345
 \end{aligned}$$

$$\begin{aligned}
 Z_{22} \text{ (new)} &= Z_{22} - \frac{(Z_{24})(Z_{42})}{Z_{33} + Z_b} & (5.103) \\
 &= j0.097 - \frac{(j0.097)(j0.097)}{j0.3353} \\
 &= j0.06894
 \end{aligned}$$

$$\begin{aligned}
 Z_{23} \text{ (new)} &= Z_{32} \text{ (new)} = Z_{32} - \frac{(Z_{34})(Z_{42})}{Z_{33} + Z_b} & (5.104) \\
 &= j0.097 - \frac{(j0.12778)(j0.097)}{j0.3353} \\
 &= j0.06003
 \end{aligned}$$

$$\begin{aligned}
 Z_{31} \text{ (new)} &= Z_{13} \text{ (new)} = Z_{13} - \frac{(Z_{14})(Z_{43})}{Z_{33} + Z_b} & (5.105) \\
 &= j0.033 - \frac{(j0.033)(j0.12778)}{j0.3353} \\
 &= j0.02042
 \end{aligned}$$

$$\begin{aligned}
 Z_{33} \text{ (new)} &= Z_{33} - \frac{(Z_{34})(Z_{43})}{Z_{33} + Z_b} & (5.106) \\
 &= j0.12778 - \frac{(j0.12778)(j0.12778)}{j0.3353} \\
 &= j0.07908
 \end{aligned}$$

$$Z_{\text{bus},5} = \begin{bmatrix} j0.02975 & j0.02345 & j0.02042 \\ j0.02345 & j0.06894 & j0.06003 \\ j0.02042 & j0.06003 & j0.07908 \end{bmatrix} \quad (5.107)$$

$$Z_{\text{bus},6} = \begin{bmatrix} j0.02975 & j0.02345 & j0.02042 & j0.02042 \\ j0.02345 & j0.06894 & j0.06003 & j0.06003 \\ j0.02042 & j0.06003 & j0.07908 & j0.07908 \\ j0.02042 & j0.06003 & j0.07908 & j0.07536 \end{bmatrix} \quad (5.108)$$

$$Z_{\text{bus},7} = \begin{bmatrix} j0.02975 & j0.02345 & j0.02942 & j0.02042 & j0.02042 \\ j0.02345 & j0.06894 & j0.06003 & j0.06003 & j0.06003 \\ j0.02042 & j0.06003 & j0.07908 & j0.07908 & j0.07908 \\ j0.02042 & j0.06003 & j0.07908 & j0.07536 & j0.07536 \\ j0.02042 & j0.06003 & j0.07908 & j0.07536 & j0.13736 \end{bmatrix} \quad (5.109)$$

$$Z_{\text{bus},8} = \begin{bmatrix} j0.02975 & j0.02345 & j0.02042 & j0.02042 & j0.02042 & j0.02042 \\ j0.02345 & j0.06894 & j0.06003 & j0.06003 & j0.06003 & j0.06003 \\ j0.02042 & j0.06003 & j0.07908 & j0.07908 & j0.07908 & j0.07908 \\ j0.02042 & j0.06003 & j0.07908 & j0.07536 & j0.07536 & j0.07536 \\ j0.02042 & j0.06003 & j0.07908 & j0.07536 & j0.13736 & j0.13736 \\ j0.02042 & j0.06003 & j0.07908 & j0.07536 & j0.13736 & j0.13986 \end{bmatrix} \quad (5.110)$$

The sixth row and column is eliminated by Kron reduction (Grainger & Stevenson 1994).

$$\begin{aligned} Z_{11(\text{new})} &= Z_{11} - \frac{(Z_{16})(Z_{61})}{Z_{kk} + Z_b} & (5.111) \\ &= j0.02975 - \frac{(j0.02042)(j0.02042)}{j0.13986} \\ &= j0.02677 \end{aligned}$$

$$\begin{aligned} Z_{21(\text{new})} &= Z_{12(\text{new})} = Z_{12} - \frac{(Z_{16})(Z_{62})}{Z_{55} + Z_b} & (5.112) \\ &= j0.02345 - \frac{(j0.02042)(j0.06003)}{j0.13986} \\ &= j0.01469 \end{aligned}$$

$$\begin{aligned}
Z_{22}(\text{new}) &= Z_{22} - \frac{(Z_{26})(Z_{62})}{Z_{kk} + Z_b} & (5.113) \\
&= j0.06894 - \frac{(j0.06003)(j0.06003)}{j0.13986} \\
&= j0.04317
\end{aligned}$$

$$\begin{aligned}
Z_{31}(\text{new}) &= Z_{13}(\text{new}) = Z_{13} - \frac{(Z_{16})(Z_{63})}{Z_{55} + Z_b} & (5.114) \\
&= j0.02042 - \frac{(j0.02042)(j0.07908)}{j0.13986} \\
&= j0.00887
\end{aligned}$$

$$\begin{aligned}
Z_{32}(\text{new}) &= Z_{23}(\text{new}) = Z_{23} - \frac{(Z_{26})(Z_{63})}{Z_{55} + Z_b} & (5.115) \\
&= j0.06003 - \frac{(j0.06003)(j0.07908)}{j0.13986} \\
&= j0.02609
\end{aligned}$$

$$\begin{aligned}
Z_{33}(\text{new}) &= Z_{33} - \frac{(Z_{36})(Z_{63})}{Z_{kk} + Z_b} & (5.116) \\
&= j0.07908 - \frac{(j0.07908)(j0.07908)}{j0.13986} \\
&= j0.03437
\end{aligned}$$

$$\begin{aligned}
Z_{41}(\text{new}) &= Z_{14}(\text{new}) = Z_{14} - \frac{(Z_{16})(Z_{64})}{Z_{55} + Z_b} & (5.117) \\
&= j0.02042 - \frac{(j0.02042)(j0.07536)}{j0.13986} \\
&= j0.00942
\end{aligned}$$

$$\begin{aligned}
Z_{42}(\text{new}) &= Z_{24}(\text{new}) = Z_{24} - \frac{(Z_{26})(Z_{64})}{Z_{55} + Z_b} & (5.118) \\
&= j0.06003 - \frac{(j0.06003)(j0.07536)}{j0.13986} \\
&= j0.02768
\end{aligned}$$

$$\begin{aligned}
Z_{43}(\text{new}) &= Z_{34}(\text{new}) = Z_{34} - \frac{(Z_{36})(Z_{64})}{Z_{55} + Z_b} & (5.119) \\
&= j0.07908 - \frac{(j0.07908)(j0.07536)}{j0.13986} \\
&= j0.03647
\end{aligned}$$

$$\begin{aligned}
Z_{44}(\text{new}) &= Z_{44} - \frac{(Z_{46})(Z_{64})}{Z_{kk} + Z_b} & (5.120) \\
&= j0.07536 - \frac{(j0.07536)(j0.07536)}{j0.13986} \\
&= j0.03475
\end{aligned}$$

$$\begin{aligned}
Z_{51}(\text{new}) &= Z_{15}(\text{new}) = Z_{15} - \frac{(Z_{16})(Z_{65})}{Z_{55} + Z_b} & (5.121) \\
&= j0.02042 - \frac{(j0.02042)(j0.13736)}{j0.13986} \\
&= j0.00037
\end{aligned}$$

$$\begin{aligned}
Z_{52}(\text{new}) &= Z_{25}(\text{new}) = Z_{52} - \frac{(Z_{56})(Z_{62})}{Z_{55} + Z_b} & (5.122) \\
&= j0.06003 - \frac{(j0.13736)(j0.06003)}{j0.13986} \\
&= j0.00107
\end{aligned}$$

$$\begin{aligned}
Z_{53}(\text{new}) &= Z_{35}(\text{new}) = Z_{35} - \frac{(Z_{36})(Z_{65})}{Z_{55} + Z_b} & (5.123) \\
&= j0.07908 - \frac{(j0.07908)(j0.13736)}{j0.13986} \\
&= j0.00141
\end{aligned}$$

$$\begin{aligned}
Z_{54}(\text{new}) &= Z_{45}(\text{new}) = Z_{54} - \frac{(Z_{56})(Z_{64})}{Z_{55} + Z_b} & (5.124) \\
&= j0.07536 - \frac{(j0.13736)(j0.07536)}{j0.13986} \\
&= j0.00135
\end{aligned}$$

$$\begin{aligned}
Z_{55 \text{ (new)}} &= Z_{55} - \frac{(Z_{56})(Z_{65})}{Z_{kk} + Z_b} & (5.125) \\
&= j0.13736 - \frac{(j0.13736)(j0.13736)}{j0.13986} \\
&= j0.00246
\end{aligned}$$

$$Z_{\text{bus}}^0 = \begin{bmatrix} j0.02677 & j0.01469 & j0.00887 & j0.00942 & j0.00037 \\ j0.01469 & j0.04317 & j0.02609 & j0.02768 & j0.00107 \\ j0.00887 & j0.02609 & j0.03437 & j0.03647 & j0.00141 \\ j0.00942 & j0.02768 & j0.03647 & j0.03475 & j0.00135 \\ j0.00037 & j0.00107 & j0.00141 & j0.00135 & j0.00246 \end{bmatrix} \quad (5.126)$$

$$\begin{aligned}
I_1 = I_2 = I_0 &= \frac{1}{Z_{44}^1 + Z_{44}^2 + Z_{44}^0} & (5.127) \\
&= \frac{1}{j0.03384 + j0.03384 + j0.03475} \\
&= -j9.763 \text{ pu}
\end{aligned}$$

$$I_{f_{\text{pu}}} = 3I_0 = 29.288 \text{ pu} \quad (5.128)$$

$$I_{\text{base}} = \frac{100 \times 10^6}{\sqrt{3} \times 132000} = 437.387 \text{ A} \quad (5.129)$$

$$I_{\text{actual}} = I_{\text{base}} \times I_{f_{\text{pu}}} = 12810.319 \text{ A} \quad (5.130)$$

The distribution of the fault currents in the positive/negative sequence diagram for Case-Study-Example 7 are shown in Figure 5-16. The distribution of fault current in the zero sequence reactance diagram where $I_{\text{fault}} = 1 \text{ pu}$, is shown in Figure 5-19 below.

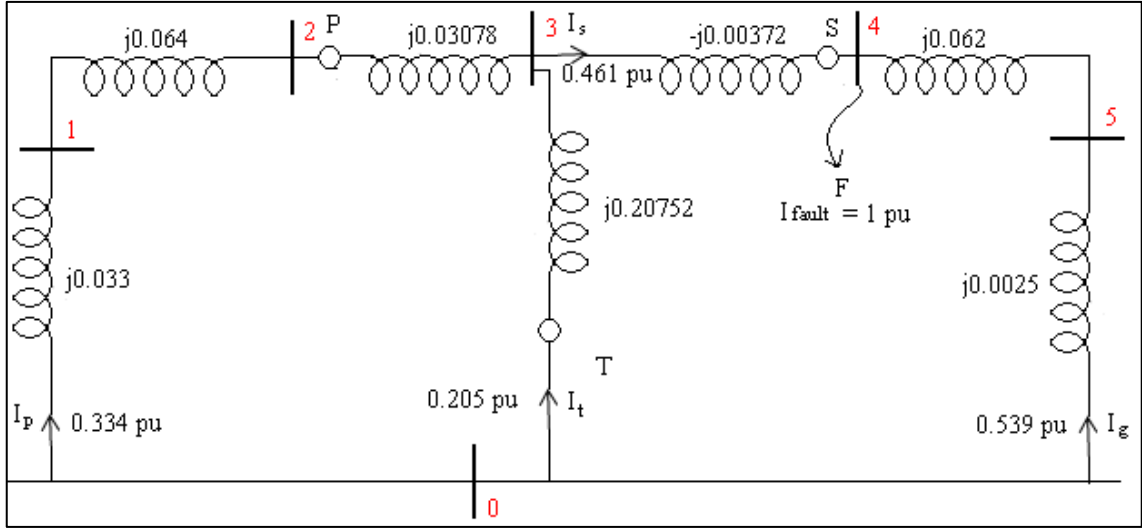


Figure 5-19: Distribution of fault current for zero sequence reactance diagram - Case-Study-Example 7

Using the current divider rule the distribution of currents for the zero sequence diagram of Case-Study-Example 7 is calculated as follows:-

$$I_s = \frac{0.062 + 0.0025}{0.07908 - 0.00372 + 0.062 + 0.0025} = 0.461 \text{ pu} \quad (5.131)$$

$$I_g = \frac{0.07908 - 0.00372}{0.07908 - 0.00372 + 0.062 + 0.0025} = 0.539 \text{ pu} \quad (5.132)$$

$$I_t = 0.461 \times \frac{0.033 + 0.064 + 0.03078}{0.20752 + 0.033 + 0.064 + 0.03078} = 0.176 \text{ pu} \quad (5.133)$$

$$I_p = 0.461 \times \frac{0.20752}{0.20752 + 0.033 + 0.064 + 0.03078} = 0.285 \text{ pu} \quad (5.134)$$

$$\begin{aligned} I_{R_{\text{bus } 2}} &= I_{\text{base}} \left(\frac{132}{400} \right) [I_1(0.4453) + I_2(0.4453) + I_0(0.334)] \quad (5.135) \\ &= 437.387 \times (-j9.763) \times 0.33(0.4453 + 0.4453 + 0.334) \\ &= -j1725.668 \text{ A} \end{aligned}$$

According to Grainger and Stevenson (1994), the voltages at Bus 2 for a fault at Bus 4 are calculated as follows:-

$$\begin{aligned} V_{1_{\text{bus } 2}} &= V_f - Z_{24}^{(1)} I_1 \quad (5.136) \\ &= 1 - (j0.02182)(-j9.763) \\ &= 0.787 \text{ pu} \end{aligned}$$

$$\begin{aligned}
V_{2_{\text{bus } 2}} &= -Z_{24}^{(2)} I_2 & (5.137) \\
&= (-j0.02182)(-j9.763) \\
&= -0.213 \text{ pu}
\end{aligned}$$

$$\begin{aligned}
V_{0_{\text{bus } 2}} &= -Z_{24}^{(0)} I_0 & (5.138) \\
&= (-j0.02768)(-j9.763) \\
&= -0.270 \text{ pu}
\end{aligned}$$

$$\begin{aligned}
V_{R_{\text{bus } 2}} &= V_{1_{\text{bus } 2}} + V_{2_{\text{bus } 2}} + V_{0_{\text{bus } 2}} & (5.139) \\
&= 0.787 - 0.213 - 0.270 \\
&= 0.304 \text{ pu} \\
&= 0.304 \times 400 / \sqrt{3} \\
&= 70.206 \text{ kV}
\end{aligned}$$

$$\begin{aligned}
V_{Y_{\text{bus } 2}} &= a^2 V_{1_{\text{bus } 2}} + a V_{2_{\text{bus } 2}} + V_{0_{\text{bus } 2}} & (5.140) \\
&= (1 \angle 240^\circ) 0.787 + (1 \angle 120^\circ) (-0.213) + (-0.270) \\
&= 1.03 \angle -122.75^\circ \text{ pu} \\
&= (1.03 \angle -122.75^\circ) \times 400 / \sqrt{3} \\
&= (237.795 \angle -122.75^\circ) \text{ kV}
\end{aligned}$$

$$\begin{aligned}
V_{B_{\text{bus } 2}} &= a V_{1_{\text{bus } 2}} + a^2 V_{2_{\text{bus } 2}} + V_{0_{\text{bus } 2}} & (5.141) \\
&= (1 \angle 120^\circ) 0.787 + (1 \angle 240^\circ) (-0.213) + (-0.270) \\
&= 1.03 \angle 122.75^\circ \text{ pu} \\
&= (1.03 \angle 122.75^\circ) \times 400 / \sqrt{3} \\
&= (237.975 \angle 122.75^\circ) \text{ kV}
\end{aligned}$$

5.8 Simulation-Example 1

$$\begin{aligned}
 Z_{AB} &= \frac{V_A - V_B}{I_A - I_B} & (5.142) \\
 &= \frac{(104.0508 \angle 30.24^\circ) \text{kV} - (104.0508 \angle -89.76^\circ) \text{kV}}{(1.1093 \angle -59.76^\circ) \text{kA} - (1.1093 \angle -179.76^\circ) \text{kA}} \\
 &= (93.8 \angle 90^\circ) \Omega
 \end{aligned}$$

$$\begin{aligned}
 Z_{BC} &= \frac{V_B - V_C}{I_B - I_C} & (5.143) \\
 &= \frac{(104.0508 \angle -89.76^\circ) \text{kV} - (104.0508 \angle 150.24^\circ) \text{kV}}{(1.1093 \angle -179.76^\circ) \text{kA} - (1.1093 \angle 60.24^\circ) \text{kA}} \\
 &= (93.8 \angle 90^\circ) \Omega
 \end{aligned}$$

$$\begin{aligned}
 Z_{CA} &= \frac{V_C - V_A}{I_C - I_A} & (5.144) \\
 &= \frac{(104.0508 \angle 150.24^\circ) \text{kV} - (104.0508 \angle 30.24^\circ) \text{kV}}{(1.1093 \angle 60.24^\circ) \text{kA} - (1.1093 \angle -59.76^\circ) \text{kA}} \\
 &= (93.8 \angle 90^\circ) \Omega
 \end{aligned}$$

$$\begin{aligned}
 Z_A &= \frac{V_A}{I_A + I_r k_0} & (5.145) \\
 &= \frac{V_A}{I_A} & I_r = (I_A + I_B + I_C) = 0 \\
 &= \frac{(104.0508 \angle 30.24^\circ) \text{kV}}{(1.1093 \angle -59.76^\circ) \text{kA}} \\
 &= (93.8 \angle 90^\circ) \Omega
 \end{aligned}$$

$$\begin{aligned}
 Z_B &= \frac{V_B}{I_B + I_r k_0} & (5.146) \\
 &= \frac{V_B}{I_B} & I_r = (I_A + I_B + I_C) = 0 \\
 &= \frac{(104.0508 \angle -89.76^\circ) \text{kV}}{(1.1093 \angle -179.76^\circ) \text{kA}} \\
 &= (93.8 \angle 90^\circ) \Omega
 \end{aligned}$$

$$\begin{aligned}
Z_C &= \frac{V_C}{I_C + I_r k_0} & (5.147) \\
&= \frac{V_C}{I_C} & I_r = (I_A + I_B + I_C) = 0 \\
&= \frac{(104.0508 \angle 150.24^\circ) \text{kV}}{(1.1093 \angle 60.24^\circ) \text{kA}} \\
&= (93.8 \angle 90^\circ) \Omega
\end{aligned}$$

5.9 Simulation-Example 2

$$\begin{aligned}
I_r &= (I_A + I_B + I_C) & (5.148) \\
&= (1.1745 \angle -57.95^\circ + 0.1307 \angle -110.58^\circ + 0.1212 \angle 88.04^\circ) \text{kA} \\
&= (1.1539 \angle -59.74^\circ) \text{kA}
\end{aligned}$$

$$\begin{aligned}
k_0 &= \frac{Z_0 - Z_1}{3Z_1} & (5.149) \\
&= \frac{j84.4 - j93.8}{3(j93.8)} \\
&= -0.0334
\end{aligned}$$

$$\begin{aligned}
Z_A &= \frac{V_A}{I_A + I_r k_0} & (5.150) \\
&= \frac{106.6192 \angle 32.11^\circ}{1.1745 \angle -57.95^\circ + ((1.1539 \angle -59.74^\circ)(-0.0334))} \\
&= (93.86 \angle 90^\circ) \Omega
\end{aligned}$$

$$\begin{aligned}
Z_B &= \frac{V_B}{I_B + I_r k_0} & (5.151) \\
&= \frac{231.7164 \angle -92.66^\circ}{(0.1307 \angle -110.58^\circ) + ((1.1539 \angle -59.74^\circ)(-0.0334))} \\
&= (2097.3493 \angle 33.61^\circ) \Omega
\end{aligned}$$

$$\begin{aligned}
Z_C &= \frac{V_C}{I_C + I_r k_0} & (5.152) \\
&= \frac{238.8967 \angle 144.93^\circ}{(0.1212 \angle 88.04^\circ) + ((1.1539 \angle -59.74^\circ)(-0.0334))} \\
&= (1539.5614 \angle 49.28^\circ) \Omega
\end{aligned}$$

Consequently using the algorithm that does not have zero sequence compensation yields the following result:-

$$\begin{aligned}
Z_A &= \frac{V_A}{I_A} & (5.153) \\
&= \frac{106.6192 \angle 32.11^\circ}{1.1745 \angle -57.95^\circ} \\
&= (90.78 \angle 90^\circ) \Omega
\end{aligned}$$

5.10 Simulation-Example 3

$$\begin{aligned}
Z_{AB} &= \frac{V_A - V_B}{I_A - I_B} & (5.154) \\
&= \frac{(238.1392 \angle 26.61^\circ) \text{kV} - (144.6990 \angle -114.97^\circ) \text{kV}}{(0.1435 \angle -11.62^\circ) \text{kA} - (1.0153 \angle -152.46^\circ) \text{kA}} \\
&= (321.027 \angle 18.02^\circ) \Omega
\end{aligned}$$

$$\begin{aligned}
Z_{BC} &= \frac{V_B - V_C}{I_B - I_C} & (5.155) \\
&= \frac{(144.6990 \angle -114.97^\circ) \text{kV} - (153.8089 \angle 170.83^\circ) \text{kV}}{(1.0153 \angle -152.46^\circ) \text{kA} - (0.9085 \angle 33.26^\circ) \text{kA}} \\
&= (93.8 \angle 90^\circ) \Omega
\end{aligned}$$

$$\begin{aligned}
Z_{CA} &= \frac{V_C - V_A}{I_C - I_A} & (5.156) \\
&= \frac{(153.8089 \angle 170.83^\circ) \text{kV} - (238.1392 \angle 26.61^\circ) \text{kV}}{(0.9085 \angle 33.26^\circ) \text{kA} - (0.1435 \angle -11.62^\circ) \text{kA}} \\
&= (459.81 \angle 152.28^\circ) \Omega
\end{aligned}$$

5.11 Simulation-Example 4

$$\begin{aligned}
 Z_{AB} &= \frac{V_A - V_B}{I_A - I_B} & (5.157) \\
 &= \frac{(232.2563 \angle 25.56^\circ) \text{kV} - (108.4328 \angle -89.99^\circ) \text{kV}}{(0.0908 \angle -8.68^\circ) \text{kA} - (1.1763 \angle 178.39^\circ) \text{kA}} \\
 &= (233.15 \angle 46.78^\circ) \Omega
 \end{aligned}$$

$$\begin{aligned}
 Z_{BC} &= \frac{V_B - V_C}{I_B - I_C} & (5.158) \\
 &= \frac{(108.4328 \angle -89.99^\circ) \text{kV} - (102.3091 \angle 152.48^\circ) \text{kV}}{(1.1763 \angle 178.39^\circ) \text{kA} - (1.1117 \angle 64.18^\circ) \text{kA}} \\
 &= (93.8 \angle 90^\circ) \Omega
 \end{aligned}$$

$$\begin{aligned}
 Z_{CA} &= \frac{V_C - V_A}{I_C - I_A} & (5.159) \\
 &= \frac{(102.3091 \angle 152.48^\circ) \text{kV} - (232.2563 \angle 25.56^\circ) \text{kV}}{(1.1117 \angle 64.18^\circ) \text{kA} - (0.0908 \angle -8.68^\circ) \text{kA}} \\
 &= (280.13 \angle 121.25^\circ) \Omega
 \end{aligned}$$

$$\begin{aligned}
 I_r &= (I_A + I_B + I_C) & (5.160) \\
 &= (0.0908 \angle -8.68^\circ + 1.1763 \angle 178.39^\circ + 1.1117 \angle 64.18^\circ) \text{kA} \\
 &= (1.1844 \angle 120.54^\circ) \text{kA}
 \end{aligned}$$

$$\begin{aligned}
 k_o &= \frac{Z_0 - Z_1}{3Z_1} & (5.161) \\
 &= \frac{j84.4 - j93.8}{3(j93.8)} \\
 &= -0.0334
 \end{aligned}$$

$$\begin{aligned}
 Z_B &= \frac{V_B}{I_B + I_r k_o} & (5.162) \\
 &= \frac{108.4328 \angle -89.99^\circ}{(1.1763 \angle 178.39^\circ) + ((1.1844 \angle 120.54^\circ)(-0.0334))} \\
 &= (93.82 \angle 90^\circ) \Omega
 \end{aligned}$$

$$\begin{aligned}
Z_C &= \frac{V_C}{I_C + I_r k_0} & (5.163) \\
&= \frac{102.3091 \angle 152.48^\circ}{(1.1117 \angle 64.18^\circ) + ((1.1844 \angle 120.54^\circ)(-0.0334))} \\
&= (93.84 \angle 90^\circ) \Omega
\end{aligned}$$

Consequently using the algorithm that does not have zero sequence compensation yields the following result:-

$$\begin{aligned}
Z_B &= \frac{V_B}{I_B} & (5.164) \\
&= \frac{108.4328 \angle -89.99^\circ}{1.1763 \angle 178.39^\circ} \\
&= (92.18 \angle 91.6^\circ) \Omega
\end{aligned}$$

$$\begin{aligned}
Z_C &= \frac{V_C}{I_C} & (5.165) \\
&= \frac{102.3091 \angle 152.48^\circ}{1.1117 \angle 64.18^\circ} \\
&= (90.78 \angle 90^\circ) \Omega
\end{aligned}$$

5.12 Simulation-Example 5

$$\begin{aligned}
Z_{AB} &= \frac{V_A - V_B}{I_A - I_B} & (5.166) \\
&= \frac{(231.8061 \angle 27.87^\circ) \text{kV} - (238.1392 \angle -93.39^\circ) \text{kV}}{(0.1564 \angle -34.99^\circ) \text{kA} - (0.1435 \angle -131.62^\circ) \text{kA}} \\
&= (1836.19 \angle 53.67^\circ) \Omega
\end{aligned}$$

$$\begin{aligned}
Z_{BC} &= \frac{V_B - V_C}{I_B - I_C} & (5.167) \\
&= \frac{(238.1392 \angle -93.39^\circ) \text{kV} - (230.5368 \angle 145.87^\circ) \text{kV}}{(0.1435 \angle -131.62^\circ) \text{kA} - (0.1997 \angle 99.44^\circ) \text{kA}} \\
&= (1311.53 \angle 37.33^\circ) \Omega
\end{aligned}$$

$$\begin{aligned}
Z_{CA} &= \frac{V_C - V_A}{I_C - I_A} & (5.168) \\
&= \frac{(230.5368 \angle 145.87^\circ) \text{kV} - (231.8061 \angle 27.87^\circ) \text{kV}}{(0.1997 \angle 99.44^\circ) \text{kA} - (0.1564 \angle -34.99^\circ) \text{kA}} \\
&= (1205.53 \angle 57.66^\circ) \Omega
\end{aligned}$$

$$\begin{aligned}
3I_0 = I_r &= (I_A + I_B + I_C) & (5.169) \\
&= (0.1564 \angle -34.99^\circ + 0.1435 \angle -131.62^\circ + 0.1997 \angle 99.44^\circ) \text{kA} \\
&= (0) \text{A}
\end{aligned}$$

$$\begin{aligned}
Z_A &= \frac{V_A}{I_A + I_r k_0} & (5.170) \\
&= \frac{(231.8061 \angle 27.87^\circ) \text{kV}}{(0.1564 \angle -34.99^\circ) \text{kA}} \quad I_r = (I_A + I_B + I_C) = 0 \\
&= (1482.14 \angle 62.86^\circ) \Omega
\end{aligned}$$

$$\begin{aligned}
Z_B &= \frac{V_B}{I_B + I_r k_0} & (5.171) \\
&= \frac{(238.1392 \angle -93.39^\circ) \text{kV}}{(0.1435 \angle -131.62^\circ) \text{kA}} \quad I_r = (I_A + I_B + I_C) = 0 \\
&= (1659.51 \angle 38.23^\circ) \Omega
\end{aligned}$$

$$\begin{aligned}
Z_C &= \frac{V_C}{I_C + I_r k_0} & (5.172) \\
&= \frac{(230.5368 \angle 145.87^\circ) \text{kV}}{0.1997 \angle 99.44^\circ \text{kA}} \quad I_r = (I_A + I_B + I_C) = 0 \\
&= (1154.42 \angle 46.43^\circ) \Omega
\end{aligned}$$

5.13 Simulation-Example 6

$$\begin{aligned}
 Z_{AB} &= \frac{V_A - V_B}{I_A - I_B} & (5.173) \\
 &= \frac{(209.4747 \angle 10.96^\circ) \text{kV} - (104.0508 \angle -89.76^\circ) \text{kV}}{(0.6525 \angle -7.06^\circ) \text{kA} - (1.1093 \angle -179.76^\circ) \text{kA}} \\
 &= (142.53 \angle 37.5^\circ) \Omega
 \end{aligned}$$

$$\begin{aligned}
 Z_{BC} &= \frac{V_B - V_C}{I_B - I_C} & (5.174) \\
 &= \frac{(104.0508 \angle -89.76^\circ) \text{kV} - (215.8681 \angle 162.69^\circ) \text{kV}}{(1.1093 \angle -179.76^\circ) \text{kA} - (0.4694 \angle 10.42^\circ) \text{kA}} \\
 &= (169.31 \angle 137.6^\circ) \Omega
 \end{aligned}$$

$$\begin{aligned}
 Z_{CA} &= \frac{V_C - V_A}{I_C - I_A} & (5.175) \\
 &= \frac{(215.8681 \angle 162.69^\circ) \text{kV} - (209.4747 \angle 10.96^\circ) \text{kV}}{(0.4694 \angle 10.42^\circ) \text{kA} - (0.6525 \angle -7.06^\circ) \text{kA}} \\
 &= (1659.02 \angle 38.22^\circ) \Omega
 \end{aligned}$$

$$\begin{aligned}
 Z_A &= \frac{V_A}{I_A + I_r k_0} & (5.176) \\
 &= \frac{(209.4747 \angle 10.96^\circ) \text{kV}}{(0.6525 \angle -7.06^\circ) \text{kA}} \quad I_r = (I_A + I_B + I_C) = 0 \\
 &= (321.03 \angle 18.02^\circ) \Omega
 \end{aligned}$$

$$\begin{aligned}
Z_B &= \frac{V_B}{I_B + I_r k_0} & (5.177) \\
&= \frac{(104.0508 \angle -89.76^\circ) \text{kV}}{(1.1093 \angle -179.76^\circ) \text{kA}} \quad I_r = (I_A + I_B + I_C) = 0 \\
&= (93.8 \angle 90^\circ) \Omega
\end{aligned}$$

$$\begin{aligned}
Z_C &= \frac{V_C}{I_C + I_r k_0} & (5.178) \\
&= \frac{(215.8681 \angle 162.69^\circ) \text{kV}}{(0.4694 \angle 10.42^\circ) \text{kA}} \quad I_r = (I_A + I_B + I_C) = 0 \\
&= (459.88 \angle 152.27^\circ) \Omega
\end{aligned}$$

5.14 Simulation-Example 7

$$\begin{aligned}
Z_{AB} &= \frac{V_A - V_B}{I_A - I_B} & (5.179) \\
&= \frac{(207.4943 \angle 11.19^\circ) \text{kV} - (104.0508 \angle -89.76^\circ) \text{kV}}{(0.6513 \angle -8.5^\circ) \text{kA} - (1.1093 \angle -179.76^\circ) \text{kA}} \\
&= (141.91 \angle 38.39^\circ) \Omega
\end{aligned}$$

$$\begin{aligned}
Z_{BC} &= \frac{V_B - V_C}{I_B - I_C} & (5.180) \\
&= \frac{(104.0508 \angle -89.76^\circ) \text{kV} - (213.7173 \angle 162.64^\circ) \text{kV}}{(1.1093 \angle -179.76^\circ) \text{kA} - (0.4759 \angle 12.24^\circ) \text{kA}} \\
&= (167.61 \angle 136.78^\circ) \Omega
\end{aligned}$$

$$\begin{aligned}
Z_{CA} &= \frac{V_C - V_A}{I_C - I_A} & (5.181) \\
&= \frac{(213.7173 \angle 162.64^\circ) \text{kV} - (207.4943 \angle 11.19^\circ) \text{kV}}{(0.4759 \angle 12.24^\circ) \text{kA} - (0.6513 \angle -8.5^\circ) \text{kA}} \\
&= (1532.66 \angle 44.45^\circ) \Omega
\end{aligned}$$

$$\begin{aligned}
Z_A &= \frac{V_A}{I_A + I_r k_0} & (5.182) \\
&= \frac{(207.4943 \angle 11.19^\circ) \text{kV}}{(0.6513 \angle -8.5^\circ) \text{kA}} \quad I_r = (I_A + I_B + I_C) = 0 \\
&= (318.58 \angle 19.69^\circ) \Omega
\end{aligned}$$

$$\begin{aligned}
Z_B &= \frac{V_B}{I_B + I_r k_0} & (5.183) \\
&= \frac{(104.0508 \angle -89.76^\circ) \text{kV}}{(1.1093 \angle -179.76^\circ) \text{kA}} \quad I_r = (I_A + I_B + I_C) = 0 \\
&= (93.8 \angle 90^\circ) \Omega
\end{aligned}$$

$$\begin{aligned}
Z_C &= \frac{V_C}{I_C + I_r k_0} & (5.184) \\
&= \frac{(213.7173 \angle 162.64^\circ) \text{kV}}{(0.4759 \angle 12.24^\circ) \text{kA}} \quad I_r = (I_A + I_B + I_C) = 0 \\
&= (449.08 \angle 150.4^\circ) \Omega
\end{aligned}$$

5.15 Simulation-Example 8

$$\begin{aligned}
Z_{AB} &= \frac{V_A - V_B}{I_A - I_B} & (5.185) \\
&= \frac{(166.6363 \angle 45.53^\circ) \text{kV} - (238.1392 \angle -93.39^\circ) \text{kV}}{(0.7604 \angle -86^\circ) \text{kA} - (0.1435 \angle -131.62^\circ) \text{kA}} \\
&= (568.71 \angle 147.02^\circ) \Omega
\end{aligned}$$

$$\begin{aligned}
Z_{BC} &= \frac{V_B - V_C}{I_B - I_C} & (5.186) \\
&= \frac{(238.1392 \angle -93.39^\circ) \text{kV} - (157.0144 \angle 130.82^\circ) \text{kV}}{(0.1435 \angle -131.62^\circ) \text{kA} - (0.8669 \angle 87.21^\circ) \text{kA}} \\
&= (374.8 \angle 21.99^\circ) \Omega
\end{aligned}$$

$$\begin{aligned}
Z_{CA} &= \frac{V_C - V_A}{I_C - I_A} & (5.187) \\
&= \frac{(157.0144 \angle 130.82^\circ) \text{kV} - (166.6363 \angle 45.53^\circ) \text{kV}}{(0.8669 \angle 87.21^\circ) \text{kA} - (0.7604 \angle -86^\circ) \text{kA}} \\
&= (135.04 \angle 89.64^\circ) \Omega
\end{aligned}$$

$$\begin{aligned}
3I_0 = I_r &= (I_A + I_B + I_C) & (5.188) \\
&= (0.7604 \angle -86^\circ + 0.1435 \angle -131.62^\circ + 0.8669 \angle 87.21^\circ) \text{kA} \\
&= (0) \text{A}
\end{aligned}$$

The sum of line currents entering a delta connection will always summate to zero (ISU 2014).

$$\begin{aligned}
Z_A &= \frac{V_A}{I_A + I_r k_0} & (5.189) \\
&= \frac{(166.6363 \angle 45.53^\circ) \text{kV}}{(0.7604 \angle -86^\circ) \text{kA}} \quad I_r = (I_A + I_B + I_C) = 0 \\
&= (219.14 \angle 131.53^\circ) \Omega
\end{aligned}$$

$$\begin{aligned}
Z_B &= \frac{V_B}{I_B + I_r k_0} & (5.190) \\
&= \frac{(238.1392 \angle -93.39^\circ) \text{kV}}{(0.1435 \angle -131.62^\circ) \text{kA}} \quad I_r = (I_A + I_B + I_C) = 0 \\
&= (1659.51 \angle 38.23^\circ) \Omega
\end{aligned}$$

$$\begin{aligned}
Z_C &= \frac{V_C}{I_C + I_r k_0} & (5.191) \\
&= \frac{(157.0144 \angle 130.82^\circ) \text{kV}}{(0.8669 \angle 87.21^\circ) \text{kA}} \quad I_r = (I_A + I_B + I_C) = 0 \\
&= (181.12 \angle 43.61^\circ) \Omega
\end{aligned}$$

5.16 Simulation-Example 9

$$\begin{aligned}
 Z_{AB} &= \frac{V_A - V_B}{I_A - I_B} & (5.192) \\
 &= \frac{(150.4786 \angle 19.38^\circ) \text{kV} - (104.0508 \angle -89.76^\circ) \text{kV}}{(0.8048 \angle -44.45^\circ) \text{kA} - (1.1093 \angle -179.76^\circ) \text{kA}} \\
 &= (117.88 \angle 65.77^\circ) \Omega
 \end{aligned}$$

$$\begin{aligned}
 Z_{BC} &= \frac{V_B - V_C}{I_B - I_C} & (5.193) \\
 &= \frac{(104.0508 \angle -89.76^\circ) \text{kV} - (152.3302 \angle 159.19^\circ) \text{kV}}{(1.1093 \angle -179.76^\circ) \text{kA} - (0.7803 \angle 46.74^\circ) \text{kA}} \\
 &= (122.41 \angle 112.87^\circ) \Omega
 \end{aligned}$$

$$\begin{aligned}
 Z_{CA} &= \frac{V_C - V_A}{I_C - I_A} & (5.194) \\
 &= \frac{(152.3302 \angle 159.19^\circ) \text{kV} - (150.4786 \angle 19.38^\circ) \text{kV}}{(0.7803 \angle 46.74^\circ) \text{kA} - (0.8048 \angle -44.45^\circ) \text{kA}} \\
 &= (251.09 \angle 87.14^\circ) \Omega
 \end{aligned}$$

$$\begin{aligned}
 Z_A &= \frac{V_A}{I_A + I_r k_0} & (5.195) \\
 &= \frac{(150.4786 \angle 19.38^\circ) \text{kV}}{(0.8048 \angle -44.45^\circ) \text{kA}} \quad I_r = (I_A + I_B + I_C) = 0 \\
 &= (186.98 \angle 63.83^\circ) \Omega
 \end{aligned}$$

$$\begin{aligned}
 Z_B &= \frac{V_B}{I_B + I_r k_0} & (5.196) \\
 &= \frac{(104.0508 \angle -89.76^\circ) \text{kV}}{(1.1093 \angle -179.76^\circ) \text{kA}} \quad I_r = (I_A + I_B + I_C) = 0 \\
 &= (93.8 \angle 90^\circ) \Omega
 \end{aligned}$$

$$\begin{aligned}
 Z_C &= \frac{V_C}{I_C + I_r k_0} & (5.197) \\
 &= \frac{(152.3302 \angle 159.19^\circ) \text{kV}}{(0.7803 \angle 46.74^\circ) \text{kA}} \quad I_r = (I_A + I_B + I_C) = 0 \\
 &= (195.22 \angle 112.45^\circ) \Omega
 \end{aligned}$$

5.17 Simulation-Example 10

$$\begin{aligned}
 Z_{AB} &= \frac{V_A - V_B}{I_A - I_B} & (5.198) \\
 &= \frac{(85.6359 \angle 30.27^\circ) \text{kV} - (85.6359 \angle -89.73^\circ) \text{kV}}{(1.2489 \angle -59.73^\circ) \text{kA} - (1.2489 \angle -179.73^\circ) \text{kA}} \\
 &= (68.57 \angle 90^\circ) \Omega
 \end{aligned}$$

$$\begin{aligned}
 Z_{BC} &= \frac{V_B - V_C}{I_B - I_C} & (5.199) \\
 &= \frac{(85.6359 \angle -89.73^\circ) \text{kV} - (85.6359 \angle 150.27^\circ) \text{kV}}{(1.2489 \angle -179.73^\circ) \text{kA} - (1.2489 \angle 60.27^\circ) \text{kA}} \\
 &= (68.57 \angle 90^\circ) \Omega
 \end{aligned}$$

$$\begin{aligned}
 Z_{CA} &= \frac{V_C - V_A}{I_C - I_A} & (5.200) \\
 &= \frac{(85.6359 \angle 150.27^\circ) \text{kV} - (85.6359 \angle 30.27^\circ) \text{kV}}{(1.2489 \angle 60.27^\circ) \text{kA} - (1.2489 \angle -59.73^\circ) \text{kA}} \\
 &= (68.57 \angle 90^\circ) \Omega
 \end{aligned}$$

$$\begin{aligned}
 3I_0 = I_r &= (I_A + I_B + I_C) & (5.201) \\
 &= (1.2489 \angle -59.73^\circ + 1.2489 \angle -179.73^\circ + 1.2489 \angle 60.27^\circ) \text{kA} \\
 &= (0) \text{A}
 \end{aligned}$$

$$\begin{aligned}
 Z_A &= \frac{V_A}{I_A + I_r k_0} & (5.202) \\
 &= \frac{V_A}{I_A} & I_r = (I_A + I_B + I_C) = 0 \\
 &= \frac{(85.6359 \angle 30.27^\circ) \text{kV}}{(1.2489 \angle -59.73^\circ) \text{kA}} \\
 &= (68.57 \angle 90^\circ) \Omega
 \end{aligned}$$

$$\begin{aligned}
Z_B &= \frac{V_B}{I_B + I_r k_0} & (5.203) \\
&= \frac{V_B}{I_B} & I_r = (I_A + I_B + I_C) = 0 \\
&= \frac{(85.6359 \angle -89.73^\circ) \text{kV}}{(1.2489 \angle -179.73^\circ) \text{kA}} \\
&= (68.57 \angle 90^\circ) \Omega
\end{aligned}$$

$$\begin{aligned}
Z_C &= \frac{V_C}{I_C + I_r k_0} & (5.204) \\
&= \frac{V_C}{I_C} & I_r = (I_A + I_B + I_C) = 0 \\
&= \frac{(85.6359 \angle 150.27^\circ) \text{kV}}{(1.2489 \angle 60.27^\circ) \text{kA}} \\
&= (68.57 \angle 90^\circ) \Omega
\end{aligned}$$

5.18 Simulation-Example 11

$$\begin{aligned}
I_r &= (I_A + I_B + I_C) & (5.205) \\
&= (1.3023 \angle -58.18^\circ + 0.1185 \angle 161.92^\circ + 0.2859 \angle 103.56^\circ) \text{kA} \\
&= (0.9402 \angle -57.37^\circ) \text{kA}
\end{aligned}$$

$$\begin{aligned}
k_0 &= \frac{Z_0 - Z_1}{3Z_1} & (5.206) \\
&= \frac{Z_{ps0} - Z_{ps}}{3Z_{ps}} \\
&= \frac{0.042063 - 0.042857}{3(0.042857)} \\
&= -0.006176
\end{aligned}$$

$$\begin{aligned}
Z_A &= \frac{V_A}{I_A + I_r k_0} & (5.207) \\
&= \frac{87.3827 \angle 31.93^\circ}{1.3023 \angle -58.18^\circ + ((0.9402 \angle -57.37^\circ)(-0.006176))} \\
&= (67.4 \angle 90.1^\circ) \Omega
\end{aligned}$$

Consequently using the algorithm that does not have zero sequence compensation yields the following result:-

$$\begin{aligned}
 Z_A &= \frac{V_A}{I_A} & (5.208) \\
 &= \frac{87.3827 \angle 31.93^\circ}{1.3023 \angle -58.18^\circ} \\
 &= (67.1 \angle 90.1^\circ) \Omega
 \end{aligned}$$

The equation for the residual compensation factor or ‘k’ factor that measures the autotransformer’s positive sequence impedance Z_{Tps} for a single line to ground fault through an autotransformer is shown below (Ziegler 2011):-

$$k_0 = \frac{Z_{0 \text{ total}} - (Z_{Tps} + Z_{1 \text{ line}})}{3 \times Z_{Tps}} \quad (5.209)$$

Since the model for a 3 winding isolation transformer and an autotransformer is the same the above equation will be used in this case study.

$$Z_{0 \text{ total}} = Z_{p0} + \frac{Z_{s0} (Z_{1 \text{ Source}} + Z_{p0} + Z_{t0})}{Z_{t0}} \quad (5.210)$$

Where $Z_{1 \text{ Source}}$ is the total positive sequence source impedance up to the 3 winding transformer.

$$\begin{aligned}
 Z_{0 \text{ total}} &= j0.047388 & (5.211) \\
 &+ \frac{-j0.005183(0.082461 \angle 89.58^\circ + j0.047388 + j0.193691)}{j0.193691} \\
 &= 0.03873 \angle 90^\circ
 \end{aligned}$$

$$\begin{aligned}
 k_0 &= \frac{0.03873 - 0.042857}{3 \times 0.042857} & (5.212) \\
 &= -0.0321
 \end{aligned}$$

$$\begin{aligned}
\text{Therefore, } Z_{\text{measured}} &= \frac{V_a}{I_a + I_r k_0} & (5.213) \\
&= \frac{87.3827 \angle 31.93^\circ}{1.3023 \angle -58.18^\circ + 0.9402 \angle -57.37^\circ (-0.0321)} \\
&= (68.7 \angle 90^\circ) \Omega
\end{aligned}$$

5.19 Simulation-Example 12

$$\begin{aligned}
Z_{AB} &= \frac{V_A - V_B}{I_A - I_B} & (5.214) \\
&= \frac{(238.5276 \angle 26.61^\circ) \text{kV} - (136.3586 \angle -120.52^\circ) \text{kV}}{(0.1417 \angle -10.69^\circ) \text{kA} - (1.1360 \angle -152.07^\circ) \text{kA}} \\
&= (288.62 \angle 14.58^\circ) \Omega
\end{aligned}$$

$$\begin{aligned}
Z_{BC} &= \frac{V_B - V_C}{I_B - I_C} & (5.215) \\
&= \frac{(136.3586 \angle -120.52^\circ) \text{kV} - (144.4102 \angle 175.78^\circ) \text{kV}}{(1.1360 \angle -152.07^\circ) \text{kA} - (1.0291 \angle 32.86^\circ) \text{kA}} \\
&= (68.57 \angle 90^\circ) \Omega
\end{aligned}$$

$$\begin{aligned}
Z_{CA} &= \frac{V_C - V_A}{I_C - I_A} & (5.216) \\
&= \frac{(144.4102 \angle 175.78^\circ) \text{kV} - (238.5276 \angle 26.61^\circ) \text{kV}}{(1.0291 \angle 32.86^\circ) \text{kA} - (0.1417 \angle -10.69^\circ) \text{kA}} \\
&= (397.2 \angle 156.2^\circ) \Omega
\end{aligned}$$

5.20 Simulation-Example 13

$$\begin{aligned}
Z_{AB} &= \frac{V_A - V_B}{I_A - I_B} & (5.217) \\
&= \frac{(206.9766 \angle 26.16^\circ) \text{kV} - (89.2765 \angle -89.90^\circ) \text{kV}}{(0.2569 \angle -50.63^\circ) \text{kA} - (1.3174 \angle 178.80^\circ) \text{kA}} \\
&= (172.94 \angle 52.9^\circ) \Omega
\end{aligned}$$

$$\begin{aligned}
Z_{BC} &= \frac{V_B - V_C}{I_B - I_C} & (5.218) \\
&= \frac{(89.2765 \angle -89.90^\circ) \text{kV} - (84.1099 \angle 152.51^\circ) \text{kV}}{(1.3174 \angle 178.80^\circ) \text{kA} - (1.2465 \angle 63.76^\circ) \text{kA}} \\
&= (68.57 \angle 90^\circ) \Omega
\end{aligned}$$

$$\begin{aligned}
Z_{CA} &= \frac{V_C - V_A}{I_C - I_A} & (5.219) \\
&= \frac{(84.1099 \angle 152.51^\circ) \text{kV} - (206.9766 \angle 26.16^\circ) \text{kV}}{(1.2465 \angle 63.76^\circ) \text{kA} - (0.2569 \angle -50.63^\circ) \text{kA}} \\
&= (193.5 \angle 117.81^\circ) \Omega
\end{aligned}$$

$$\begin{aligned}
I_r &= (I_A + I_B + I_C) & (5.220) \\
&= (0.2569 \angle -50.63^\circ + 1.3174 \angle 178.80^\circ + 1.2465 \angle 63.76^\circ) \text{kA} \\
&= (1.1227 \angle 122.49^\circ) \text{kA}
\end{aligned}$$

$$\begin{aligned}
k_0 &= \frac{0.03873 - 0.042857}{3 \times 0.042857} & (5.221) \\
&= -0.0321 & \text{(from Simulation-Example 11)}
\end{aligned}$$

$$\begin{aligned}
Z_B &= \frac{V_B}{I_B + I_r k_0} & (5.222) \\
&= \frac{89.2765 \angle -89.90^\circ}{(1.3174 \angle 178.80^\circ) + ((1.1227 \angle 122.49^\circ)(-0.0321))} \\
&= (68.8 \angle 90^\circ) \Omega
\end{aligned}$$

$$\begin{aligned}
Z_C &= \frac{V_C}{I_C + I_r k_0} & (5.223) \\
&= \frac{84.1099 \angle 152.51^\circ}{(1.2465 \angle 63.76^\circ) + ((1.1227 \angle 122.49^\circ)(-0.0321))} \\
&= (68.48 \angle 90.2^\circ) \Omega
\end{aligned}$$

Consequently using an algorithm that does not have zero sequence compensation yields the following result:-

$$\begin{aligned} Z_B &= \frac{V_B}{I_B} && (5.224) \\ &= \frac{89.2765\angle-89.90^\circ}{1.3174\angle178.80^\circ} \\ &= (67.77\angle91.3^\circ)\Omega \end{aligned}$$

$$\begin{aligned} Z_C &= \frac{V_C}{I_C} && (5.225) \\ &= \frac{84.1099\angle152.51^\circ}{1.2465\angle63.76^\circ} \\ &= (67.48\angle88.75^\circ)\Omega \end{aligned}$$

6 CONCLUSIONS AND RECOMMENDATIONS

6.1 Conclusions

Distance protection applied to reach through power transformers are traditionally used to provide backup protection for generator transformers and line bank transformers. The Eskom Transmission setting philosophy states that the HV and MV IDMT overcurrent elements must be stable at 2 x full load current of the transformer (Eskom 2006). This has resulted in MV and HV overcurrent protection not detecting uncleared MV multiphase busbar faults in substations with low MV fault levels which are located far away from generating stations.

According to the DigSilent simulations summarised in Tables 4-17 and 4-18, accurate measurement is possible for multiphase faults through Dyn1, YNynd1, YNa0d1, YNyn and YNd1 three phase power transformers. The multiphase faults are 3 phase, phase-to-phase and phase-to-phase-to-ground faults. It must be noted that only the earth element measures accurately for phase-to-phase and phase-to-phase-to-ground faults through Dyn1 and YNd1 transformers. The distance relay employed must measure all six fault loops simultaneously. The GE D30 relay will measure the correct distance to phase-to-phase faults through any star/delta or delta/star transformer using the inputs detailed in the relay's manual. The GE D30 relay will also measure the correct distance to fault through YNd1 and Dyn1 transformers during phase-to-phase-to-ground faults as shown in Sections 4.2.4 and 4.3.4

It was shown that Ziegler's 'k' factor for autotransformers provided the most accurate results for distance measurement through YNynd1 and YNa0d1 transformers during single-line-to-ground faults. Distance measurement through YNd1 and Dyn1 transformers are not possible for single-line-to-ground faults using the traditional algorithms for distance protection.

Vector group compensation for CTs and VTs when connected to distance elements are not required when both instrument transformers are located on the same side of power transformers. The Zone of protection for transformer distance protection is determined by the location of the VT. Consequently it is recommended that CT compensation be applied when the instrument transformers are not located on the same side of the power transformer. This has been detailed in Section 2.

The change in transformer impedance introduced by tap-changers can be accommodated in settings calculations. The effects of transformer inrush current on distance relays is mitigated by using 2nd harmonic blocking and supervising the distance element with overcurrent and undervoltage elements.

Therefore, this study concludes that the impedance function in transformer IEDs can be set to provide backup protection for the transformer, busbar and the line.

6.2 Recommendations

This study recommends that the application of distance protection through transformers be applied in the Eskom transmission network. However the vector group of the transformer and effects of the tap-changer must be considered for the settings. In multifunction transformer protection IEDs with both distance and differential functions, it is recommended that the distance function be set to provide backup protection for the transformer, busbar and the line.

REFERENCES

ABB. 2011. *Distribution automation handbook. Section 8.8. Protection of meshed networks.* Finland.

ABB. 2004. *Transformer handbook.* Business Unit Transformers Power Technologies Division, Switzerland, 99.

Alstom. 2011. *Network protection and automation guide.* 1st ed. Levallois-Perret, France: Alstom, 11-17, 11-18.

Alworthy. G. 1999. *Impedance relays.* Eskom Manual Compilation, 12-16.

Andrichak, J. G. & Alexander, G. E. n.d. *Distance relays fundamentals.* GER-3966, Malvern, PA.

Basler Electric. 2007. *Transformer protection application guide.* Revised 06/07

Blackburn, J. L. & Domin, T. J. 2007. *Protective relaying principles and applications.* 3rd ed. London: CRC Press, 4, 12, 323.

Cigré. 2008. *Modern distance protection functions and applications.* Working Group B5.15.

Eaton. 2014. *EDR-4000 Eaton distribution relay.* Available:

http://es.eaton.com/protectiverelays/Documentation/EDR4000/IM02602006E_Instruction.PDF [Accessed 13 July 2014]

Ederhoff, K. B. 2010. Power system calculations. Part 2. Industry Applications Society Annual Meeting, Houston, Texas.

Electric Power Research Institute (ERPI). 2009. *Transformer Guidebook Development.* The Copper Book. 1-5.

Eskom. 2006. *Protection setting philosophy for transmission and sub-transmission grids.* TPL41-9.

GEC Alstom Measurements Limited. 1987. *Protective Relays Application Guide*. 3rd ed. Stafford, England: GEC Alstom, 58, 59, 180, 198.

GE. 2014a. *Line Protection with distance relays*. Available:
<http://www.gedigitalenergy.com/multilin/notes/artsci/art14.pdf> [13 July 2014]

GE. 2014b. *Transformer Protection Principles*. Available:
<http://www.gedigitalenergy.com/smartgrid/Mar07/article5.pdf> [20 July 2014]

GE Multilin. 2011. *D30 Line Distance Protection System*. Revision 5.9x, 10-7 to 10-9, 5-117

Goosen, P. V. 2004. *Transmission division power transformer specification*. TECSC0009, Eskom Transmission.

Grainger, J. J. & Stevenson, W. D. 1994. *Power systems analysis*. New York: McGraw Hill, 416.

Guzman, A. Altuve, H. & Tziouvaras, D. 2005. *Power transformer protection improvements with numerical relays*. Schweitzer Engineering Laboratories, Inc. Pullman WA, USA.

Han, Z., Liu, S., Gao, S., Yip, T. & Bo, Z. 2009. Research on transformer backup distance protection. Conference proceeding, The International Conference on Electrical Engineering.

Heathcote, M. J. 1998. *The J & P Transformer book. A practical technology of the power transformer*. 12th ed. Oxford: Newnes, 34.

Herrmann, H. J. 2005. *Transmission protection and monitoring with multifunction relays. Survey of German practice*, Siemens, Nuremberg, Germany, Cigre.

Horowitz, S. H., Phadke, A. G. & Niemira J. K. 2008. *Power system relaying*. 3rd ed. West Sussex, England: John Wiley & Sons, Ltd, 203.

IEC. 1997-10. *Power transformers – application guide, IEC 60076-8*. International Electrotechnical Commission, first edition.

IS. 2009. *Power transformers, Part 8: Applications guide (ETD16: Transformers)* IS 2026-8, Bureau of Indian Standards

ISU. 2014. *Iowa State University*. Available: www.ee.iastate.edu/~jdm/.../notes6_SymmetricalComponents2_post.doc [Accessed 26 August 2014].

Jewalikar, S. 2008. *Backup to busbar protection with numerical distance protection*. 15th National Power Systems Conference, IIT Bombay.

Mason, C. R. 1956. *The art and science of protective relaying*. General Electric series, John Wiley, 321.

Mekic, F., Girgis, R., Gajic, Z. & teNyenhuis, E. 2006. Power transformer characteristics and their effect on protective relays. 33rd Western Protective Relay Conference.

Mooney, J. & Samineni, S. 2007. *Distance relay response to transformer energisation: problems and solutions*. Schweitzer Engineering Laboratories Inc. Pullman WA, USA.

Perez, L. 2006. A brief overview of polarised Mho characteristics in steady-state.

Perera, R. & Kasztenny, B 2014. Application considerations when protecting lines with tapped and in-line transformers. Published in: *Protective Relay Engineers, 2014, 67th Annual Conference (IEEE)* College Station, Texas.

Schweitzer, E. O. & Roberts, J. 1993. Distance relay element design. Conference paper: Protective Relay Engineers, 1993, 46th Annual Conference, Texas A&M University, College Station, Texas.

Shepherd, J. Morton, A. H. & Spence, L. F. 1993. *Higher electrical engineering*. 2nd ed. Singapore: Longman Publishers, 283.

Short, T. A. 2005. *Electric power distribution equipment and systems*. Boca Raton, FL: CRC Taylor & Francis, 226.

Shukri, Z., Hairi, M. H. & Mohd Zin A. A 2005. *Application of distance function as backup protection for grid transformer in TNB 500/275/132kV System*. Cigre.

Teffo, R. 2013. Impact of transformer inrush on impedance protection. Eskom Protection Workshop, held at Eskom Academy of Learning, Midrand, SA.

Theraja, B. L. & Theraja, A. K 2005. AC & DC machines. , In: *A Textbook of Electrical Technology in S.I. system of units*. Volume 2. New Delhi: S. Chand and Company, 1216.

Verzosa, Q. n.d. *Ground distance relays – understanding the various methods of residual compensation, setting the resistive reach of polygon characteristics, and ways of modelling and testing the relay*. Doble Engineering Company, Watertown MA, USA.

Winders, J. J 2002. *Power transformers. Principles and applications*. New York: Marcel Dekker Incorporated, 137.

WSU. 2014. Washington State University. Available:

<http://conferences.wsu.edu/forms/hrs/HRS14/2014HRS/Lectures/Concurrent/PowerTransformer-SubCom.pdf> [Accessed 12 August 2014]

Zhang, X. Echeverria, A. n.d. Three-winding autotransformer fault study and impact on protection application. New York Power Authority

Ziegler, G. 2008. *Numerical distance protection: principles and Application*. 3rd ed. Munich, Germany: Publicis Corporate Publishing, 122, 124.

Ziegler, G. 2011. *Numerical Distance Protection. Principles and Application*. 4th ed. Munich, Germany: Publicis Corporate Publishing, 177.

Zimmerman, K. & Roth, D. 2005. Evaluation of distance and directional relay elements on lines with power transformers or open-delta VTs. Schweitzer Engineering Laboratories, Inc. Pullman WA, USA.

Zocholl, S., Guzman, A. & Benmouyal, G. 2000. Performance analysis of traditional and improved transformer differential protective relays. Schweitzer Engineering Laboratories, Inc. Pullman WA, USA.

APPENDIX 1

Winding Symbol			Impedance %						Subclauses
			Excited winding, 3-limb core			Excited winding, 5-limb core (or shell)			
(1)	(2)	(3)	(1)	(2)	(3)	(1)	(2)	(3)	
Y N	Y	*	≈ 50	-		≈ 10 ⁴	-		4.3.4.4
Y	Y N	*	-	≈ 60		-	≈ 10 ⁴		4.3.4.4
Y N	Y N		a ₁ z ₁₂	a ₂ z ₁₂		z ₁₂	z ₁₂		4.7.1
Y N	D		a ₁ z ₁₂	-		z ₁₂	-		4.7.2
D	Y N		-	a ₂ z ₁₂		-			4.7.2
Y N	Y	Y*	≈ 50	-	-	≈ 10 ⁴	-	-	4.3.4.4
Y	Y N	Y*	-	≈ 60	-	-	≈ 10 ⁴	-	4.3.4.4
Y	Y	YN *	-	-	≈ 70	-	-	≈ 10 ⁴	4.3.4.4
Y N	Y N	Y	a ₁ z ₁₂	a ₂ z ₁₂	-	z ₁₂	z ₁₂	-	4.7.1
Y N	Y	YN		-	a ₃ z ₁₃	z ₁₃	-	z ₁₃	4.7.1
Y	Y N	YN	-		a ₃ z ₂₃	-	z ₂₃	z ₂₃	4.7.1
Y N	Y N	D	a ₁ (z ₁ + z ₂ z ₃)	a ₂ (z ₂ + z ₁ z ₃)	-	z ₁ + z ₂ z ₃	z ₂ + z ₁ z ₃	-	4.7.2
Y N	D	D	a ₁ (z ₁ + z ₂ z ₃)	-	-	z ₁ + z ₂ z ₃	-	-	4.7.2
Y N	Y	D		-	-	z ₁₃	-	-	4.7.2
D	Y N	YN	-	a ₂ (z ₂ + z ₁ z ₃)	a ₃ (z ₃ + z ₁ z ₂)	-	z ₂ + z ₁ z ₂	z ₃ + z ₁ z ₃	4.7.2
D	Y N	Y	-	a ₂ z ₁₂	-	-	z ₁₂	-	4.7.2
D	Y	YN	-	-	a ₃ z ₁₃	-	-	z ₁₃	4.7.2
D	Y N	D	-	a ₂ (z ₂ + z ₁ z ₃)	-	-	z ₂ + z ₁ z ₃	-	4.7.2

NOTES

z₁₂, z₁₃ and z₂₃ are short-circuit positive sequence impedances

$$z_1 = \frac{z_{12} + z_{13} - z_{23}}{2}, \text{ similarly } z_2 \text{ and } z_3$$

$$z_1 \parallel z_2 = \frac{z_1 z_2}{z_1 + z_2}, \text{ similarly } z_1 \parallel z_3 \text{ and } z_2 \parallel z_3$$

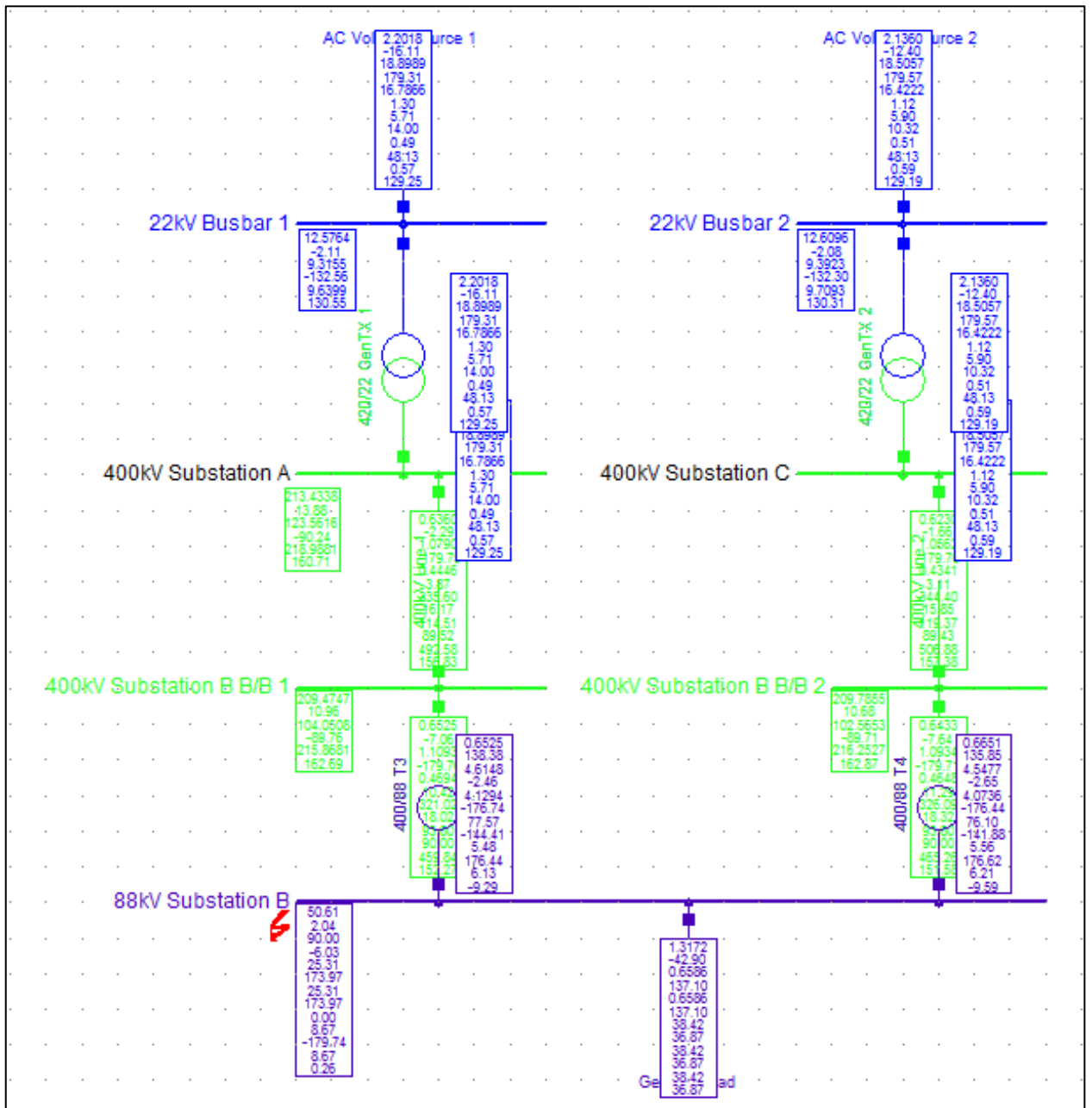
a₁, a₂ and a₃ are multiplying factors generally in the range 0.8 < a₁ < a₂ < a₃ < 1

Particular aspects of zero sequence impedance properties are given in 4.7.1, 4.7.2 and 4.7.3

Connections marked with an asterisk (*) indicate cases where the zero sequence impedance is a magnetising impedance of relatively high or very high value, depending on the nature of the magnetic circuit

Zero Sequence Impedance of Transformers – Typical values (IEC 1997-10)

APPENDIX 2



Digsilent Power Factory Simulation – Phase-to-phase fault – Section 4.3.2

APPENDIX 3

3-Winding Transformer Type - Transmission Library\3-winding transformers\Umfoloji 400/88/22 T1 - YYD KUBEN.TypTr3

<p>Basic Data</p> <p>Load Flow</p> <p>VDE/IEC Short-Circuit</p> <p>Complete Short-Circuit</p> <p>ANSI Short-Circuit</p> <p>IEC 61363</p> <p>RMS-Simulation</p> <p>EMT-Simulation</p> <p>Harmonics/Power Quality</p> <p>Protection</p> <p>Optimal Power Flow</p> <p>Reliability</p> <p>Generation Adequacy</p> <p>Description</p>	<div style="display: flex; justify-content: space-between;"> <div> <p>Name: <input type="text" value="Umfoloji 400/88/22 T1 - YYD KUBEN"/></p> </div> <div style="text-align: right;"> <input type="button" value="OK"/> <input type="button" value="Cancel"/> </div> </div> <div style="display: flex; justify-content: space-between; margin-top: 10px;"> <div> <p>Rated Power</p> <p>HV-Side: <input type="text" value="315"/> MVA</p> <p>MV-Side: <input type="text" value="315"/> MVA</p> <p>LV-Side: <input type="text" value="40"/> MVA</p> </div> <div> <p>Rated Voltage</p> <p>HV-Side: <input type="text" value="400"/> kV</p> <p>MV-Side: <input type="text" value="88"/> kV</p> <p>LV-Side: <input type="text" value="22"/> kV</p> </div> </div> <div style="margin-top: 10px;"> <p>Vector Group</p> <p>HV-Side: <input type="text" value="YN"/> Phase Shift: <input type="text" value="0"/> *30deg</p> <p>MV-Side: <input type="text" value="YN"/> Phase Shift: <input type="text" value="0"/> *30deg</p> <p>LV-Side: <input type="text" value="D"/> Phase Shift: <input type="text" value="1"/> *30deg</p> <p>Name: <input type="text" value="YNOyn0d1"/></p> </div> <p style="font-size: small; color: red; margin-top: 5px;">Hint: The short-circuit voltages refer to the corresponding min. rated Powers e.g. uk(HV-MV) is referred to the minimum of Sr(HV) and Sr(MV)</p> <div style="border: 1px solid gray; padding: 5px; margin-top: 5px;"> <p>Positive Sequence Impedance</p> <table style="width: 100%; border-collapse: collapse;"> <tr> <td style="width: 50%; border-right: 1px solid gray; padding: 2px;"> <p>Short-Circuit Voltage uk</p> <p>HV-MV: <input type="text" value="13.5"/> %</p> <p>MV-LV: <input type="text" value="8.23"/> %</p> <p>LV-HV: <input type="text" value="10.18"/> %</p> </td> <td style="width: 50%; padding: 2px;"> <p>SHC-Voltage, Real Part</p> <p>HV-MV: <input type="text" value="0"/> %</p> <p>MV-LV: <input type="text" value="0"/> %</p> <p>LV-HV: <input type="text" value="0"/> %</p> </td> </tr> </table> </div> <div style="border: 1px solid gray; padding: 5px; margin-top: 5px;"> <p>Zero Sequence Impedance</p> <table style="width: 100%; border-collapse: collapse;"> <tr> <td style="width: 50%; border-right: 1px solid gray; padding: 2px;"> <p>Short-Circuit Voltage uk0</p> <p>HV-MV: <input type="text" value="13.25"/> %</p> <p>MV-LV: <input type="text" value="7.5403"/> %</p> <p>LV-HV: <input type="text" value="9.643"/> %</p> </td> <td style="width: 50%; padding: 2px;"> <p>SHC-Voltage, Real Part</p> <p>HV-MV: <input type="text" value="0"/> %</p> <p>MV-LV: <input type="text" value="0"/> %</p> <p>LV-HV: <input type="text" value="0"/> %</p> </td> </tr> </table> </div> <div style="margin-top: 10px;"> <input type="button" value="Pocket Calculator"/> <p style="font-size: x-small; margin-top: 5px;">A tool that transforms commonly measured impedance values into equivalent star-impedances</p> </div>	<p>Short-Circuit Voltage uk</p> <p>HV-MV: <input type="text" value="13.5"/> %</p> <p>MV-LV: <input type="text" value="8.23"/> %</p> <p>LV-HV: <input type="text" value="10.18"/> %</p>	<p>SHC-Voltage, Real Part</p> <p>HV-MV: <input type="text" value="0"/> %</p> <p>MV-LV: <input type="text" value="0"/> %</p> <p>LV-HV: <input type="text" value="0"/> %</p>	<p>Short-Circuit Voltage uk0</p> <p>HV-MV: <input type="text" value="13.25"/> %</p> <p>MV-LV: <input type="text" value="7.5403"/> %</p> <p>LV-HV: <input type="text" value="9.643"/> %</p>	<p>SHC-Voltage, Real Part</p> <p>HV-MV: <input type="text" value="0"/> %</p> <p>MV-LV: <input type="text" value="0"/> %</p> <p>LV-HV: <input type="text" value="0"/> %</p>
<p>Short-Circuit Voltage uk</p> <p>HV-MV: <input type="text" value="13.5"/> %</p> <p>MV-LV: <input type="text" value="8.23"/> %</p> <p>LV-HV: <input type="text" value="10.18"/> %</p>	<p>SHC-Voltage, Real Part</p> <p>HV-MV: <input type="text" value="0"/> %</p> <p>MV-LV: <input type="text" value="0"/> %</p> <p>LV-HV: <input type="text" value="0"/> %</p>				
<p>Short-Circuit Voltage uk0</p> <p>HV-MV: <input type="text" value="13.25"/> %</p> <p>MV-LV: <input type="text" value="7.5403"/> %</p> <p>LV-HV: <input type="text" value="9.643"/> %</p>	<p>SHC-Voltage, Real Part</p> <p>HV-MV: <input type="text" value="0"/> %</p> <p>MV-LV: <input type="text" value="0"/> %</p> <p>LV-HV: <input type="text" value="0"/> %</p>				

Digsilent Power Factory – Star/Star/Delta – TX3 and TX4 Data

APPENDIX 4

Standard Number	Nominal Voltage (kV)			Ratings Main/Tertiary (MVA/MVA)				Impedance		Vector Group
	HV	MV	Tertiary	1	2	3	4	Min (%)	Ratio Max/Min	
A13	765	400	33	2000/*				12	1.30	YNa0d1
A12	400	275	22	1000/*				10	1.35	
A11	400	275	22		800/40	400/40		10	1.35	
A10	400	220	22		630/40	215/40		11	1.30	
A9	400	132	22	500/40	250/40	125/20		13	1.25	
A8	275	132	22	500/40	250/40	125/20		11	1.30	
A7	275	88	22	315/40	160/20	80/10		12	1.25	
A6	220	132	22	500/40	250/40	125/20		9	1.30	
A5	220	66	22	160/20	80/10	40/10		11	1.25	
A4	132	88	22	315/40	160/20	80/10		8	1.35	
A3	132	66	22	160/20	80/10	40/10		9	1.30	
A2	88	44	22	80/10	40/10	20/5		10	1.25	
A1	88	44	22	80/10	40/10	20/5		8	1.30	
B11	132		33	80	40	20		10	1.25	Ynd1
B10	132		22	40	20	10		10	1.25	
B9	132		11	20	10			10	1.25	
B8	88		33	80	40	20	10	9	1.25	
B7	88		22	40	20	10	5	9	1.25	
B6	88		22	20	10	5		9	1.25	
B5	88		6.6	10	5			9	1.25	
B4	66		22	40	20	10	5	8	1.25	
B3	66		11	20	10	5	2.5	8	1.25	
B2	44		11	20	10	5	2.5	7	1.25	
B1	44		6.6	100	5	2.5		7	1.25	
C2	33		11	20	10	5	2.5	7	1.25	YNyn0
C1	22		11	20	10	5	2.5	5	1.25	

Standard Eskom Transformers (Goosen, (2004))